A non-peer reviewed preprint submitted to EarthArXiv

Quantifying the Regional Dynamics and Redistribution of Physical Vulnerability in Least Developed Countries

Joshua Dimasaka[1,2*], Christian Geiß[3,4] and Emily So[1,2]

[1*] Department of Architecture, University of Cambridge, United Kingdom .
[2] Cambridge University Centre for Risk in the Built Environment, United Kingdom .
[3] Earth Observation Center, German Aerospace Center, Weßling, Germany .
[4] Institute of Geography, University of Bonn, Bonn, Germany .

*Corresponding author(s). E-mail(s): jtd33@cantab.ac.uk;

Abstract

In the margins of the accelerating development of digital technology worldwide are the Least Developed Countries (LDCs), which continually face an exacerbated risk crisis at the intersection of rapid rural-urban growth, underlying physical vulnerability, and intensifying climate hazards. Despite decades of international development commitments, the rate of built-up expansion across LDCs has significantly outpaced efforts to transition equitably towards lower physical vulnerability alongside increasing physical, socio-economic, and environmental risks. To understand the evolution of physical vulnerability over the past five decades, this study presents a comprehensive, multi-decadal quantitative spatiotemporal analysis of regional building stock composition and its redistribution dynamics across LDCs, examining aggregate regional trends, cross-country variation, and context-specific dynamics in landlocked geographies, small island developing states, African sub-regions, and post-disaster settings. Using annualised and aggregate proportional change metrics, our findings reveal that compositional redistribution has shifted predominantly towards locally sourced materials for earthen construction, which are of high vulnerability. Varying rural and urban development patterns emerge as primary drivers of redistribution trajectories, while landlocked and island nations face uniquely compounding disadvantages due to material accessibility, affordability, and resource constraints. In post-disaster contexts, the persistent prevalence of unreinforced masonry confirms that disaster occurrence has a localised effect on reshaping construction practices without robust institutional governance. These findings provide the most granular spatiotemporal evidence to date on whether LDCs are achieving significant redistribution progress and offer a quantified, prospective basis for redesigning regional vulnerability management strategies and international risk reduction frameworks that are adaptive and sensitive to the diverse and challenging realities of the built environment in LDCs, both towards and beyond 2030.

Keywords: physical vulnerability, probabilistic, least developed countries, remote sensing, deep learning, spatiotemporal

JEL Classification: O15 , O18 , O20 , Q54 , Q56 , R11 , R14 , R31 , C53 , C55 , D81 , O33 , C45

MSC Classification: 68T07 , 68T09 , 62H35 , 60G60 , 62M30 , 62P12 , 86A32 , 91B76 , 90B15

1 Introduction

In the midst of accelerating developments of digital technology across the world, a significant 12% of the global population in Least Developed Countries (LDCs) (see Figure 1) remains disproportionately suffering from a lack of quality data and technical capacity in addressing exacerbated risks from climate change, socioeconomic inequalities, food insecurity, and environmental degradation (UNICEF 2023; Pauline Dube and Sivakumar 2015; UN Population

Division 2011). LDCs also scored below average in statistical capacity indicators, thereby further hindering their progress in developing National Adaptation Programmes of Action (NAPAs) (UN 2023). These concerning issues form the basis of several international policy foci, such as the *"Leave No One Behind"* approach from the UN Sendai Framework for Disaster Risk Reduction (SFDRR) 2015-2030 (UNDRR 2025b) and the development of disaggregated data from the Doha Programme of Action for the Least Developed Countries for the Decade 2022-2031 (UN-OHRLLS 2022). However, the midterm review of the SFDRR highlights uneven progress across countries, with LDCs experiencing global disparities in equitable development (UNDRR 2023). Recent examples include the increasing drought exposure in several Asian LDCs, such as Bangladesh, Nepal, and Cambodia (Miyan 2015) and the systemic barriers, including technical, cognitive, cultural, and financial constraints, to adaptation in many African, Pacific, and Caribbean LDCs (Kuruppu and Willie 2015).

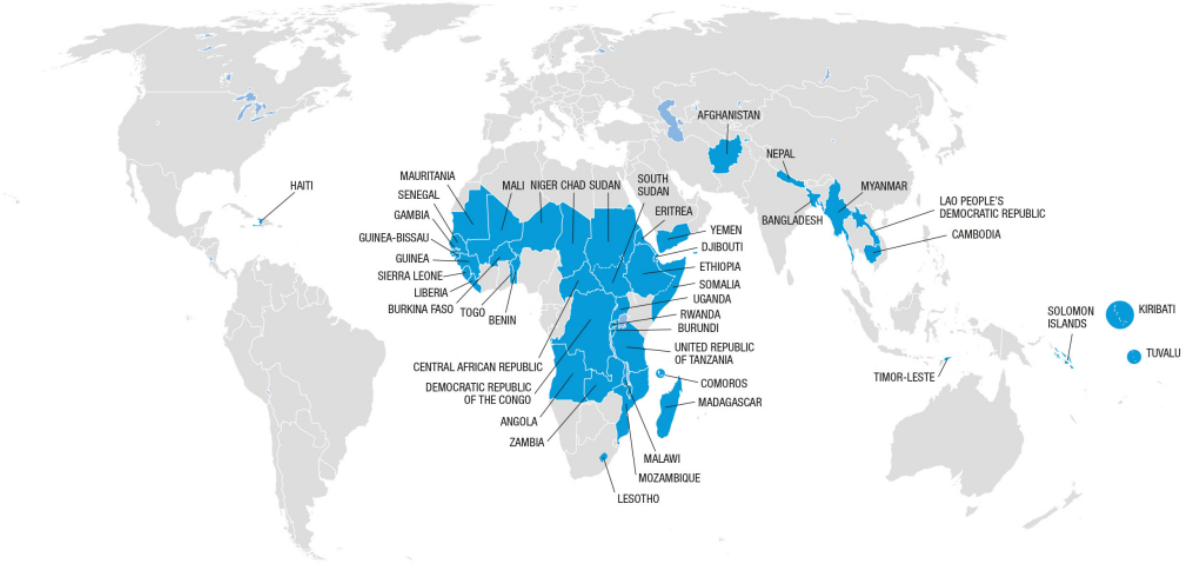

Fig. 1: 44 UN-recognised Least Developed Countries as of December 2024: Africa (32), Asia (8), Carribean (1), Pacific (3). Vanuatu, Bhutan, and Sao Tome and Principe, respectively, graduated from LDC status on December 2020, December 2023, and 2024 (UN Trade and Development 2024).

In recent years, various initiatives such as WorldPop (Tatem 2017; Stevens et al. 2015), Modelling Exposure through Earth Observation Routines (METEOR) project (Huyck et al. 2019; Winson et al. 2020), Google Open Buildings 2.5D Temporal (Sirko et al. 2021), DLR World Settlement Footprint Evolution (Marconcini et al. 2021), Global Human Settlement Layer multitemporal products (Pesaresi et al. 2024a), Microsoft Bing Quarterly Maps (Glazer et al. 2025), and Global Earthquake Model (GEM) Foundation Global Exposure Map and Vulnerability Model (Yepes-Estrada et al. 2023; Martins and Silva 2023) from the recently published UN Global Assessment Risk Report (UNDRR 2025a) have addressed this data gap by mapping the spatial and temporal distribution of exposure indicators, such as population, building geometry, built-up area or volume, and settlement footprints in many LDCs. However, most of these past efforts that deal with exposure assessment alone, such as how many more buildings have been exposed to the flooding hazard, is not adequate yet to develop a risk-informed sustainable development plan, without accounting the intersections of exposure with vulnerability and hazard (Salgado-Gálvez et al. 2026).

Disaster risk science and many civil engineering applications define risk as a physical, economic, financial, or social intersection of *exposure*, *hazard*, *vulnerability*, and *coping capacity*, depending on the characterisation and data modality of these core elements. For example, if a coastal region in an LDC built more assets exposed to the potential impacts of an earthquake and tsunami, development plans would require reducing the corresponding physical vulnerability by constructing more durable and structurally ductile structures. Thus, in the case where exposure cannot be eliminated or migrated to no-hazard zones, tackling the *regional dynamics and redistribution of physical asset vulnerability*, which can be expressed as the building typology or material characterisation, extends numerous past efforts in mapping exposure information at large scales in a disaggregated manner across space and time. This approach is particularly important in data-scarce contexts within LDCs by shaping the design of targeted regional interventions and the efficient allocation of resources (UN IAEG-DRS 2026).

To address these challenges, we present a significant extension to the existing static METEOR dataset of LDCs and comprehensively examine their regional country-level dynamics and redistribution of physical vulnerability in terms of their various development patterns. By applying a unified probabilistic spatiotemporal inference framework that uses graph deep learning, state-space modelling, and variational inference using time-series data and prior expert belief systems in a weakly supervised or coarse-to-fine-grained manner, we introduce an open geospatial dataset, **METEOR 2.5D**. This spatially refines the existing METEOR dataset (i.e., from 450-m to 100-m scale) and significantly extends it with country-wide dynamic evolution of regional exposure and physical vulnerability for 46 UN-recognised LDCs as of 2020, provided at five-year intervals between 1975 and 2030. While our other papers have already provided a detail account to the methodological technicalities of our probabilistic data-driven approach (Dimasaka et al. 2025a, 2026), the focus of this study is to underscore the complementary importance of domain insights on the applicability and scalability of evolving data-driven geospatial products with respect to the historical urban dynamic behaviour and regional disaster risk contexts in these LDCs by highlighting the important underlying regional patterns of physical vulnerability in low economies across the world.

The remainder of this paper is organised as follows: Section 2 provides a brief related work on the importance of regular measurement of vulnerability and risk, including how the framing of the term *vulnerability* from the field of *urban and building metabolism* research aligns with our specific focus on *regional dynamics and redistribution*. Section 3 presents an overview of the preparation of geospatial datasets of prior physical vulnerability and multi-temporal built-up exposure, the description of our proposed probabilistic data-driven model, and the estimation of annual proportion changes and their rates for our evaluation. Section 4 examines the aggregate regional trends and redistribution patterns in LDCs, particularly how LDCs are individually and collectively changing their composition of physical vulnerability, which we refer to as the expected annual development profile over the past five decades. This section also compares LDCs in terms of varying neighbouring development patterns, landlocked geographies, small island developing states, the African continent, and challenging post-disaster contexts.

2 Related Work

The study of regional dynamics and redistribution of physical vulnerability is integral to various applications that rely on dynamic collection, mapping, and review of risk data (UN IAEG-DRS 2026), such as international climate finance mechanisms (Patt et al. 2010), impact attribution (Füssel 2010; Paprotny et al. 2025b), policy development (Feindouno et al. 2020), and socioeconomic development forecasting (Riahi et al. 2017). From a geospatial standpoint, vulnerability can be further characterised as the spatiotemporal distribution of population (e.g., age, sex, disability, education attainment, employment, poverty), assets (e.g., quality and safety

of the built environment features), and flows (e.g., supply chain and distribution networks) (UN 2016; UN IAEG-DRS 2026). Despite widespread efforts in modelling the regional dynamics of vulnerability, considerable disagreements, ambiguities, and a lack of consensus remain across qualitative and quantitative approaches (Brien et al. 2004; Füssel 2010; Feindouno et al. 2020; Adger 2006; Paprotny et al. 2025a), which ultimately narrows its interpretation and application. Its inherently dynamic nature (Brien et al. 2004), sector- and hazard-dependent characterisation (Füssel 2010), reliance on simplified performance indicators with temporally inconsistent variability (Brien et al. 2004; Visser et al. 2020), and insufficient attention to critical distributional properties (Adger 2006) collectively represent the prevailing gaps and challenges in this field.

In particular, several studies have developed various ways to quantify vulnerability at the regional scale. Early work by Briguglio (1995) developed metrics, such as export dependence, remoteness, and insularity, that are particularly relevant to developing economies. Patt et al. (2010) derived an empirical casualty-based vulnerability model that accounts for potential changes in regional exposure and socioeconomic patterns. Closset et al. (2017) and Feindouno et al. (2020) extended the global economic vulnerability index with geophysical variables related to sea level rise, among others, which is critically relevant to small island developing states (Turvey 2007). The global open-source INFORM Risk Index (Marin et al. 2017) measures vulnerability to direct physical impacts using overlapping proxies for exposure indicators, such as population density, urban growth, economic capacity and flows, and agricultural variables (Cardona and Carreño 2011). In the METEOR project, from which this study draws inspiration and offers an extension, Winson et al. (2020) acknowledges these multiple interpretations encountered in practice, ranging from probabilistic modelling and composite proxy indicators to physical characterisation (e.g., building material and number of floors in tsunami contexts), reflecting the broad flexibility required for multi-hazard or hazard-agnostic frameworks (Papathoma and Dominey-Howes 2003; Papathoma-Köhle et al. 2007; Kappes et al. 2012). In the following section, *physical vulnerability* is used consistently to refer to building typology in order to avoid misinterpretation.

With the rapid development of Earth observation data and volunteered geographic information, the shift from a static to a dynamic characterisation of exposure and physical vulnerability has recently gained traction (Geiß a et al. 2025; Salgado-Gálvez et al. 2026), as reflected in various approaches such as cellular automata modelling (Lallemant 2015), analytical probabilistic modelling (Pittore et al. 2017), rigorous bottom-up approaches (Schorlemmer et al. 2020, 2026), geographically weighted regression and multi-agent systems (Calderon and Silva 2022), and agent-based modelling (though these still lack robust uncertainty quantification capability) (Blair and Buytaert 2016; de Ruiter and van Loon 2022; Tilloy et al. 2019). de Ruiter and van Loon (2022) further notes that this trajectory traces back to the physical-to-social shift, followed by the proliferation of composite indices and proxies, and, more recently, the growing recognition of underlying dynamics in the context of slow-onset, cascading, and shock disasters. This is particularly relevant to measuring progress under the UN Sendai Framework for Disaster Risk Reduction 2015-2030, as current practice remains short-sighted and narrow, with a disproportionate focus on disaster events (Chmutina et al. 2021) and the deterministic characterisation of hazards (Muir-Wood 2012, 2017), rather than the primary influence of vulnerability dynamics and development trajectories.

Despite these recent yet limited integrations of dynamics in practice (Hagenlocher et al. 2019), the related discipline of dynamic material flow analysis (dMFA) offers a structured approach to examining the *dynamics* and *redistribution* (Deng et al. 2023) of a system. From this perspective, the regional dynamics and redistribution of physical vulnerability can involve a correlation process between flows and stocks (van der Voet et al. 1995; Müller 2006), which can be extended to large-scale economy-wide accounting models (Wiedenhofer et al. 2019).

Specifically, past studies have applied dMFA in the context of disaster recovery and resilience (Sapountzaki 2005, 2012; Johnson et al. 2022), drawing on methods ranging from random forest modelling and remote sensing to probabilistic approaches and post-disaster field analysis across diverse geographic settings (Mao et al. 2022; Gontia et al. 2020; Silva Bustos 2001; Gallardo et al. 2014; Tanikawa et al. 2014; Lanau et al. 2019; Nie et al. 2025; Pelizari et al. 2026; Cao et al. 2018; Symmes et al. 2020; Martin del Campo et al. 2023). From this framing of dMFA to the use of Earth Observation data, our work also extends these related studies by applying emerging data-driven techniques in graph temporal learning and deep probabilistic inference to capture such correlation processes and to develop a regional accounting model of physical vulnerability.

3 Methodology

This section presents an adapted contextualisation of a unified probabilistic data-driven spatiotemporal inference framework, specifically the Graph Categorical Structured Variational Autoencoder (GraphCSVAE), which models the spatiotemporal and discrete distributions of physical vulnerability categories (Dimasaka et al. 2025a). This framework also serves as the Observation Vulnerability (**OM**) module within a broader temporal framework, the Graph Variational State-Space Model, presented in greater detail in previous chapters (Dimasaka et al. 2026). The following sections describe the data for physical vulnerability and built-up exposure, including a tabular overview of the diverse categories for each LDC. Subsequent sections then detail any new methodological choices in the model implementation, followed by a post-processing procedure for analysing regional redistribution behaviour through proportional change and its corresponding rate.

3.1 Geospatial Data Preparation

3.1.1 Prior Physical Vulnerability

This study draws on the existing static METEOR dataset, which covers UN-recognised LDCs as of 2020 at a 15-arcsecond grid resolution (approximately 500 metres at the equator) (Huyck et al. 2019; Winson et al. 2020). As highlighted in our prior work on deep spatial disaggregation (Dimasaka et al. 2025b), the degree of temporal uncertainty inherent in the METEOR dataset serves as a suitable prior for regularising the trade-off between prior information and patterns learned by the trained model. For each country, the geospatial data are initially represented as a point shapefile containing building counts per physical vulnerability category. Table 1 summarises and describes all categories of physical vulnerability from the original METEOR dataset across all LDCs considered in this study.

Building count data were pre-processed by transforming each pixel into compositional proportions relative to the total building counts across all typologies. The resulting values are bounded between 0 and 1, providing a convenient output constraint for the data-driven model. It is important to note, however, that these values are strictly interpreted as compositional proportions, or equivalently as prior probabilities, assigned as pixel labels at 100-metre resolution. They do not represent the fraction of available observations within a given 100-metre pixel grid, as the resolution of the input covariates, namely the built-up exposure data, dictates the target downscaled resolution of physical vulnerability and disregards any further intra-pixel variability information within the fixed pixel grid size limitation.

Following model training and inference, the resulting individual maps were aggregated into broader shared categories to manage the multiplicity of country-level typologies and to aid subsequent interpretation. Drawing on the pre-defined categorisation from the original METEOR study, two aggregation schemes are presented in Table 2 and Table 3, covering general material grouping and vulnerability level classification, respectively. This simplification assumes

Table 1: Building typologies present in each LDC, where a bullet (•) indicates presence and N = total count per typology/country.

Symbol	Description	N	**AFG:** Afghanistan	**AGO:** Angola	**BDI:** Burundi	**BEN:** Benin	**BFA:** Burkina Faso	**BGD:** Bangladesh	**BTN:** Bhutan	**CAF:** The Central African Republic	**COD:** The DR Congo	**COM:** Comoros	**DJI:** Djibouti	**ERI:** Eritrea	**ETH:** Ethiopia	**GIN:** Guinea	**GMB:** The Gambia	**GNB:** Guinea-Bissau	**HTI:** Haiti	**KHM:** Cambodia	**KIR:** Kiribati	**LAO:** Laos	**LBR:** Liberia	**LSO:** Lesotho	**MDG:** Madagascar	**MLI:** Mali	**MMR:** Myanmar	**MOZ:** Mozambique	**MRT:** Mauritania	**MWI:** Malawi	**NER:** Niger	**NPL:** Nepal	**RWA:** Rwanda	**SDN:** Sudan	**SEN:** Senegal	**SLB:** Solomon Islands	**SLE:** Sierra Leone	**SOM:** Somalia	**SSD:** South Sudan	**STP:** São Tomé and Príncipe	**TCD:** Chad	**TGO:** Togo	**TLS:** Timor-Leste	**TUV:** Tuvalu	**TZA:** Tanzania	**UGA:** Uganda	**VUT:** Vanuatu	**YEM:** Yemen	**ZMB:** Zambia
		362	5	8	6	9	5	9	11	8	10	7	10	10	9	8	5	7	6	8	7	7	8	7	7	7	8	12	6	9	5	12	9	8	7	3	7	10	7	4	9	7	9	4	12	9	5	9	7
A	Adobe block walls	33	•	•	•	•			•	•	•		•		•	•	•	•	•				•	•	•	•	•	•	•	•	•	•	•	•		•	•		•	•		•	•	•	•	•
C	Reinforced concrete	7														•		•																							•	•			•	•	•	•	
C3L	Low-rise nonductile concrete frame	43	•	•	•	•	•	•	•	•	•	•	•	•	•	•	•	•	•	•	•	•	•	•	•	•	•	•	•	•	•	•	•	•	•			•	•	•	•	•	•	•	•	•	•
C3M	Mid-rise nonductile concrete frame	19		•		•		•						•	•	•		•			•						•	•				•	•	•	•			•			•		•	•		•	•
C3H	High-rise nonductile concrete frame	6		•		•																										•						•			•					•	
DS	Rectangular cut-stone masonry block	1																																													•	
INF	Informal constructions.	33		•			•	•	•	•	•	•	•	•	•	•	•	•	•	•		•		•			•	•			•	•	•		•	•		•	•	•	•	•	•	•			
M	Mud walls	23				•	•	•		•	•		•		•	•	•	•							•	•	•	•	•	•				•	•			•	•			•			•	•
RE	Rammed earth	2							•																					•																		
RM	Reinforced masonry	4																							•	•		•		•																		
RS	Rubble stone masonry	21	•					•			•	•	•	•	•				•		•	•	•									•	•				•	•			•	•		•	•
RS1	Local field stones, no mortar	3							•		•	•																																				
RS2	Local field stones with mud mortar.	1																					•																									
RS3	Local field stones with lime mortar.	3							•					•									•																									
S	Steel	10	•					•					•			•			•						•	•	•	•		•																	
S1L	Low-rise steel moment frame	1																										•																			
S1M	Mid-rise steel moment frame	1																										•																			
S3	Steel light frame	8												•						•	•								•			•			•								•	•			
S5	Steel frame w/ unreinforced masonry infill	1																														•															
UCB	Unreinforced concrete block masonry	39		•	•	•	•		•	•	•	•	•	•		•	•	•	•	•	•	•	•	•	•	•		•	•	•		•	•	•	•	•	•	•	•		•	•	•	•	•	•	•
UFB	Unreinforced fired brick masonry	33	•	•	•	•		•	•	•	•	•	•	•	•				•	•	•	•	•	•			•	•	•	•		•	•	•			•		•	•	•	•	•	•	•	•	•
UFB1	Unreinforced brick masonry in mud mortar	1																														•															
W	Wood	28			•				•	•	•	•	•	•	•						•	•		•	•	•	•	•		•		•	•	•		•	•	•	•			•	•			
W1	Wood stud-wall w/ plywood sheathing	2							•											•																											
W2	Wood frame, heavy members	1							•																																							
W3	Wood light unbraced post and beam	5				•		•												•	•																					•						
W5	Wattle and daub	33		•	•	•	•	•		•	•		•	•	•						•		•	•	•			•		•		•	•	•	•		•	•	•		•	•	•	•	•	•	•

Table 2: Material groups and associated building typology symbols.

Group	Description	Detailed Types
EARTH	Load-bearing walls made from soil-based materials	**A**, **M**, **RE**, **W5**
STONE	Natural stone masonry	**RS**, **RS1**, **RS2**, **RS3**, **DS**
URM	Unreinforced brick or concrete block masonry	**UCB**, **UFB**, **UFB1**
RM	Reinforced masonry	**RM**
RC	Reinforced concrete frame systems	**C**, **C3L**, **C3M**, **C3H**
STEEL	Steel structural systems	**S**, **S1L**, **S1M**, **S3**, **S5**
WOOD	Timber structural systems	**W**, **W1**, **W2**, **W3**
INFORMAL	Informal / non-engineered construction	**INF**

Table 3: Vulnerability levels and associated building typology symbols.

Level	Structural Characteristics	Detailed Types
HIGH	Brittle, non-engineered, no reinforcement, no ductility, poor material quality	**A**, **M**, **RE**, **W5**, **RS**, **RS1**, **RS2**, **RS3**, **DS**, **UCB**, **UFB**, **UFB1**, **INF**
MODERATE	Structural frame present but non-ductile or unspecified structural detailing	**C**, **C3L**, **C3M**, **C3H**, **S5**, **W**, **W3**
LOW	Engineered and ductile systems	**RM**, **S**, **S1L**, **S1M**, **S3**, **W1**, **W2**

that the diversity of physical vulnerability can be reduced to three broad levels, implying the homogeneity and dominance of a few building typologies over more complex, heterogeneous, or hybrid ones. Nonetheless, this aggregation facilitates global comparative analysis across LDCs and provides valuable spatiotemporal insights into the overall trends and trajectories of physical vulnerability for subsequent risk assessments.

3.1.2 Multi-Temporal Built-up Exposure

Using the geographical extents defined by the prior information on physical vulnerability, we processed the global, high-resolution, multi-temporal gridded data on total built-up volume from the Global Human Settlement Layer (GHS-BUILT-V R2023A) at five-year intervals from 1975 to 2030 at 100-m spatial resolution (Pesaresi and Politis 2023). The same spatial resolution was applied to the physical vulnerability maps using nearest-neighbour resampling to ensure a resolution-consistent dataset. It is worth noting that this built-up exposure dataset carries uncertainties from spatiotemporal interpolation and extrapolation, including reported limitations in the accuracy and completeness of validation (Pesaresi et al. 2024b,a), which may introduce modelling bias into the resulting posterior distribution of physical vulnerability. While the use of raw satellite imagery, such as synthetic aperture radar and multispectral data as in our previous studies (Dimasaka et al. 2024), or global embeddings such as TESSERA (Feng et al. 2025) and AlphaEarth (Brown et al. 2025), could provide additional variability to enhance the learning and discriminative capacity of the trained model, our work instead demonstrates a simple implementation that relates the categorical distributions of physical vulnerability to rich graph-based patterns derived from built-up geometry. This geometrical information is indirectly relevant to building typology characterisation, as demonstrated in our prior study (Dimasaka et al. 2025b) using the African exposure dataset (Paul et al. 2022).

3.2 Probabilistic Data-Driven Model

The probabilistic data-driven framework known as the Observation Vulnerability (**OM**) module from the Graph Variational State-Space Model (Dimasaka et al. 2026) was applied

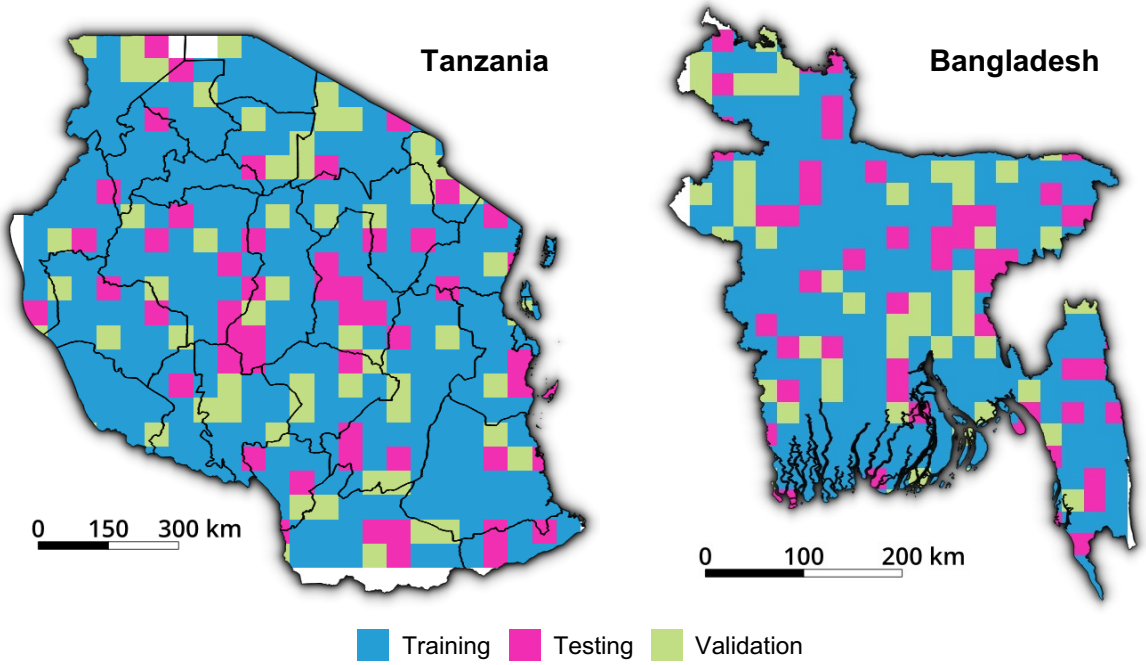

Fig. 2: Example split of a country data into training, testing, and validation sets.

to train country-specific models and infer spatiotemporal patterns for all 46 LDCs across their respective sets of physical vulnerability categories. This module implements the Graph Categorical Structured Variational Autoencoder (Dimasaka et al. 2025a), but rather than using high-resolution Google Open Buildings 2.5D data at 50-centimetre resolution, it incorporates coarser-grained built-up exposure data for the year 2020 from the Global Human Settlement Layer at 100-metre resolution to support larger-scale mapping. The year 2020 was selected on the basis of its largest temporal overlap with the physical vulnerability data, indicating that all other temporal periods are effectively inferred. Unlike the previous high-resolution implementation, which is well-suited for capturing finer-grained, short-term post-disaster settlement behaviour, this coarser-grained approach enables continental-scale application at national extents across all 46 LDCs. The change in spatial resolution was also necessitated by computational constraints.

Rather than training a single unified model for all LDCs, individual models were trained per country to better capture the distinct patterns and distributions of physical vulnerability, as reflected in Table 1. While this substantially simplified the modelling approach, it introduced a separate challenge in partitioning each country's geographical extent into square tiles for training, testing, and validation. For instance, Solomon Islands is an archipelagic country with a considerably smaller landmass than Rwanda, which exhibits more spatially distributed patterns. A variable tile-size approach was therefore adopted to ensure that the resulting proportions of non-overlapping tile counts are sufficient to support deep learning.

Following the dataset split, each tile was assessed for the completeness and diversity of physical vulnerability categories present before being randomly assigned to the training, testing, or validation set, ensuring an even distribution of data quality across all sets. Figure 2 illustrates the 70-15-15 dataset split for Tanzania and Bangladesh, based on the diversity and completeness of available physical vulnerability categories.

For each country, the framework generates a posterior distribution of physical vulnerability by balancing new information derived from multi-temporal built-up patterns against the prior information preserved from the METEOR physical vulnerability maps. The graph-structured representation incorporates neighbourhood information from eight-directional adjacency among

100-metre pixels, establishing a learning propagation mechanism as the parameters of a three-layer graph convolutional neural network (Kipf and Welling 2016) converge to an optimal solution. The variational autoencoder learns a structured latent representation consistent with the discrete categorical nature of physical vulnerability, extending the analytical Bayesian formulations of Pittore et al. (2020) and Porter et al. (2014) through the reparameterisation trick of Jang et al. (2016). Model training optimises the combined loss comprising the reconstruction of decoded built-up exposure patterns, a Kullback-Leibler divergence loss for the encoded posterior distributions of physical vulnerability, and a supervised cross-entropy loss within a semi-supervised variational learning scheme (Kingma et al. 2014). For downstream inference, the trained model was applied to newly prepared overlapping tiles and then aggregated pixel-wise to generate the final maps. For pixels without prior information from the METEOR dataset, we set a uniform prior weight across all physical vulnerability categories, which was subsequently adjusted in deriving the posterior based on the learned patterns of the built-up volume. This major assumption provides an initial estimate of the posterior distribution of physical vulnerability in the absence of prior information, although the assignment of prior weights remains flexible and can be further refined in future studies.

3.3 Estimating Proportion Change and Rate

Using the posterior compositional distributions of physical vulnerability alongside multi-temporal built-up volume in cubic metres, we derived estimated built-up volumes for each physical vulnerability category and temporal period. Beyond analysing country-level totals and visualising spatiotemporal trends through maps and charts, we further characterise the dynamics of the distribution of the physical vulnerability share, analogous to the ”distributional pie” concept frequently employed in economic policy analyses. Two metrics are computed: (1) the average annual proportion change (AAPC), and (2) its rate (APRC) over time. A positive time-averaged annual proportion change (AAPC) indicates a growing share or distribution of a given category. Given the slow and gradual nature of physical vulnerability dynamics over the 55-year study period, this annualised metric is contextualised in terms of the fractional shift, whether an increase or decrease, since net changes in proportions necessarily balance out. The rate (APRC) describes the pace of distributional shifts through time, which is essential for assessing whether an LDC has been reducing its physical vulnerability through regional redistribution across material groups or vulnerability levels.

3.4 Limitations

While this work presents an initial and substantive step towards understanding the regional dynamics and redistribution of physical vulnerability across LDCs, several methodological limitations bound the interpretation of our findings in the succeeding sections and, at the same time, define a clear agenda for future extension. In addition to the challenging state of data availability in LDCs, the probabilistic data-driven model considered the following methodological limitations that shape the current scope of this study.

- The static nature and fixed number of building typologies representing the prior physical vulnerability data for each LDC lack temporally fine-grained information that could otherwise refine the posterior compositions. This limitation necessitates the use of a uniform prior weight assumption, which affects the downstream inference implementation.
- The coarse spatial resolution of the multi-temporal built exposure and prior vulnerability data, at 100 metres and 500 metres, respectively, compounds the uncertainty arising from the proportion of built-up within the grid and the epistemic noise inherent to the model.

- The five-year temporal resolution of the multi-temporal built exposure data averages over unobserved finer annual trends, potentially introducing under- or over-estimation in the resulting annualised metrics of proportional change.
- The simplification of diverse building typologies into eight broad material classes and three vulnerability levels necessarily disregards more complex, heterogeneous, or hybrid construction forms and local construction practices.
- The reliance on a single exposure data source limits the discriminative learning capability of the model to built-up geometrical information, which is only indirectly relevant to building typology characterisation and could have been substantially improved through the incorporation of auxiliary data streams, when available.

Nonetheless, this work is intended to provide a quantitative demonstration for a growing and important area of study of physical vulnerability and risk modelling. This study also envisions that this framework can be extended to building- or community-scale applications and large-scale, economy-wide accounting models that provide auditing capabilities and evidence-based tools for measuring progress for international frameworks, towards and beyond 2030.

4 Results and Discussion

4.1 Aggregate Regional Trends and Redistribution Patterns in LDCs

4.1.1 Understanding the Changing Composition in Annual Development Profile

Figure 3 reveals a sustained and accelerating growth in total built-up volume across LDCs over the past five decades, with projections extending to 2030. Across this period, total built-up volume rises from 114 km^3 in 1975 to a projected 431 km^3 by 2030. This is equivalent to an average annual increase of 5.76 km^3, which represents the total built-up volume illustrated in Figure 3c and Figure 3d. To contextualise this rate, this corresponds to constructing roughly one hectare[1] of single-storey informal settlement (≈40,000 m^3, assuming 4 m average height) to the built environment of LDCs every four minutes (i.e., 5.76 km^3/yr ≈ 40,000 m^3 per ~4 min). These findings underscore the rapid pace and extensive scale of built-up expansion in LDCs, reinforcing the urgency of addressing their disproportionate exposure to climate change and other forms of natural hazards.

Disaggregating total built-up volume by material type and vulnerability level further shows the deeply uneven and persistently high vulnerability of built-up growth across LDCs. Derived from remotely sensed spatiotemporal data using our proposed probabilistic data-driven model, Figure 3a shows that three material types, namely **EARTH** (earthen construction), **URM** (unreinforced masonry), and **RC** (reinforced concrete), dominate the total built-up volume throughout the observed period. This material composition is consistent with the vulnerability trends in Figure 3b, wherein the **HIGH** (brittle, non-engineered systems) and **MODERATE** (with inadequate structural detailing) curves remain prevalent and exhibit concerning widening gaps from the **LOW** (ductile, engineering systems) curve over time. Together, these findings suggest that LDCs have not only remained disproportionately locked into high-vulnerability construction, but that the rate of built-up expansion has significantly outpaced current efforts to transition the built environment towards lower physical vulnerability levels.

Beyond the dominant material types and vulnerability levels, the more granular trends across both charts reveal important insights into the trajectory and composition of built-up growth in LDCs. In Figure 3b, the **LOW** vulnerability curve remains comparatively flat throughout the period, while both the **HIGH** and **MODERATE** vulnerability curves exhibit an accelerated growth phase before 2020, followed by a gradual deceleration towards 2030. Correspondingly,

[1] 1 hectare = 10,000 m^2

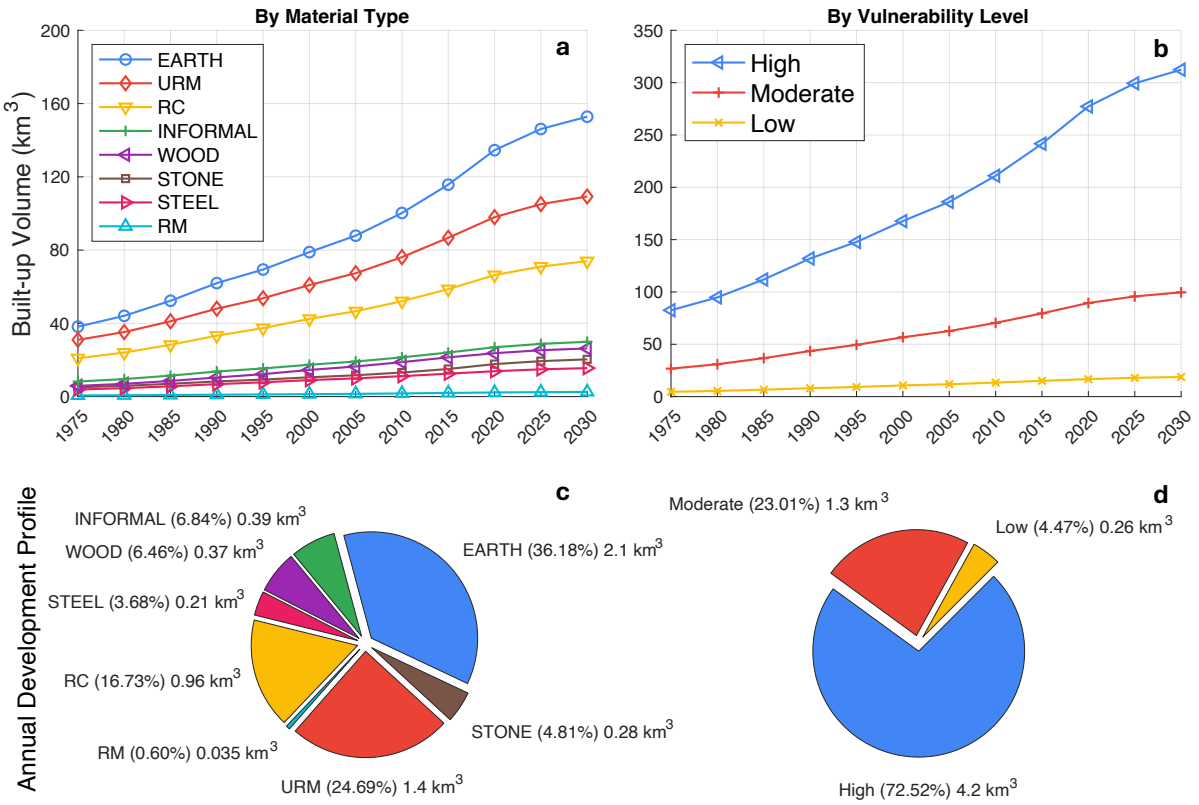

Fig. 3: Changes in built-up volume according to the inferred compositions by material type (**a**) and vulnerability level (**b**), with their respective annual development profiles (**c-d**) projected and averaged from the five-year intervals. These proportions were calculated from the total built-up volume from the Global Human Settlement Layer (GHS-BUILT-V R2023A) at five-year intervals from 1975 to 2030 (Pesaresi and Politis 2023).

Figure 3a shows that the remaining material types, namely **STONE** (stone masonry), **RM** (reinforced masonry), **STEEL** (steel structures), **WOOD** (timber structures), and **INFORMAL** (makeshift, non-engineered), contribute only marginally to overall built-up volume trends across LDCs, reinforcing the dominant role of **EARTH**, **URM**, and **RC** in shaping physical vulnerability.

Comparing the rates of change in built-up volume characterises the expected annual development profile by material type in Figure 3c and by vulnerability level in Figure 3d, revealing a highly concerning built-up growth towards higher vulnerability. On one hand, **EARTH**-made buildings lead at +2.1 km^3 per year, outpacing **URM** by 1.5×, **RC** by 2×, **STONE** by 7.5×, **WOOD** by 5.7×, **INFORMAL** by 5.4×, **STEEL** by 10×, and **RM** by 60×. Expressed as a share of the aforementioned simplified settlement block, this translates to approximately +36% (**EARTH**), +25% (**URM**), +17% (**RC**), +7% (**INFORMAL**), +6% (**WOOD**), +5% (**STONE**), +4% (**STEEL**), and +0.04% (**RM**) on average. Correspondingly, the annual development profile is expected to have **HIGH** accounting for +4.2 km^3 annually, compared to **MODERATE** at +1.3 km^3 (3.2x lower) and **LOW** at merely +0.26 km^3 (16.2x lower), which is roughly +73%, +23%, and +4%, respectively. These rates provide strong quantitative evidence that incremental reductions in physical vulnerability cannot be achieved through passive growth trajectories alone, and that targeted urban policies and community development plans are crucial to effective redirection and redistribution of built-up expansion towards vulnerability reduction targets.

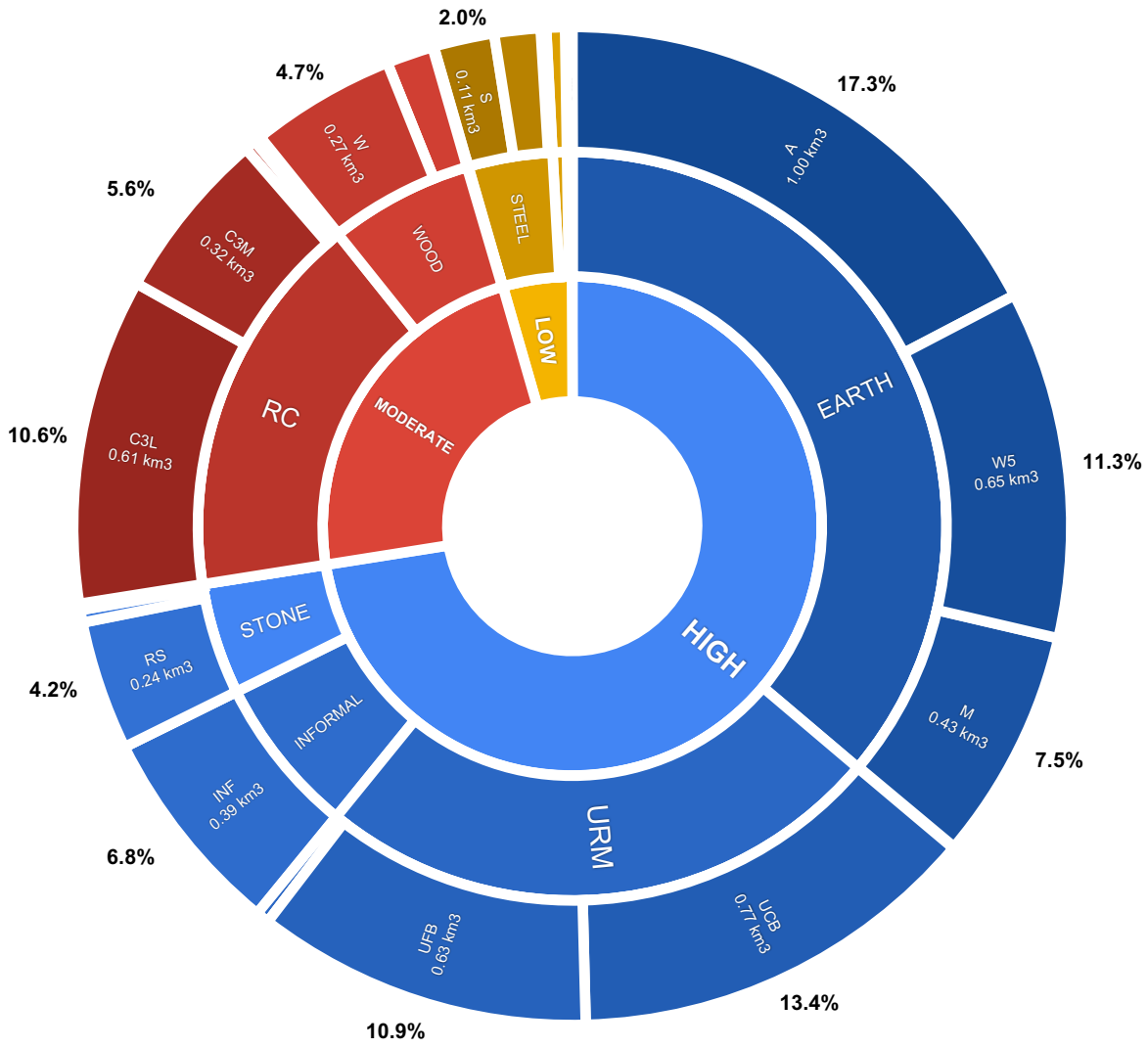

Fig. 4: Three-level composition of annual development profiles (in km^3 and %) across LDCs by vulnerability, material, and building typology.

We further investigated the trends in specific building typologies to identify particular construction materials and to understand the main drivers of the dominance of high-vulnerability built-up growth established in our previous analysis. In Figure 4, among **EARTH**-made buildings, **A** (adobe block walls), which exists in 33 of 47 LDCs, emerges as the single largest contributor, growing at +1 km^3 per year and accounting for +17.3% of the annual development profile across LDCs (i.e, 17.3% of +5.76 km^3 per year). This significant change is also equivalent to communicating that, in every hour, roughly three hectares of single-storey **A**-made settlements are added to the building stock across LDCs. This is followed by **UCB** (unreinforced concrete block masonry) in 39 LDCs at +13.4%, **W5** (wattle and daub) in 33 LDCs at +11.3%, and **UFB** (unreinforced fired brick masonry) in 33 LDCs at +10.9%. Critically, all four of these leading building typologies, under **EARTH** and **URM**, belong to the **HIGH** vulnerability level, collectively accounting for over half of the annual development profile. The remaining notable contribution comes from **C3L** at +10.6%, which manifests primarily in the **MODERATE** vulnerability curve, representing the only substantial share associated

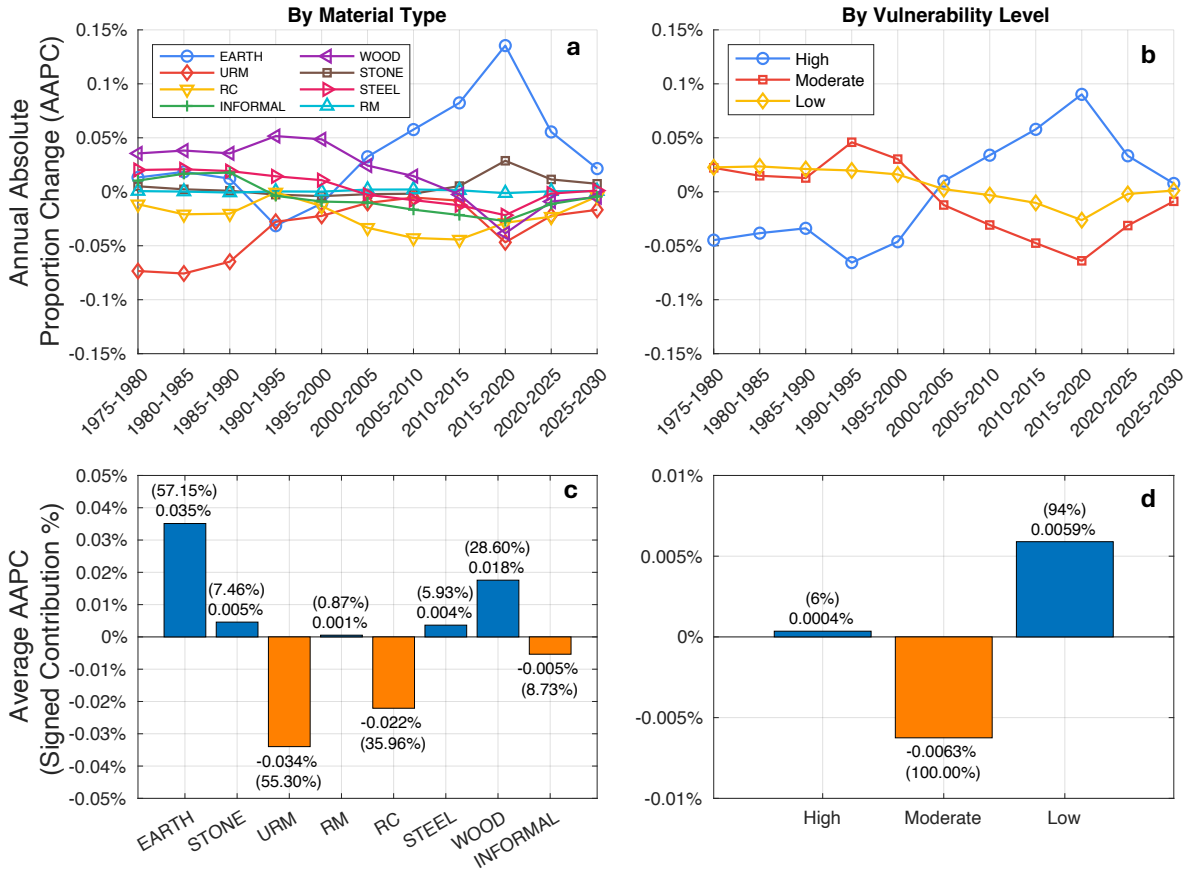

Fig. 5: Changes in absolute proportion change (AAPC) by material type (**a**) and vulnerability level (**b**) with corresponding charts on their averages and signed contributions (**c-d**).

with a lower risk level. Nevertheless, it is important to note that **RC** construction across LDCs remains predominantly non-ductile without proper structural detailing (Huyck et al. 2019). While a paradigm shift in building typology and construction practices would demand a difficult transformation of indigenous knowledge systems across LDCs, these findings highlight the importance of considering the existing dominant materials in designing targeted retrofit strategies.

4.1.2 Measuring the Gain & Loss of Pie Share by Absolute Proportion Change

Complementing the preceding analysis of absolute built-up volume, this section shifts focus to the compositional dynamics of the building stock, specifically, how the proportional share of each material type and vulnerability level has redistributed across LDCs over time. To capture this, we introduce the annual absolute proportion change (AAPC) metric, which quantifies the signed incremental shift in the pie share of a given material type or vulnerability level at each point in time. As shown in Figure 5a and Figure 5b, the AAPC trends reveal the direction and magnitude of these proportional changes over the observed period, while Figure 5c and Figure 5d provide the time-averaged AAPC values, enabling direct comparison of the relative pace of compositional change across material types and vulnerability levels. Consequently, these measures provide insights into the gradual, cumulative, and policy-driven redistribution of the collective vulnerability profile of the built environment across LDCs. Unlike absolute built-up volume metrics, which reflect the scale of growth, AAPC examines whether such gain or loss of pie share is gradually shifting the building stock towards or away from lower vulnerability

targets, offering a more holistic understanding to evaluate the effectiveness of building stock management efforts at both the country and global level.

The AAPC trends in Figure 5a and Figure 5b exhibit high temporal variability, with two particularly notable inflection points that reveal the underlying dynamics of compositional redistribution across material types and vulnerability levels. In the early period, the AAPC of **URM** under the **HIGH** vulnerability curve is markedly negative, indicating a declining proportional share driven by the concurrent expansion of other material types. Both figures then show a sharp peak in the **EARTH** and **HIGH** curves over the 2015–2020 period, reflecting the persistence of indigenous construction knowledge and practice. This is consistent with the accelerated growth phase previously identified in Figure 3a and Figure 3b, which is a period of rapid built-up expansion that produced significant shifts in the proportional composition of both material types and vulnerability levels.

The subsequent decline in AAPC after 2015–2020 in Figure 5a and Figure 5b is, however, partly a result of a methodological assumption inherent to the limitation of prior data in our probabilistic inference framework. The estimated temporal signature of the prior METEOR data is approximately 2019, representing the point of largest spatiotemporal alignment or overlap on the map. Beyond this horizon, projected urban development is extrapolated from learned patterns encoded in the graphical structure of the deep learning, combined with a uniform prior distribution across building typologies. Despite the neighbourhood-aware learning capability of our graph-based model, the *static* nature of the prior METEOR data is a key limitation in interpreting post-2019 trends, as the observed compositional behaviour after 2020 reflects both the gradual dampening of the accelerated growth phase and the transition from directly observed data to inferred projections or extrapolations. Nonetheless, these findings underscore a broader methodological challenge wherein, across LDCs, limited and often coarse-grained representation of prior data presents a unique regularisation trade-off between new information derived from multi-temporal exposure data and the constraints of a static prior knowledge system.

Moreover, the time-averaged AAPC values in Figure 5c and Figure 5d further substantiate the long-term direction of compositional redistribution, revealing a persistent shift towards higher-vulnerability material types at the expense of those associated with lower risk. When assessed across all 46 LDCs, these time-averaged AAPC values are expected to be small percentages of *annual absolute proportion change*, which considered the averaging effect over the 1975-2030 horizon and the aggregation effect across all LDCs.

By material type, Figure 5c shows that five categories exhibit a net annually expanding proportional share, namely **EARTH** (+0.035%), **WOOD** (+0.018%), **STONE** (+0.005%), **STEEL** (+0.004%), and **RM** (+0.001%), whereas **URM** (-0.034%), **RC** (-0.022%), and **INFORMAL** (-0.005%) register a net decline. The notably small time-averaged AAPC of **RM** at +0.001% reflects that, although its built-up volume grows by +0.035 km^3 per year and accounts for +0.60% of the annual development profile across LDCs (see Figure 3c), this share has seen only a marginal increment over the 55-year study period because **RM** is not present in many LDCs, as shown in Table 2. Another way to interpret these small percentages is through the example of **EARTH** (+0.035%) wherein its proportional share expands from +33.56% in 1975 to +35.48% in 2030, resulting in a total proportion increase of +1.93% over the 55-year period (i.e., 55 x 0.035%/year = +1.93 in 55 years). Assuming a unit hectare of single-storey settlement of any material type, this +1.93% corresponds to a redistribution where 193 m^2 shifts toward **EARTH**-made construction. The following subsection 4.2 examines these small percentages in each country to illustrate the regions with significant proportional changes.

Nevertheless, analysing their signed contributions, either across LDCs or in each LDC, also explains how the compositions of each material type and vulnerability level are shifting. For example, the **EARTH** and **WOOD** alone account for +57% and +29% of the total positive

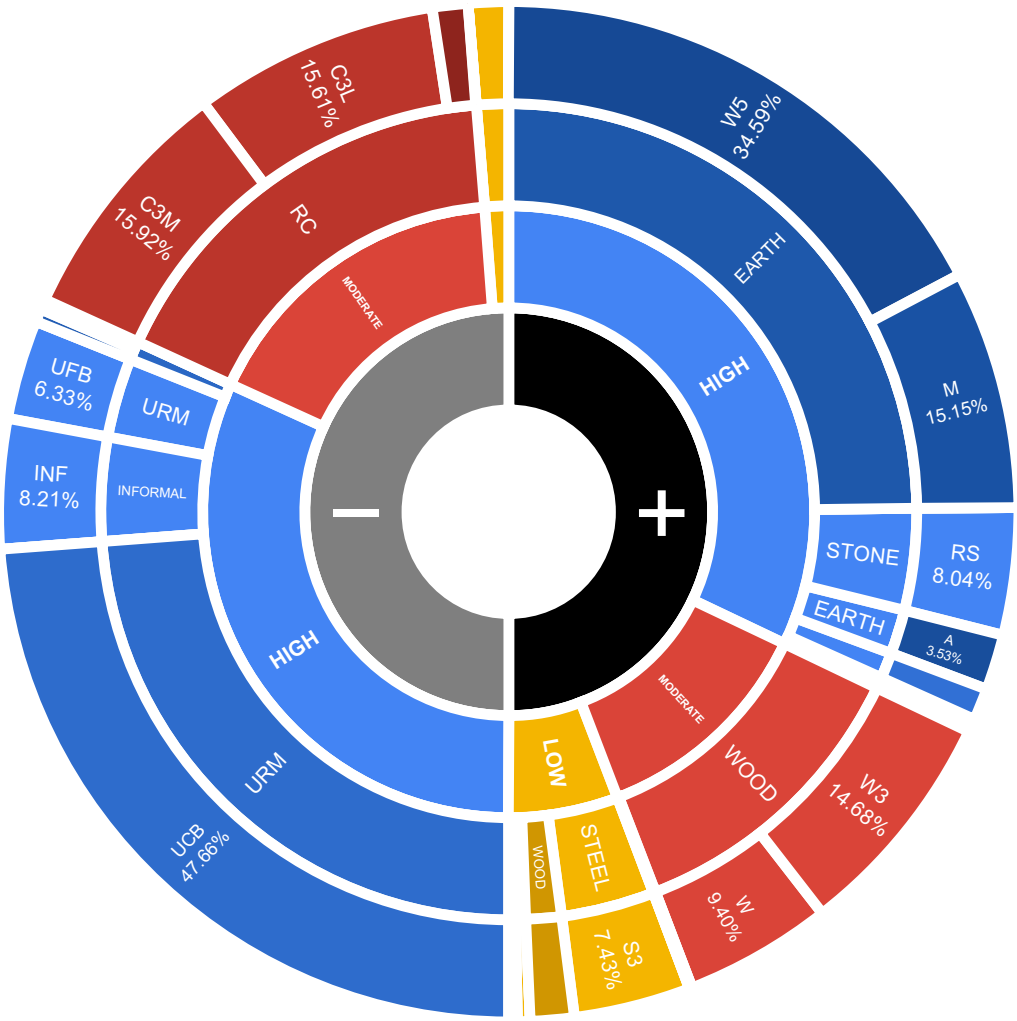

Fig. 6: Three-level composition of average annual absolute proportion change (Average AAPC) (in %) across LDCs by signed contribution, vulnerability, material, and building typology. This particular sunburst illustration has an overall 200% size with 100% assigned to each signed contribution to visualise the interactions of gain and loss of pie share.

proportional shift, respectively, while **URM** and **RC** absorb -55% and -36% of the total negative shift. Critically, since these values represent a zero-sum redistribution rather than net gain, the declining share of **URM** and **RC** does not imply a reduction in vulnerability; it is rather offset by the expanding dominance of **EARTH**. At the vulnerability level, Figure 5d shows that 94% and 6% of the positive distributional shift in **MODERATE** is sourced from **HIGH** and **LOW**, respectively. This is consistent with the widening **HIGH–LOW** and **MODERATE–LOW** gaps previously identified in Figure 3b. Overall, these compositional trends indicate that the collective efforts of LDCs have thus far achieved only marginal progress in reducing the dominance of **HIGH**-vulnerability construction.

Zooming into the specific building typologies driving the bidirectional proportional shift in Figure 6 further clarifies where compositional redistribution is occurring and where the most

critical policy gaps remain across vulnerability levels. Within the **HIGH** vulnerability level, **W5** (wattle and daub) at +34.59% in 28 of 47 LDCs, **M** (mud walls) at +15.15% in 23 LDCs, and **RS** (rubble stone masonry) at +8.04% in 21 LDCs register the largest positive proportional gain. However, this is substantially outpaced by the negative shifts of **UCB** (unreinforced concrete block masonry) at -47.66%, in 39 LDCs and **UFB** (unreinforced fired brick masonry) at -6.33% in 33 LDCs. While the declining shares of **UCB** and **UFB** reflect a recognisable collective effort to reduce the most prevalent high-vulnerability typologies, the continued positive gain of **W5**, **M**, and **RS** signals that these typologies now require prioritised and targeted policy intervention to sustain and accelerate the overall reduction in **HIGH** vulnerability level proportion.

At the **MODERATE** vulnerability level, similar findings show select typologies indicating both optimistic structural transitions and areas requiring renewed policy attention. The positive proportional gain of **W3** (unbraced light wood frame) at +14.68% in 5 LDCs and **W** (wood) at +9.4% in 28 LDCs provides a basis for targeted policies for further vulnerability reduction efforts within the **MODERATE** level. Notably, the declining proportional share of non-ductile reinforced concrete **RC** typologies, specifically **C3L** (low-rise) and **C3M** (mid-rise), alongside the positive shift of **S3** (steel light frame) towards **LOW** vulnerability, provides a spatiotemporally derived quantitative evidence that LDCs are aligning with the global trend of prohibiting non-ductile RC systems in building codes due to their inherent poor resistance under earthquake and typhoon loading, and expanding the adoption of steel-based structural systems (ICBO 1979). Overall, these typology-level findings offer the most granular evidence yet of where LDCs are making measurable compositional progress and where deliberate policy redirection, particularly towards **W5**, **W**, **M**, **RS**, and **W3**, and the continued phase-out of non-ductile systems, remains crucial to achieving a sustained reduction of physical vulnerability.

4.1.3 Evaluating the Growth & Shrink of Pie Share by Relative Proportion Change

Building on the absolute proportional shifts examined previously, this section elevates the analysis to the dynamics of redistribution itself, introducing the annual relative proportion change (ARPC) metric to capture how fast each material type and vulnerability level is gaining (growth) or losing (shrink) its pie share *relative to its own preceding measurement*. As shown in Figure 7a and Figure 7b, the ARPC trends broadly corroborate the AAPC insights from Figure 5 wherein **WOOD** and **STEEL** exhibit a noticeable positive ARPC prior to 2000, before being overtaken by **STONE** and **EARTH**, which both peak over the 2015–2020 period. Indeed, this temporal pattern reflects the rural-to-urban transition, wherein development radiating outward from capital cities tends to adopt predominant local materials such as **EARTH**, while densifying areas within and around urban centres continue to urbanise in constrained and limited spaces with material types of lower vulnerability levels. Therefore, the AAPC and ARPC consistently support that the compositional redistribution in LDCs has shifted towards **EARTH**-dominant, high-vulnerability construction in continually expanding patterns of human settlements over the past five decades.

Examining the time-averaged ARPC values in Figure 7c reveals an important distinction in the relative pace of growth and shrinkage that are not explicitly described by absolute magnitude alone. The relative proportional share of **EARTH**-, **STONE**-, **RM**-, and **STEEL**-made buildings has grown at comparable rates, yet that of **WOOD**-made buildings has expanded threefold, with its proportional share growing at an average of +0.32% per year, peaking at approximately +0.8%to +0.9% during the 1990–2000 period across 33 LDCs. This disproportionate growth in **WOOD**-made buildings, namely **W** (mostly present in all LDCs), **W1**, **W2**, and **W3**, supports the relative affordability, versatility, and lower construction workload of wood compared to other material types, over the 1975–2010 period. Particularly, **WOOD**-made buildings, such as palm wood and other salvaged forms, become the main rural housing typology in Haiti due to the widespread deforestation (IOM 2020). Conversely, **URM**, **RC**, and **INFORMAL**

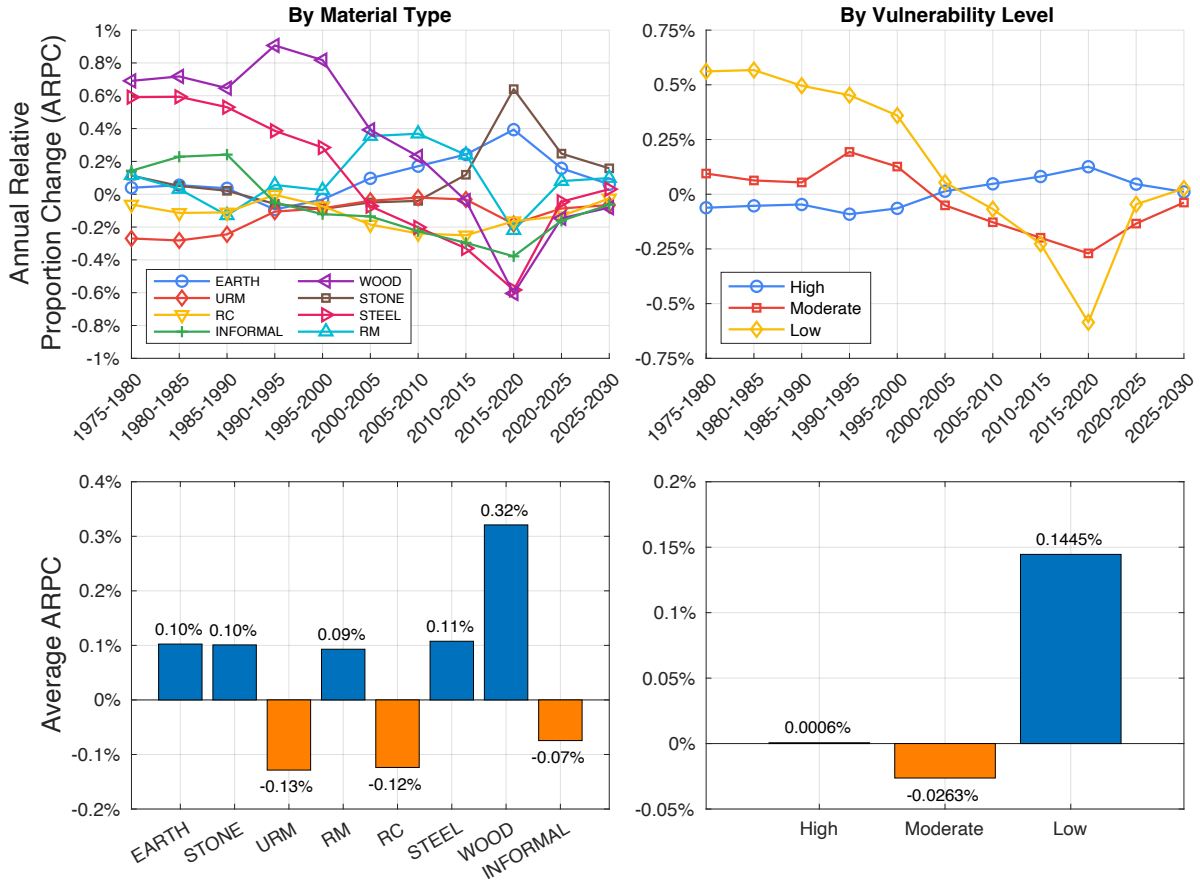

Fig. 7: Changes in built-up volume by material type (**a**) and vulnerability level (**b**) with corresponding charts on mean annual proportion changes (**c-d**) and their rates (**e-f**).

exhibit comparable negative ARPC values, suggesting a similar pace of net shrink from the overall building stock composition. These relative growth and shrinkage differences highlight that even material types with insignificant absolute shares can influence the trajectory of compositional redistribution of the physical vulnerability across LDCs, particularly when the rates of proportional change are sustained over multi-decadal horizons.

Over the past five decades, Figure 7d shows that LDCs have collectively registered a net positive ARPC at +0.1445% in the **LOW** vulnerability level, indicating that the relative annual rate of proportional change has been aligned with vulnerability reduction efforts. The interpretation of ARPC at +0.1445% is also equivalent to communicating that the absolute proportion of **LOW** vulnerability level at 4.04% in 1975 is expected to increase to 4.37% in 2030 (i.e., $4.04\% \times (1+0.1435/100)^{(2030-1975)} = 4.37\%$. In contrast, the **MODERATE** vulnerability level records substantially smaller with a net negative ARPC value, underscoring that the pace of transition away from higher-vulnerability construction remains inadequate. However, these averaged rates are sensitive to high temporal variability, as shown in Figure 7a and Figure 7b, illustrating that trajectories of compositional redistribution are neither fixed nor deterministic. Beyond 2030, whether LDCs sustain and boost the net positive ARPC signal of the **LOW** level will crucially depend on the proactive and prospective design of national building code regulations and urban development policies moving forward.

4.2 Cross-Country Variation in Redistribution Change Rate

This section shifts the lens from aggregate global trends to cross-country variation, examining how the rate of compositional redistribution in physical vulnerability differs across individual

LDCs and what these differences reveal about the collective trajectory towards vulnerability reduction over the past five decades. Figure 8 and Figure 9 provide a comparative breakdown of the underlying dynamics of material type and vulnerability level change rates across individual LDC members, providing quantified evidence to support the design of large-scale, targeted incentive mechanisms for top-to-bottom policy solutions. While high temporal variability across LDCs has been established in the preceding analyses, this section extends that discussion by understanding the spatial dimension of cross-country differences, specifically, how clusters of LDCs are moving towards adequate vulnerability reduction trajectories with respect to their inherently unique development patterns. These country-level dynamics are particularly significant for scientific and policy discourse on regional cooperation because of the shared and transboundary nature of climate and disaster risks at the regional scale, thereby justifying both the motivation and the opportunity for coordinated and cross-border management of physical risks. The continent-level grouping and country profiles of all LDCs are presented as supplementary information in Section A and Section B, respectively. In the following subsections, we contextualise the discussion into five major patterns of redistribution dynamics in terms of varying neighbouring development patterns, landlocked geographies, small island developing states, the African continent, and challenging post-disaster contexts.

4.2.1 Redistribution Dynamics in Varying Development Patterns

Among African LDCs, three geographically adjacent countries, namely Sudan (**SDN**), Somalia (**SOM**), and Ethiopia (**ETH**), illustrate how contrasting urbanisation patterns can produce strikingly divergent compositional redistribution trajectories even within the same regional neighbourhood. The relative proportional share of **EARTH**-made buildings in Somalia and Ethiopia expands at the highest positive ARPC of +0.71% and +0.64%, respectively, while that of **RC** declines at an ARPC of -0.37% and -0.43%, consistent with dispersed and fragmented rural population growth of Somali inter-riverine communities (Osman and Abebe 2023) and Ethiopian pastoralist groups (Woube 1995) where internal migration, affordability constraints, recurring conflicts, and environmental depletion sustain dependence on **EARTH**-made construction. Sudan presents the inverse trajectory in which the relative proportional share of **EARTH**-made buildings marginally contracts at an ARPC of -0.05%, while that of **RC** expands substantially at an ARPC of +0.97%, reflecting a high-city, space-limited concentration of more formal construction activity, particularly along the Nile river system (Ranganathan et al. 2011).

These divergences among material types are also consistent with our results for the vulnerability level. The relative proportional share of **HIGH** vulnerability in Somalia and Ethiopia grows at an ARPC of +0.064% and +0.605%, respectively, while that of **MODERATE** declines at an ARPC of -0.219% and -0.320%, with no building typology present at the **LOW** level, whereas, in Sudan, the relative proportional share of **HIGH** contracts at an ARPC of -0.068% while that of **MODERATE** expands at an ARPC of +0.527%. These findings demonstrate that geographic proximity does not necessarily imply homogeneous vulnerability trajectories, but the degree of urban concentration versus rural dispersion is a key factor in determining whether the compositional redistribution of a country's building stock moves towards or away from lower physical vulnerability.

A contrasting but equally insightful redistribution dynamics emerges among three neighbouring Asian LDCs, namely Cambodia (**KHM**), Myanmar (**MMR**), and Laos (**LAO**), wherein all three register a net shrinking relative proportional share of **HIGH** vulnerability, yet through different compositional trajectories. Cambodia leads the group with the largest contraction in the relative proportional share of **URM**, declining at an ARPC of -0.14%, while the relative proportional shares of **EARTH**, **WOOD**, and **INFORMAL** expand at ARPCs of +0.06%, +0.09%, and +0.11%, respectively, alongside a notable contraction in that of non-ductile **RC** at an ARPC of -0.36%, reflecting clustered rural and village-scale development

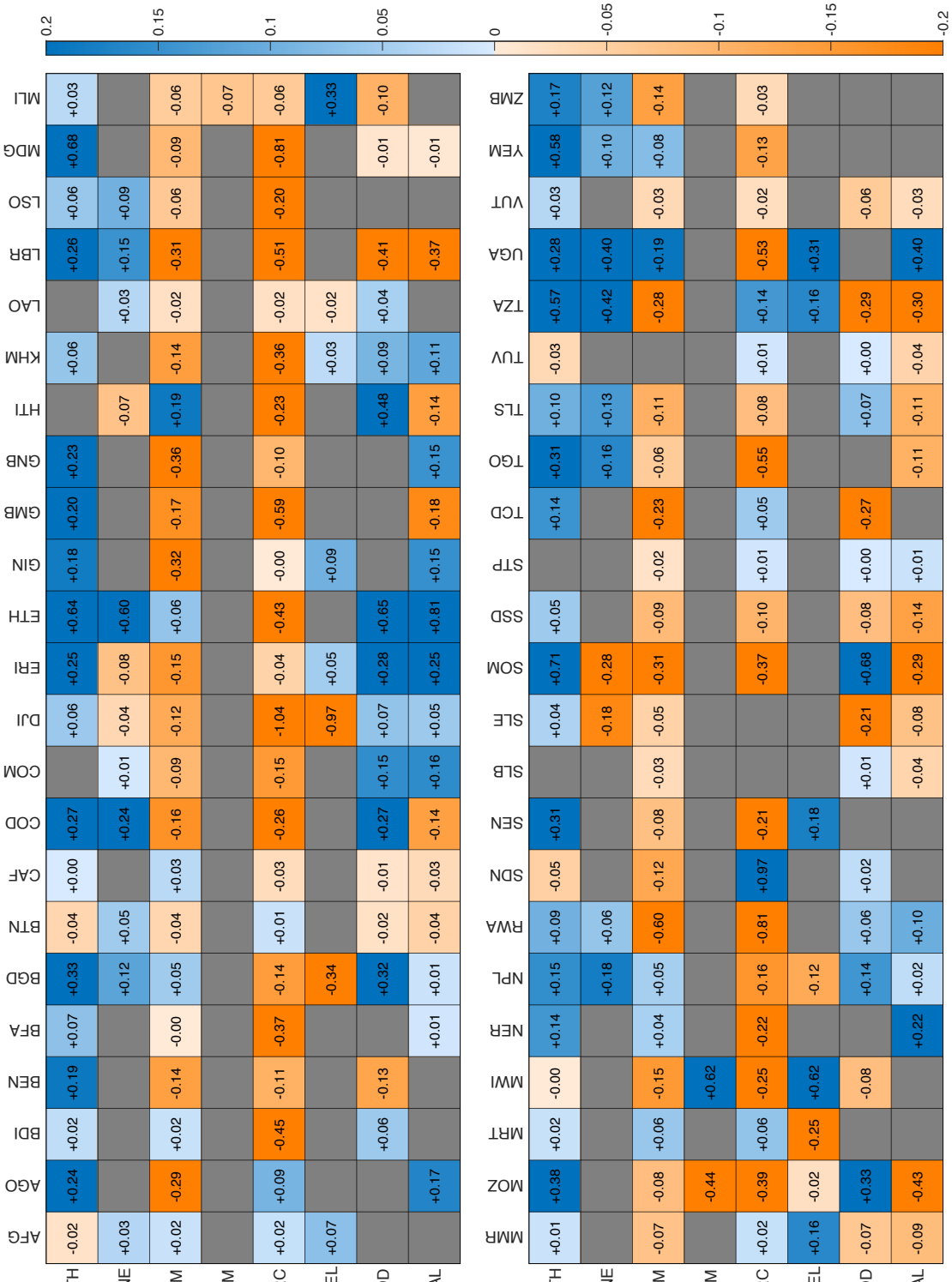

Fig. 8: Annual relative proportion change (ARPC) of LDCs by material type.

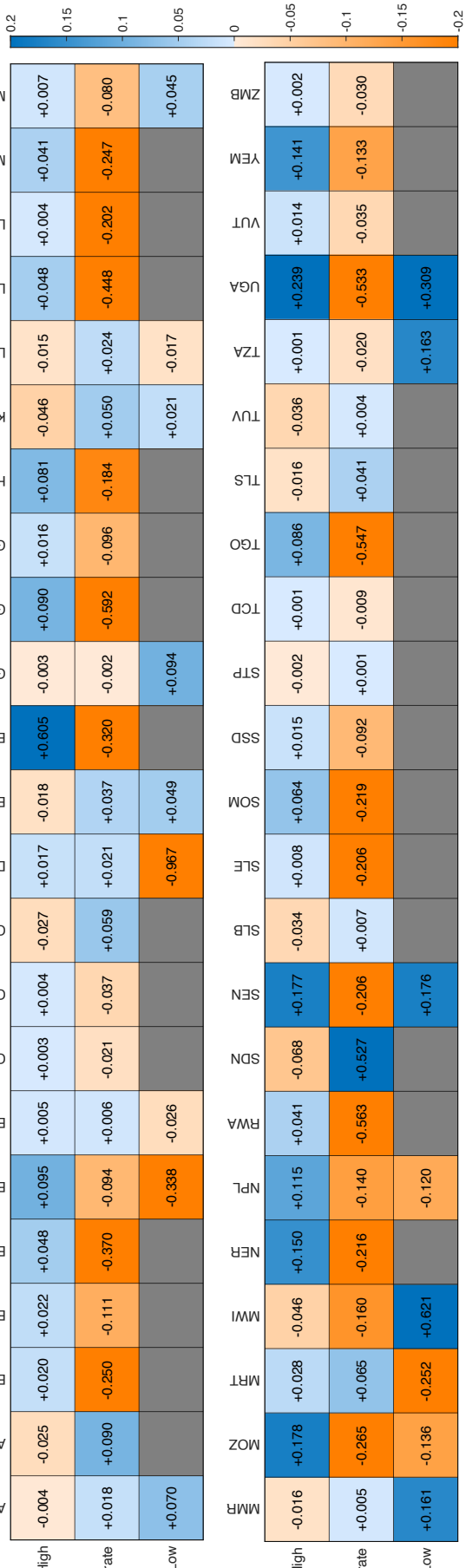

Fig. 9: Annual relative proportion change (ARPC) of LDCs by vulnerability level.

(Fox 2002) favouring traditional and informal materials. Myanmar presents a different pathway, where the relative proportional shares of **INFORMAL** and **WOOD** contract at ARPCs of -0.09% and -0.07%, while those of **STEEL** and **RC** expand at ARPCs of +0.16% and +0.02%, consistent with rapid urbanisation near economic centres of Yangon, Mandalay, and Nay Pyi Taw (Myint et al. 2023). Laos, in turn, registers an expanding relative proportional share of **WOOD** at an ARPC of +0.04%, while those of **RC** and **STEEL** contract at an ARPC of -0.02%, reflecting dispersed rural development constrained by its landlocked geography and limited habitable land (Li et al. 2023). Despite their divergent material trajectories, the shared net contraction in the relative proportional share of **HIGH** vulnerability across all three countries suggests that meaningful progress in compositional redistribution is achievable through multiple development pathways, provided that the dominant urbanisation pattern of each country, whether concentrated, clustered, or dispersed, is explicitly accounted for in policy design for vulnerability and risk reduction.

The six African and Asian LDCs examined, namely Sudan, Somalia, Ethiopia, Cambodia, Myanmar, and Laos, collectively exemplify how the spatial characteristics of urbanisation fundamentally shape the direction and pace of compositional redistribution in physical vulnerability. Shifting the relative proportional share of a country's building stock towards lower vulnerability levels is not a straightforward process, but is deeply conditioned by existing development patterns, geographic constraints, socioeconomic capacity, and the institutional strength to enforce building regulations, all of which considerably vary even among geographically adjacent countries. Our results offer a comparable spatiotemporal quantification of these shared and divergent settlement behaviours over the past five decades, capturing the degree of urban concentration, clustering, and dispersion as a primary differentiating element in how the relative compositional redistribution of physical vulnerability changes at the country level. These findings present a direct implication for regional policy design, suggesting that effective interventions must be calibrated to the country-specific urbanisation patterns.

4.2.2 Redistribution Dynamics in Landlocked Geographies

Traditionally, most human settlements evolve near rivers and water bodies where access to transportation, commerce, trade, and livelihood is available. However, landlocked geographies impose a fundamental constraint on urbanisation patterns where limited access to transportation and trade networks for specific material types influences the compositional redistribution of their physical vulnerability (Faye et al. 2004). As shown in Figure 8, the majority of landlocked LDCs, namely Afghanistan (**AFG**), Burundi (**BDI**), Burkina Faso (**BFA**), Bhutan (**BTN**), the Central African Republic (**CAF**), Ethiopia (**ETH**), Laos (**LAO**), Lesotho (**LSO**), Niger (**NER**), Nepal (**NPL**), Rwanda (**RWA**), South Sudan (**SSD**), Chad (**TCD**), Uganda (**UGA**), and Zambia (**ZMB**), register a growing relative proportional share of **EARTH**-, **STONE**-, and **WOOD**-made buildings, reflecting a dependence on locally sourced construction materials driven by constrained supply chains for **RC** and **STEEL**. Malawi (**MWI**) stands as a notable exception wherein its proximity to Lake Malawi provides meaningful economic and trade leverage (De Weerdt et al. 2023), enabling access to industrial construction materials and registering a growth rate in the relative proportional share of **RC**-made buildings at an ARPC of +0.62%. These material-level patterns are consistent with Figure 9, where most landlocked LDCs record a net positive ARPC at the **HIGH** vulnerability level, with the exception of Afghanistan and Laos, which show movement towards **MODERATE**, and Malawi, which trends towards **LOW**, primarily driven by accelerating **RM** development, despite **EARTH**-made buildings remaining prevalent. These findings suggest that access to construction materials is not merely an economic consideration but a primary factor for how the relative proportional share of physical vulnerability is distributed across landlocked LDCs.

Beyond the material composition itself, these patterns of regional dynamics and redistribution highlight the broader and more systemic challenge wherein the geographical location serves simultaneously as a resource constraint and an element of physical vulnerability, compounding the resulting risk of landlocked LDCs. While income levels, urbanisation rates, and conflicts introduce additional complexity (Faye et al. 2004), our results show that landlocked LDCs consistently exhibit a compositional redistribution away from industrial construction materials towards locally sourced alternatives, alongside higher levels of informal construction. This pattern indicates that both affordability and accessibility of construction materials are crucial in shaping vulnerability outcomes. Despite having access alone, the financial burden of trade costs in supply chains remains a significant barrier to delivering essential construction materials at scale, such as in Kigali, Rwanda (Bah et al. 2018). Therefore, geographical location raises an important concern for equitable global risk governance, wherein landlocked LDCs face a compounded disadvantage amplified by accessibility and affordability constraints, suggesting that targeted policy instruments should explicitly account for these inequities between landlocked and non-landlocked countries in vulnerability and risk reduction efforts.

4.2.3 Redistribution Dynamics in Small Island Developing States

Alongside landlocked geographies, the remoteness and limited size of Small Island Developing States (SIDS) introduce a distinct set of constraints on building stock composition and its redistribution dynamics, shaped by restricted resource access, water insecurity, acute exposure to sea level rise and storms, limited infrastructure, and small population and economic bases (Scandurra et al. 2018; Gheuens et al. 2019; Vousdoukas et al. 2023). Among the LDC-classified SIDS examined, namely Comoros (**COM**) and São Tomé and Príncipe (**STP**) from Africa, Timor-Leste (**TLS**) from Asia, Solomon Islands (**SLB**), Tuvalu (**TUV**), and Vanuatu (**VUT**) from the Pacific, and Haiti (**HTI**) from the Caribbean, the changes in relative proportional share of physical vulnerability are predominantly driven by locally sourced materials such as **WOOD**, **INFORMAL**, **STONE**, and **EARTH**. As shown in Figure 8, all these SIDS register an increasing relative proportional share of **MODERATE** vulnerability, while the declining relative proportional share of **URM** corresponds to a net negative ARPC at the **HIGH** level. Figure 9 further shows that Tuvalu records the largest contraction in the relative proportional share of **HIGH** vulnerability at an ARPC of -0.036%, driven primarily by a shift towards **RC** at an ARPC of +0.01% and contractions in **EARTH** and **INFORMAL** at ARPCs of -0.03% and -0.04%, respectively. This is followed by Solomon Islands at -0.034%, Comoros at -0.027%, Timor-Leste at -0.06%, and São Tomé and Príncipe at -0.002%, primarily attributed to respective contractions in the relative proportional share of **URM** at ARPCs of -0.03%, -0.09%, -0.11%, and -0.02%, alongside expansions in the relative proportional share of **WOOD** at ARPCs of +0.01%, +0.15%, +0.07%, and +0.001%, respectively. Vanuatu presents a notable exception, where the relative proportional share of **HIGH** vulnerability grows instead, driven by an expanding share of **EARTH**, a locally sourced material that has greater physical vulnerability than **WOOD**.

Across all these SIDS, redistribution dynamics are confined to movement between **HIGH** and **MODERATE** vulnerability levels, with no observable shift towards **LOW**, reflecting both the limited access to construction materials necessary for **STEEL** structures, heavy **WOOD** members, and **RM** or reinforced masonry. The absence of **LOW**-level redistribution across these SIDS reveals a distinct two-mode dynamic that sets them apart from other LDC contexts, highlighting important implications for how vulnerability and risk are assessed and governed in small island settings. Unlike other LDCs, where redistribution spans all three vulnerability levels, the limited characteristics of building stock composition of these SIDS can also partly be attributed to the low data availability in many SIDS (Hambleton and Jeyaseelan 2024). Hence, this limitation is an important area for future extension, particularly in specifying prior

knowledge for model training and inference, as well as in the tiling and splitting of a country dataset into training, testing, and validation sets.

Nonetheless, this pattern, alongside the previously established constraints of landlocked geographies and varying development patterns, underscores that remoteness and size present a uniquely compounding challenge in vulnerability and risk reduction efforts. These findings point to an important methodological and policy concern wherein quantitative or qualitative regional risk assessments that group developing economies into a single comparative basket are not straightforward, and must explicitly account for the inequities and resource constraints in SIDS, as also emphasised in the midterm review of the SFDRR (UNDRR 2023).

4.2.4 Redistribution Dynamics in African Continent

In the southern and eastern regions of African LDCs, the redistribution dynamics of physical vulnerability exhibit a heterogeneous and polarised pattern, wherein diverging development trajectories coexist even among geographically neighbouring countries. Tanzania (**TZA**) and Eritrea (**ERI**) both register expanding relative proportional shares of **STEEL** at ARPCs of +0.16% and +0.05%, respectively, alongside notable contractions in the relative proportional share of **URM** at ARPCs of -0.28% and -0.15%, reflecting a collective movement towards lower vulnerability levels. Angola (**AGO**) exhibits a similar trajectory, with the relative proportional share of **RC** expanding at an ARPC of +0.09%, positively reinforced by a contraction in the relative proportional share of **URM** at an ARPC of -0.16%. Conversely, the Democratic Republic of Congo (**COD**), Mozambique (**MOZ**), Madagascar (**MDG**), and Djibouti (**DJI**) register expanding relative proportional shares of **EARTH** at ARPCs of +0.27%, +0.38%, +0.68%, and +0.06%, respectively, with corresponding contractions in both **URM** and non-ductile **RC** at ARPCs of (-0.16%, -0.26%), (-0.08%, -0.39%), (-0.09%, -0.81%), and (-0.12%, -1.04%), resulting in an opposite movement towards higher vulnerability levels. This divergence indicates unequal development patterns across neighbouring countries in the southern and eastern African group, wherein the coexistence of formal and locally sourced construction materials produces a polarised profile of regional vulnerability.

In contrast, the western African LDCs, namely Senegal (**SEN**), Guinea (**GIN**), Mali (**MLI**), Guinea-Bissau (**GNB**), Benin (**BEN**), Sierra Leone (**SLE**), Liberia (**LBR**), Togo (**TGO**), the Gambia (**GMB**), display a more uniform and homogeneous redistribution pattern, but are equally concerning because of its consistent trajectory towards higher vulnerability levels. Across this group, the relative proportional share of **EARTH** consistently expands while those of **URM** and **RM** contract, with limited growth in more formal construction materials, indicating a collective shift towards locally sourced and higher-vulnerability materials. Among them, Guinea, Guinea-Bissau, and Liberia register the largest contractions in the relative proportional share of **URM** at ARPCs of -0.32%, -0.36%, and -0.31%, while Liberia, Togo, and the Gambia record the largest contractions in non-ductile **RC** at ARPCs of -0.51%, -0.55%, and -0.59%. Despite the expanding relative proportional shares of **EARTH** in Senegal, Guinea-Bissau, Liberia, and the Gambia at ARPCs of +0.31%, +0.18%, +0.26%, and +0.20%, an interesting expansion in the relative proportional share of **STEEL**-made buildings is observed in Senegal, Guinea, and Mali at ARPCs of +0.18%, +0.09%, and +0.33%, respectively, reflecting localised efforts towards lower vulnerability levels in many dense village towns. The uniformity of these patterns across the western group suggests a networked or shared development dynamic, wherein vulnerability and risk continue to accumulate despite incremental material improvements, in stark contrast to the polarised heterogeneity observed in the southern and eastern group.

Collectively, the redistribution dynamics across both African groups reveal that the concentration of low economies within a single continent, combined with strong neighbourhood effects, compounds the challenges of vulnerability and risk reduction. The two groups present fundamentally different development profiles: the western group exhibits a more uniform,

collectively drifting pattern, whereas the southern and eastern groups display a more polarised and diverging one. Consistent with the recently conducted large-scale risk assessment on the spatial distribution of annualised earthquake-induced economic loss and damaged buildings (Paul and Silva 2025), these differences do not only reflect the inherent capabilities and development disparities across the African continent, but also carry direct implications for the design of regional cooperation strategies, wherein interconnectedness of geographically neighbouring economies plays a key role.

4.2.5 Redistribution Dynamics in Challenging Post-Disaster Contexts

The occurrence and intensity of disasters can also shape the development patterns across LDCs and their associated redistribution dynamics. While the majority of LDCs register a net decline in relative proportional share of **URM** (unreinforced masonry), a subset of countries presents a contrasting and concerning trajectory wherein post-disaster contexts have not translated into a meaningful reduction in **URM** construction, adding to the accumulation of regional vulnerability over the past five decades. Haiti (**HTI**), (**UGA**), Yemen (**YEM**), Ethiopia (**ETH**), Mauritania (**MRT**), Nepal (**NPL**), Bangladesh (**BGD**), Niger (**NER**), the Central African Republic (**CAF**), Burundi (**BDI**), and Afghanistan (**AFG**) all register net positive ARPCs in the relative proportional share of **URM** at +0.19%, +0.19%, +0.08%, +0.06%, +0.06%, +0.05%, +0.05%, +0.04%, +0.03%, +0.02%, and +0.02%, respectively. It is important to note that these findings modelled that all **URM** are considered similar across these countries, following the prior assumption from the METEOR project (Huyck et al. 2019).

These figures are notable given the documented disasters of each country: Haiti experienced two large earthquakes in 2010 and 2021 (Miyamoto et al. 2024), yet increased awareness for enhanced construction quality may have been spatially concentrated near and around the impacted area of Port-au-Prince only (Miyamoto et al. 2024); Uganda experienced widespread **URM** destruction in the 2016 M-5.9 earthquake (Alaneme and Okotete 2018; Mulibo 2019); Yemen suffered comparable losses following the 1982 Mw-5.2 earthquake (Ambraseys and Melville 1983); Ethiopia documented cracks in many masonry houses from the 1979 M-4.1, 1983 M-5.1, and 1989 M-5.8 earthquakes (Getu 2020); Mauritania and Niger were severely affected by the 2022 flooding (IFRC 2024, 2022); Bangladesh with over 563,877 houses destroyed from 2007 Cyclone Sidr (Mukhopadhyay and Chandra Dutta 2012); Nepal from the 2015 Mw 7.8 Gorkha earthquake, in which unreinforced masonry accounted for the majority of building damage (Brando et al. 2015), yet traditional housing practice continues to sustain an expanding relative proportional share (Vibhāga 2012); the Central African Republic from recurrent seasonal flooding (Runge and Nguimalet 2005; Nguimalet et al. 2025); Burundi from floods and landslides (Nkunzimana et al. 2019); and Afghanistan from the 2022 M-6.2 earthquake (Sonda et al. 2026). Across all these cases, the persistent and even growing relative proportional share of **URM** following repeated disaster events reveals that disaster occurrence alone is insufficient to reshape construction practice towards lower vulnerability typologies in low-income economies where affordability constraints and weak institutional enforcement remain a serious systemic inertia and policy bottleneck to transformation (Oliver-Smith 1991). These findings also show the importance of calibrating the ARPC at the country level, as well as localised ARPCs, in identifying whether vulnerability reduction efforts are spatially equitable, given that substantial exposure extends beyond the perimeters of post-disaster zones.

5 Conclusion

This study addressed the critical challenge of measuring and tracking the physical vulnerability of built environments across LDCs, with a particular focus on how the composition of building stock has redistributed across vulnerability levels over the past five decades. By leveraging

probabilistic data-driven modelling with multi-temporal remote sensing data, this study also quantified the distributional pie and its pace and direction, providing contextualised insights into regional dynamics and redistribution with respect to varying development patterns and other distinct geographical constraints, such as landlockedness and remoteness, across LDCs. Our main findings and policy-relevant recommendations comprehensively support and extend our informed understanding of the evolution of physical vulnerability over the past five decades.

- Across LDCs, the pace of built-up expansion has significantly outpaced current efforts to transition the built environment toward lower physical vulnerability levels, necessitating a more proactive regional approach to vulnerability reduction rather than relying on incremental changes from passive urban growth trajectories.
- The ”distributional pie” analysis through annualised metrics (AAPC & APRC) consistently supports that the compositional redistribution in LDCs has shifted towards locally sourced materials for earthen construction, which are of high vulnerability, recommending prioritised and targeted context-sensitive policy enforcements and interventions to accelerate shifting particular building typologies towards lower physical vulnerability and risk, despite the increasing exposure from rural and urban growth.
- The reported high temporal variability in APRC supports the importance of sustained regional efforts in influencing the trajectory of compositional redistribution of physical vulnerability across LDCs, underscoring the long-term effect of proactive, prospective, and contextualised designs of national building code regulation as a shared, cooperative, and socio-economically differentiated responsibility, rather than an isolated national policy obligation.
- The cross-country variation analysis reveals how various development patterns in neighbouring, landlocked, and island LDCs, including the localised effect of post-disaster settings, motivate an opportunity for coordinated and cross-border management of physical vulnerability and risks due to its inherently shared and transboundary nature at the regional scale.

This research provided an initial and substantive step towards catalysing opportunities to develop auditing capabilities and evidence-based tools for tracking progress against international frameworks, towards and beyond 2030. The insights revealed on the scale, pace, and contextualised challenges to an equitable global risk governance clearly present an indispensable basis for scientific and policy discourse for shaping inclusive and difference-sensitive regional cooperation strategies and risk-informed sustainable development plans across LDCs, while directly accounting for the shared and transboundary nature of risks and the inherently dynamic nature of physical vulnerability.

6 Data and Code Availability

Two parts of spatiotemporal data are publicly available at https://doi.org/10.5281/zenodo.16608380 (Dimasaka et al. 2025c) and https://doi.org/10.5281/zenodo.16695059 (Dimasaka et al. 2025d). The code is also accessible at https://github.com/riskaudit/GraphVSSM (Dimasaka 2025).

Acknowledgments

This work is funded by the UKRI Centre for Doctoral Training in Application of Artificial Intelligence to the study of Environmental Risks (AI4ER) (EP/S022961/1). We are thankful to Charles Huyck for sharing technical details of the METEOR products and Dr. Robert Muir-Wood for his valuable advice on spatiotemporal disaster risk quantification auditing.

References

Adger WN (2006) Vulnerability. Global environmental change 16(3):268–281

Alaneme KK, Okotete EA (2018) Critical evaluation of seismic activities in africa and curtailment policies–a review. Geoenvironmental Disasters 5(1):24

Ambraseys NN, Melville C (1983) Seismicity of yemen. Nature 303(5915):321–323

Bah EhM, Faye I, Geh ZF (2018) The construction cost conundrum in africa. In: Housing market dynamics in Africa. Springer, p 159–214

Blair P, Buytaert W (2016) Socio-hydrological modelling: a review asking "why, what and how?". Hydrology and Earth System Sciences 20(1):443–478

Brando G, Rapone D, Spacone E, et al (2015) Reconnaissance report on the 2015 gorkha earthquake effects in nepal. XVI Convegno Anidis

Brien K, Eriksen S, Schjolden A, et al (2004) What's in a word? conflicting interpretations of vulnerability in climate change research. Climate Policy 7

Briguglio L (1995) Small island developing states and their economic vulnerabilities. World Development 23(9):1615–1632

Brown CF, Kazmierski MR, Pasquarella VJ, et al (2025) Alphaearth foundations: An embedding field model for accurate and efficient global mapping from sparse label data. arXiv preprint arXiv:250722291

Calderon A, Silva V (2022) Forecasting seismic risk within the context of the sendai framework: An application to the dominican republic. Int J Disaster Risk Reduct 82:103364

Martin del Campo F, Singh SJ, Fishman T, et al (2023) The bahamas at risk: Material stocks, sea-level rise, and the implications for development. Journal of Industrial Ecology 27(4):1165–1183

Cao Z, Shen L, Zhong S, et al (2018) A probabilistic dynamic material flow analysis model for chinese urban housing stock. Journal of Industrial Ecology 22(2):377–391

Cardona OD, Carreño ML (2011) Updating the indicators of disaster risk and risk management for the americas. IDRiM Journal 1(1):27–47

Chmutina K, Von Meding J, Sandoval V, et al (2021) What we measure matters: The case of the missing development data in sendai framework for disaster risk reduction monitoring. International Journal of Disaster Risk Science 12(6):779–789

Closset M, Feindouno S, Guillaumont P, et al (2017) A Physical Vulnerability to Climate Change Index: Which are the most vulnerable developing countries? URL https://hal.science/hal-01719925, ferdi Working paper P213

De Weerdt J, Pienaar L, Hami E, et al (2023) Leveraging Urbanization for Inclusive Development in Malawi. Tech. rep., International Food Policy Research Institute

Deng T, Zhang Y, Fu C (2023) Modelling dynamic interactions between material flow and stock: A review of dynamic material flow analysis. Ecological Indicators 156:111098

Dimasaka J (2025) Graph Variational State-Space Model for Probabilistic Spatiotemporal Inference of Dynamic Exposure and Vulnerability for Regional Disaster Resilience Assessment. URL github.com/riskaudit/GraphVSSM

Dimasaka J, Geiß C, So E (2024) Global mapping of exposure and physical vulnerability dynamics in least developed countries using remote sensing and machine learning. URL https://arxiv.org/abs/2404.01748, arXiv:2404.01748

Dimasaka J, Geiß C, Muir-Wood R, et al (2025a) Graphcsvae: Graph categorical structured variational autoencoder for spatiotemporal auditing of physical vulnerability towards sustainable post-disaster risk reduction. arXiv preprint arXiv:250910308

Dimasaka J, Geiß C, So E (2025b) Deepc4: Deep conditional census-constrained clustering for large-scale multitask spatial disaggregation of urban morphology. URL https://arxiv.org/abs/2507.22554, arXiv:2507.22554

Dimasaka J, Geiß C, So E (2025c) METEOR 2.5D: An Open Geospatial Dataset of Spatiotemporal Evolution of Physical Vulnerability in UN-recognized Least Developed Countries (as of 2020) at Five-year Intervals, 1975-2030 (Part 1 of 2) . https://doi.org/10.5281/zenodo.16608380, URL https://doi.org/10.5281/zenodo.16608380

Dimasaka J, Geiß C, So E (2025d) METEOR 2.5D: An Open Geospatial Dataset of Spatiotemporal Evolution of Physical Vulnerability in UN-recognized Least Developed Countries (as of 2020) at Five-year Intervals, 1975-2030 (Part 2 of 2) . https://doi.org/10.5281/zenodo.16695059, URL https://doi.org/10.5281/zenodo.16695059

Dimasaka J, Geiß C, So E (2026) Graphvssm: Graph variational state-space model for probabilistic spatiotemporal inference of dynamic exposure and vulnerability for regional disaster resilience assessment. Proceedings of the AAAI Conference on Artificial Intelligence 40(45):38376–38384. https://doi.org/10.1609/aaai.v40i45.41178, URL https://ojs.aaai.org/index.php/AAAI/article/view/41178

Faye ML, McArthur JW, Sachs JD, et al (2004) The challenges facing landlocked developing countries. Journal of Human Development 5(1):31–68

Feindouno S, Guillaumont P, Simonet C (2020) The physical vulnerability to climate change index: An index to be used for international policy. Ecological Economics 176:106752

Feng Z, Atzberger C, Jaffer S, et al (2025) Tessera: Temporal embeddings of surface spectra for earth representation and analysis. arXiv preprint arXiv:250620380

Fox J (2002) Understanding a dynamic landscape: Land use, land cover, and resource tenure in northeastern cambodia. In: Linking People, Place, and Policy: A GIScience Approach. Springer, p 113–130

Füssel HM (2010) How inequitable is the global distribution of responsibility, capability, and vulnerability to climate change: A comprehensive indicator-based assessment. Global environmental change 20(4):597–611

Gallardo C, Sandberg NH, Brattebø H (2014) Dynamic-mfa examination of chilean housing stock: long-term changes and earthquake damage. Building Research & Information 42(3):343–358

Geißa C, Pelizaria P, Taubenböcka H (2025) Seismic exposure and risk assessment. Data-Driven Earth Observation for Disaster Management: From Theory to Practical Applications p 15

Getu SB (2020) The disaster profile of Ethiopia. Tech. rep., University of Oviedo, Department of MedicineUnit for Research in Emergency and Disaster

Gheuens J, Nagabhatla N, Perera EDP (2019) Disaster-risk, water security challenges and strategies in small island developing states (sids). Water 11(4):637

Glazer T, Hacheme GQ, Zaytar A, et al (2025) TEMPO: Global Temporal Building Density and Height Estimation from Satellite Imagery. arXiv preprint arXiv:251112104

Gontia P, Thuvander L, Wallbaum H (2020) Spatiotemporal characteristics of residential material stocks and flows in urban, commuter, and rural settlements. Journal of Cleaner Production 251:119435

Hagenlocher M, Meza I, Anderson CC, et al (2019) Drought vulnerability and risk assessments: state of the art, persistent gaps, and research agenda. Environmental Research Letters 14(8):083002

Hambleton IR, Jeyaseelan S (2024) The silent barrier: exploring data availability in small island developing states. Revista Panamericana de Salud Pública 48:e80

Huyck C, Hu Z, Amyx P, et al (2019) METEOR: exposure data classification, metadata population and confidence assessment. Report M3. 2/P. Technical Report M3. 2/P, British Geological Survey

ICBO (1979) Uniform Building Code. Tech. rep., International Conference of Building Official, available at https://digitalassets.lib.berkeley.edu/ubc/UBC_1979.pdf

IFRC (2022) Floods in Niger in 2022 - Needs and responses - Situation as of 31 December 2022. Tech. rep., UN Office for the Coordination of Humanitarian Affairs, available at https://reliefweb.int/report/niger/les-inondations-au-niger-en-2022-besoins-et-reponses-situation-au-31-decembre-2022

IFRC (2024) Mauritania: Floods - DREF Operation - Final Report No. MDRMR014. Tech. rep., International Federation of Red Cross

IOM (2020) Shelter Projects - Haiti: 16 Case Studies. Tech. rep., Global Shelter Cluster

Jang E, Gu S, Poole B (2016) Categorical reparameterization with gumbel-softmax. arXiv:161101144

Johnson K, Mortensen S, Gueguen-Teil C, et al (2022) Displaced by climate and disaster-induced relocations: experiences of cascading displacement in fiji and the philippines. Disasters 46(2):499–525

Kappes MS, Papathoma-Köhle M, Keiler M (2012) Assessing physical vulnerability for multi-hazards using an indicator-based methodology. Applied Geography 32(2):577–590

Kingma DP, Mohamed S, Jimenez Rezende D, et al (2014) Semi-supervised learning with deep generative models. Adv Neural Inf Process Syst 27

Kipf TN, Welling M (2016) Semi-supervised classification with graph convolutional networks. arXiv:160902907

Kuruppu N, Willie R (2015) Barriers to reducing climate enhanced disaster risks in least developed country-small islands through anticipatory adaptation. Weather and Climate Extremes 7:72–83

Lallemant D (2015) Modeling the future disaster risk of cities to envision paths towards their future resilience. Stanford University

Lanau M, Liu G, Kral U, et al (2019) Taking stock of built environment stock studies: Progress and prospects. Environmental science & technology 53(15):8499–8515

Li S, Liang Y, Deng X, et al (2023) Exploring the spatial heterogeneity of rural development in laos based on rural building spatial database. Land 12(11):2008

Mao T, Liu Y, Chen WQ, et al (2022) Quantifying spatiotemporal dynamics of urban building and material metabolism by combining a random forest model and gis-based material flow analysis. Frontiers in Earth Science 10:944865

Marconcini M, Metz-Marconcini A, Esch T, et al (2021) Understanding current trends in global urbanisation-the world settlement footprint suite. GI_Forum 9(1):33–38

Marin F, Vernaccini L, Poljansek K, et al (2017) INFORM Index for Risk Management: Concept and Methodology, Version 2017. Tech. rep., Joint Research Centre (JRC), European Commission

Martins L, Silva V (2023) Global Vulnerability Model of the GEM Foundation. https://doi.org/10.5281/zenodo.8391743

Miyamoto HK, Sechi GJ, Victor G, et al (2024) Haiti earthquake 2021: findings from the repair and damage assessment of 179,800 buildings. Int J Disaster Risk Reduct 107:104402

Miyan MA (2015) Droughts in asian least developed countries: Vulnerability and sustainability. Weather and climate extremes 7:8–23

Muir-Wood R (2012) The use of catastrophe loss modelling methodologies to design and monitor disaster resilience goals and indicators in a post-mdg framework. Washington, DC: RMS

Muir-Wood R (2017) Sendai Framework's targets based on too little data: RMS. Interview by ReinsuranceNews URL https://www.reinsurancene.ws/sendai-frameworks-targets-based-on-too-little-data-rms

Mukhopadhyay P, Chandra Dutta S (2012) Strongest cyclone of the new millennium in the bay of bengal: strategy of rvs for nonengineered structures. Natural hazards review 13(2):97–105

Mulibo GD (2019) Investigation of macroseismic intensity of the mw5. 9 september 10, 2016 kagera earthquake: implications for site effect amplification. Journal of African Earth Sciences 159:103568

Müller DB (2006) Stock dynamics for forecasting material flows—case study for housing in the netherlands. Ecological economics 59(1):142–156

Myint ZN, May Y, Kraas F (2023) Sustainable urban development for myanmar. Journal of Myanmar Academy of Arts and Science 21(5):42–47

Nguimalet CR, Ayissou LS, Mebourou EK, et al (2025) Rising peak and flooding of the ubangi river in 2019 at bangui, central african republic. Hydrological Sciences Journal 70(5):695–716

Nie Y, Mao T, Liu Y, et al (2025) A satellite-driven model for monitoring urban material metabolism, embodied emissions, and carbonation. Environmental Science & Technology 59(46):24816–24829

Nkunzimana A, Bi S, Jiang T, et al (2019) Spatiotemporal variation of rainfall and occurrence of extreme events over burundi during 1960 to 2010. Arabian Journal of Geosciences 12(5):176

Oliver-Smith A (1991) Successes and failures in post-disaster resettlement. Disasters 15(1):12–23

Osman AA, Abebe GK (2023) Rural displacement and its implications on livelihoods and food insecurity: the case of inter-riverine communities in somalia. Agriculture 13(7):1444

Papathoma M, Dominey-Howes D (2003) Tsunami vulnerability assessment and its implications for coastal hazard analysis and disaster management planning, gulf of corinth, greece. NHESS 3(6):733–747

Papathoma-Köhle M, Neuhäuser B, Ratzinger K, et al (2007) Elements at risk as a framework for assessing the vulnerability of communities to landslides. NHESS 7(6):765–779

Paprotny D, 't Hart CMP, Morales-Nápoles O (2025a) Evolution of flood protection levels and flood vulnerability in europe since 1950 estimated with vine-copula models. Natural Hazards 121(5):6155–6184

Paprotny D, et al (2025b) Attribution of flood impacts shows strong benefits of adaptation in europe since 1950. Science Advances 11(33):eadt7068

Patt AG, Tadross M, Nussbaumer P, et al (2010) Estimating least-developed countries' vulnerability to climate-related extreme events over the next 50 years. Proceedings of the National Academy of Sciences 107(4):1333–1337

Paul N, Silva V (2025) Probabilistic seismic risk assessment of africa. Int J Disaster Risk Reduct 119:105303

Paul N, Silva V, Amo-Oduro D (2022) Development of a uniform exposure model for the african continent for use in disaster risk assessment. Int J Disaster Risk Reduct 71:102823

Pauline Dube O, Sivakumar M (2015) Global environmental change and vulnerability of least developed countries to extreme events: Editorial on the special issue. Weather and Climate Extremes 7:2–7

Pelizari PA, Geiß C, Taubenböck H (2026) Bottom-up building exposure modeling with multimodal earth vision. ISPRS Journal of Photogrammetry and Remote Sensing 231:357–375

Pesaresi M, Politis P (2023) GHS-BUILT-V R2023A - GHS built-up volume grids derived from joint assessment of Sentinel2, Landsat, and global DEM data, multitemporal (1975-2030. Tech. rep.

Pesaresi M, et al (2024a) Advances on the global human settlement layer by joint assessment of earth observation and population survey data. International Journal of Digital Earth 17(1):2390454

Pesaresi M, et al (2024b) Operational procedure for multi-temporal assessment of built-up surfaces and volumes in the Global Human Settlement Layer R2023A. Publications Office of the European Union, https://doi.org/doi/10.2760/664949

Pittore M, Wieland M, Fleming K (2017) Perspectives on global dynamic exposure modelling for geo-risk assessment. Natural Hazards 86(Suppl 1):7–30

Pittore M, Haas M, Silva V (2020) Variable resolution probabilistic modeling of residential exposure and vulnerability for risk applications. Earthq Spectra 36(1_suppl):321–344

Porter K, Hu Z, Huyck C, et al (2014) User guide: Field sampling strategies for estimating building inventories. GEM Foundation

Ranganathan R, Briceno-Garmendia CM, Ranganathan R (2011) Sudan's infrastructure: A continental perspective. World Bank

Riahi K, Van Vuuren DP, Kriegler E, et al (2017) The shared socioeconomic pathways and their energy, land use, and greenhouse gas emissions implications: An overview. Global environmental change 42:153–168

de Ruiter MC, van Loon AF (2022) The challenges of dynamic vulnerability and how to assess it. IScience 25(8)

Runge J, Nguimalet CR (2005) Physiogeographic features of the oubangui catchment and environmental trends reflected in discharge and floods at bangui 1911–1999, central african republic. Geomorphology 70(3-4):311–324

Salgado-Gálvez MA, Ramalingam NR, Jalayer F, et al (2026) Exposure modelling. In: Probabilistic Tsunami Hazard and Risk Analysis: A Cookbook. Springer, p 265–305

Sapountzaki K (2005) Coping with seismic vulnerability: small manufacturing firms in western athens. Disasters 29(2):195–212

Sapountzaki K (2012) Vulnerability management by means of resilience. Natural Hazards 60(3):1267–1285

Scandurra G, Romano A, Ronghi M, et al (2018) On the vulnerability of small island developing states: A dynamic analysis. Ecological Indicators 84:382–392

Schorlemmer D, Beutin T, Cotton F, et al (2020) Global dynamic exposure and the openbuildingmap-a big-data and crowd-sourcing approach to exposure modeling. In: EGU Gen. Assem. Conf. Abstr., p 18920

Schorlemmer D, Oostwegel L, Calliku D, et al (2026) Every building on earth–the global dynamic exposure model. Research Square Preprint

Silva Bustos NA (2001) Vulnerabilidad sìsmica estructural en viviendas sociales, y evaluaciòn preliminar de riesgo sìsmico en la regiòn metropolitana. Tech. rep., Universidad de Chile

Sirko W, Kashubin S, Ritter M, et al (2021) Continental-scale building detection from high resolution satellite imagery. arXiv preprint arXiv:210712283 URL: https://beta.source.coop/repositories/cholmes/google-open-buildings/description/. Accessed: 2024-07-30

Sonda D, Miyamoto HK, Kast S, et al (2026) Traditional masonry performance in the 2022 afghanistan earthquake. In: Saloustros S, Beyer K (eds) Structural Analysis of Historical Constructions. Springer Nature Switzerland, Cham, pp 1424–1435

Stevens FR, Gaughan AE, Linard C, et al (2015) Disaggregating census data for population mapping using random forests with remotely-sensed and ancillary data. PloS one 10(2):e0107042

Symmes R, Fishman T, Telesford JN, et al (2020) The weight of islands: Leveraging grenada's material stocks to adapt to climate change. Journal of Industrial Ecology 24(2):369–382

Tanikawa H, Managi S, Lwin CM (2014) Estimates of lost material stock of buildings and roads due to the great east japan earthquake and tsunami. Journal of Industrial Ecology 18(3):421–431

Tatem AJ (2017) Worldpop, open data for spatial demography. Scientific data 4(1):1–4

Tilloy A, Malamud BD, Winter H, et al (2019) A review of quantification methodologies for multi-hazard interrelationships. Earth-Science Reviews 196:102881

Turvey R (2007) Vulnerability assessment of developing countries: the case of small-island developing states. Development Policy Review 25(2):243–264

UN (2016) Report of the open-ended intergovernmental expert working group on indicators and terminology relating to disaster risk reduction. A/71/644. Tech. rep.

UN (2023) Report of the Fifth United Nations Conference on Least Developed Countries. Tech. rep., available at https://www.un.org/ldc5/sites/www.un.org.ldc5/files/ldc5_report-en.pdf

UN IAEG-DRS (2026) The Global Disaster-Related Statistics Framework (G-DRSF). Tech. rep., UN Inter-Agency Expert Group on Disaster-related Statistics

UN-OHRLLS (2022) Doha Programme of Action for the Least Developed Countries for the Decade 2022-2031. Tech. rep., United Nations Office of the High Representative for the Least Developed Countries, Landlocked Developing Countries and Small Island Developing States, Geneva

UN Population Division (2011) Special Buleetin on the Population Dynamics in Least Developed Countries, May 2011. Tech. rep., available at https://www.unfpa.org/sites/default/files/pub-pdf/LDC_Fact_Sheet.pdf

UN Trade and Development (2024) Least Developed Countries. URL https://unctad.org/sites/default/files/inline-images/2024-12-13_ldc-map.png

UNDRR (2023) Summary of the High-Level Meeting of the United Nations General Assembly on the Midterm Review of the implementation of the Sendai Framework for Disaster Risk Reduction 2015–2030. sendaiframework-mtr.undrr.org/media/88350, accessed: 2023-07-01

UNDRR (2025a) Global Assessment Report on Disaster Risk Reduction 2025: Resilience Pays: Financing and Investing for our Future. Tech. rep., United Nations Office for Disaster Risk

Reduction, Geneva

UNDRR (2025b) UNDRR Strategic Framework 2026-2030. Tech. rep., United Nations Office for Disaster Risk Reduction, Geneva

UNICEF (2023) Analysis of the CCRI for Least Developed Countries. Tech. rep., UNICEF Climate, Environment, Energy and Disaster Risk Reduction (CEED)

Vibhāga NKT (2012) National Population and Housing Census 2011: National report, vol 1. Government of Nepal, National Planning Commission Secretariat, Central . . .

Visser H, De Bruin S, Martens A, et al (2020) What users of global risk indicators should know. Global Environmental Change 62:102068

van der Voet E, Kleijn R, van Oers L, et al (1995) Substance flows through the economy and environment of a region. Environmental Science and Pollution Research 2(2):89–89

Vousdoukas MI, Athanasiou P, Giardino A, et al (2023) Small island developing states under threat by rising seas even in a 1.5 c warming world. Nature sustainability 6(12):1552–1564

Wiedenhofer D, Fishman T, Lauk C, et al (2019) Integrating material stock dynamics into economy-wide material flow accounting: concepts, modelling, and global application for 1900–2050. Ecological economics 156:121–133

Winson A, Jordan C, Garcia-Bajo M, et al (2020) METEOR: methods for analysing multi-hazards with exposure. Report M6. 2/P. Tech. rep., British Geological Survey

Woube M (1995) Southward-northward resettlement in ethiopia. Northeast African Studies 2(1):85–106

Yepes-Estrada C, Calderon A, Costa C, et al (2023) Global building exposure model for earthquake risk assessment. Earthq Spectra 39(4):2212–2235

A Annual Development Profile by Continent, Country, and Vulnerability

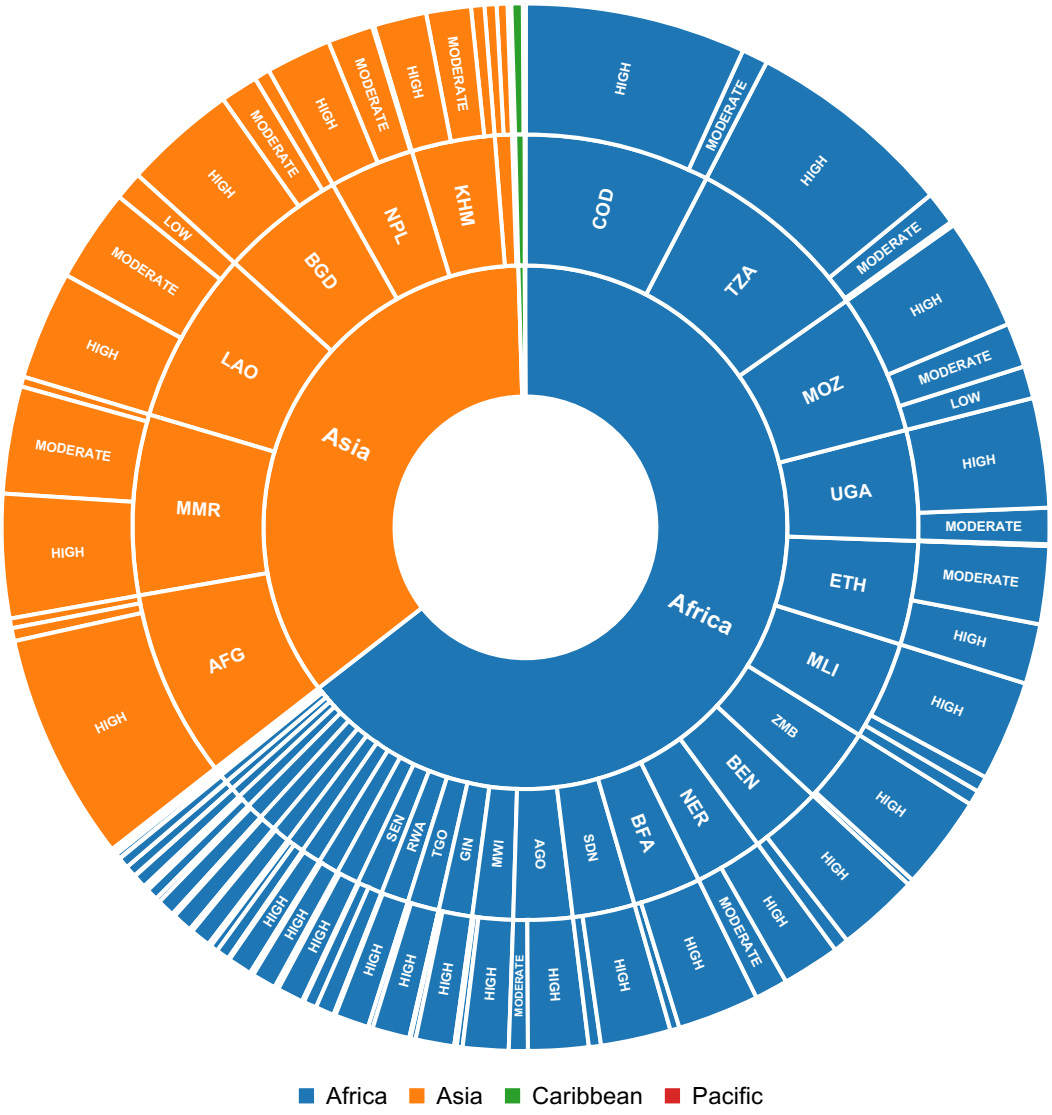

Fig. A.1: Three-level composition of annual development profiles across LDCs by continent, country, and vulnerability level.

B Country-Specific Physical Vulnerability Profiles

B.1 AFG: Kabul, Afghanistan

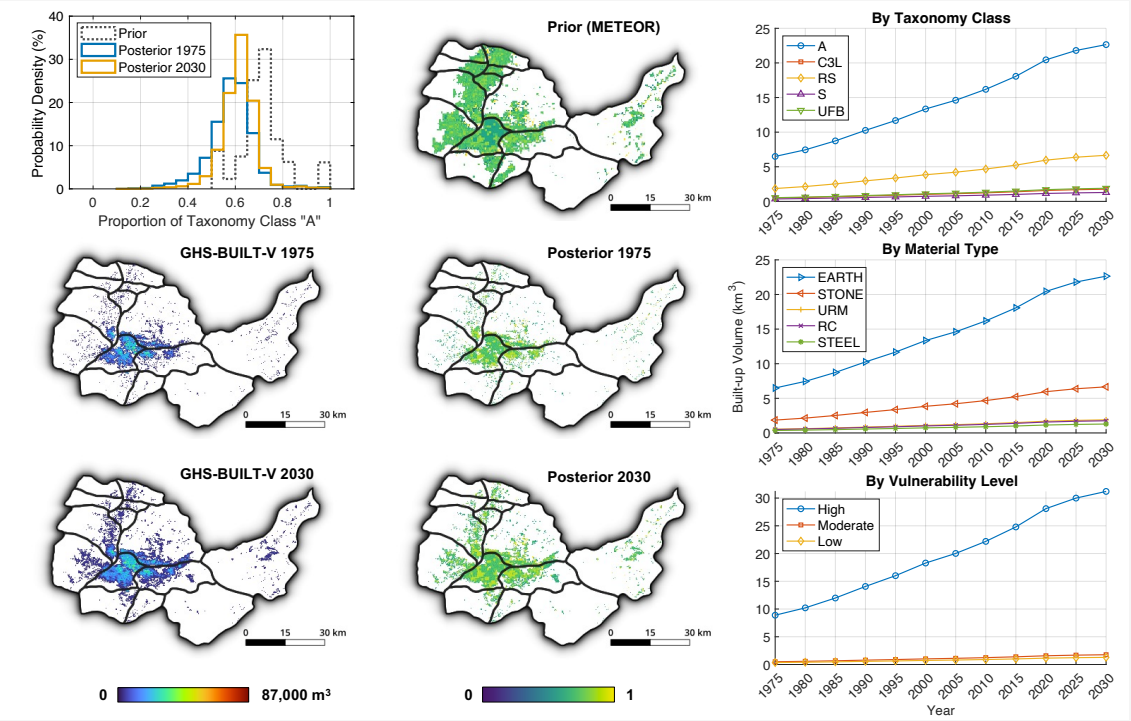

B.2 AGO: Luanda, Angola

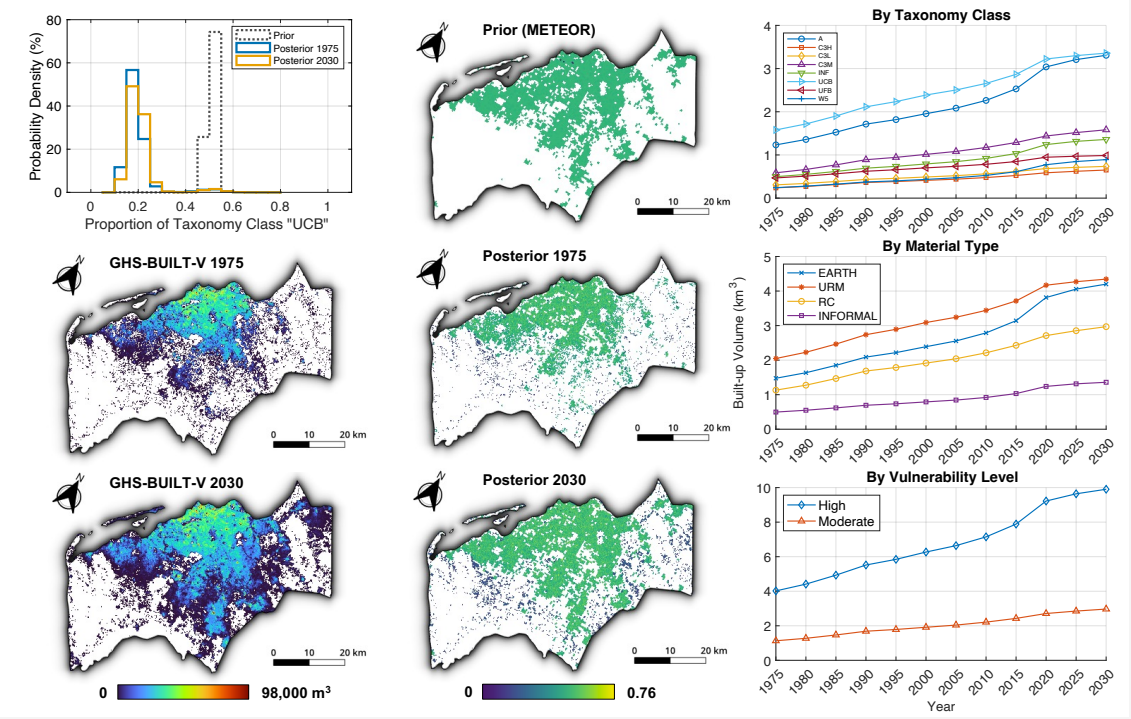

B.3 BDI: Bujumbura Mairie, Burundi

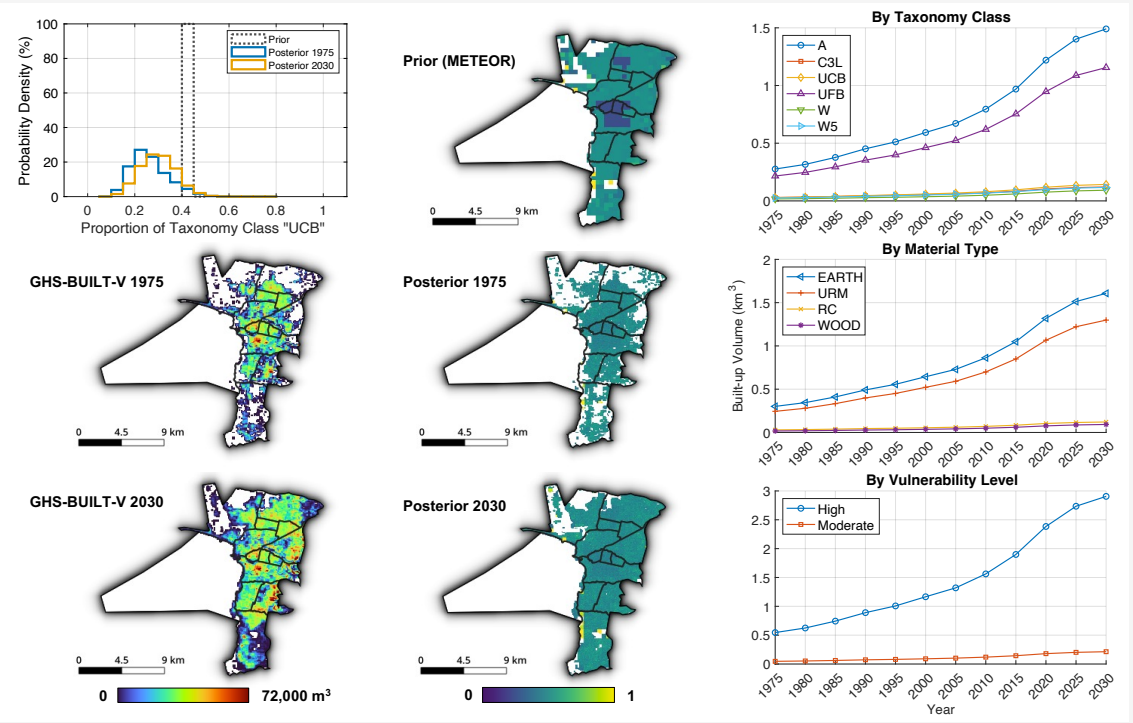

B.4 BEN: Ouémé, Benin

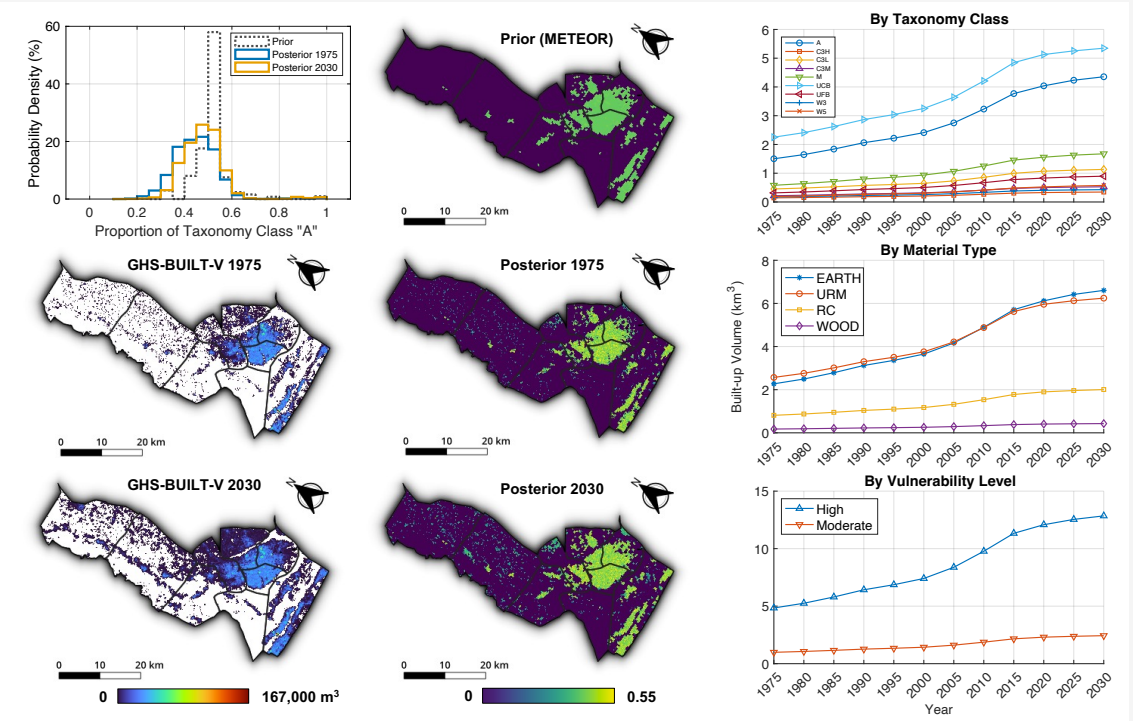

B.5 BFA: Centre Region, Burkina Faso

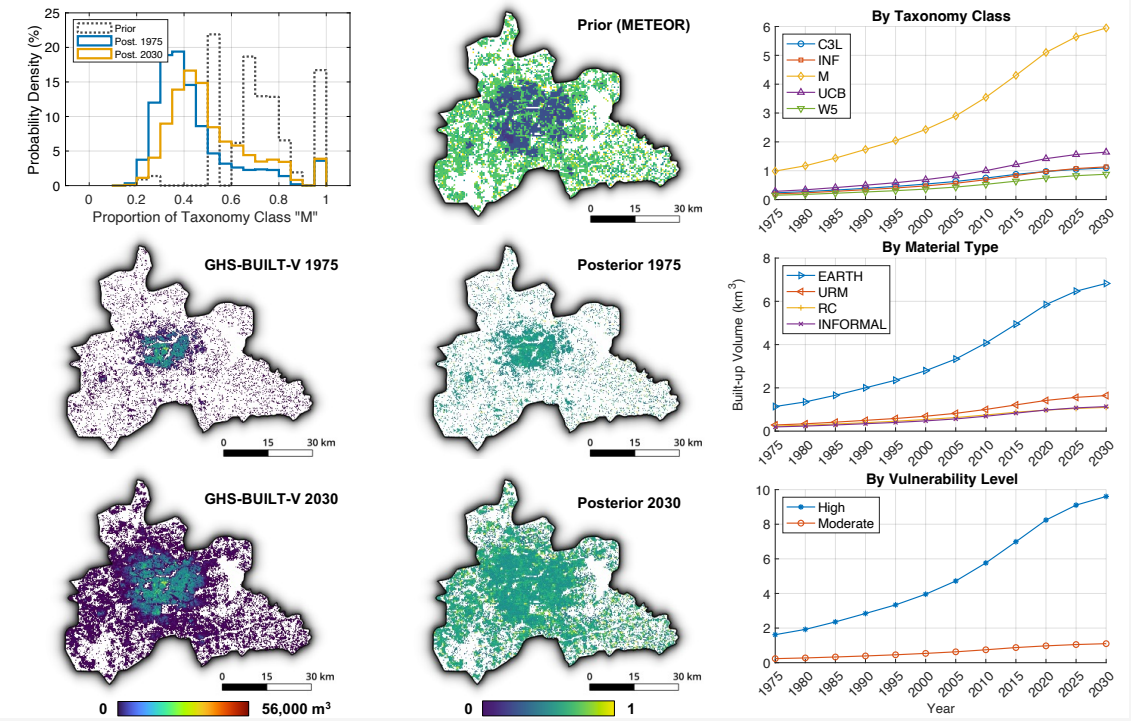

B.6 BGD: Dhaka City, Bangladesh

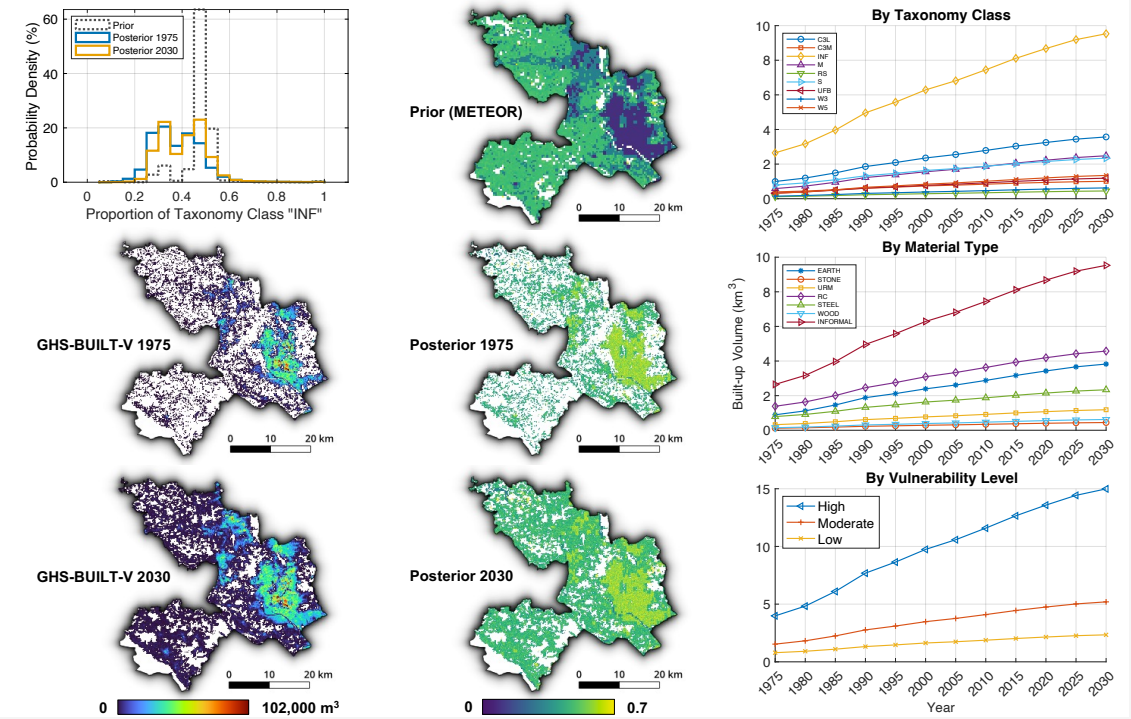

B.7 BTN: Samtse, Bhutan

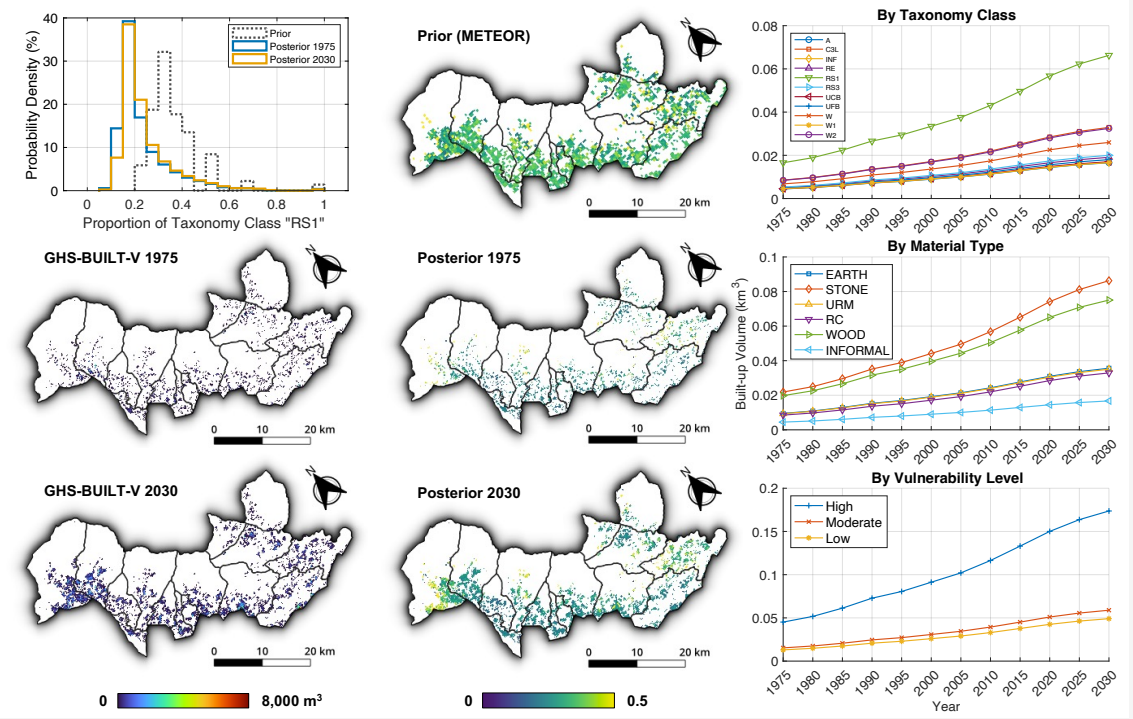

B.8 CAF: Bangui, The Central African Republic

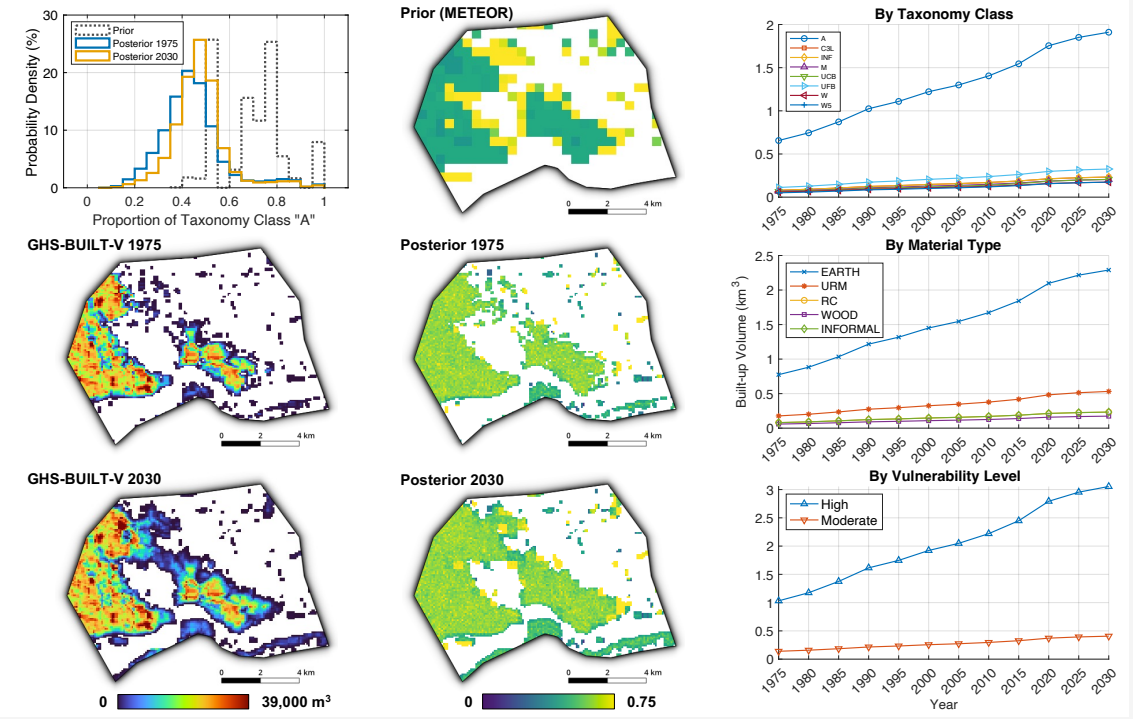

B.9 COD: Kinshasa, Democratic Republic of the Congo

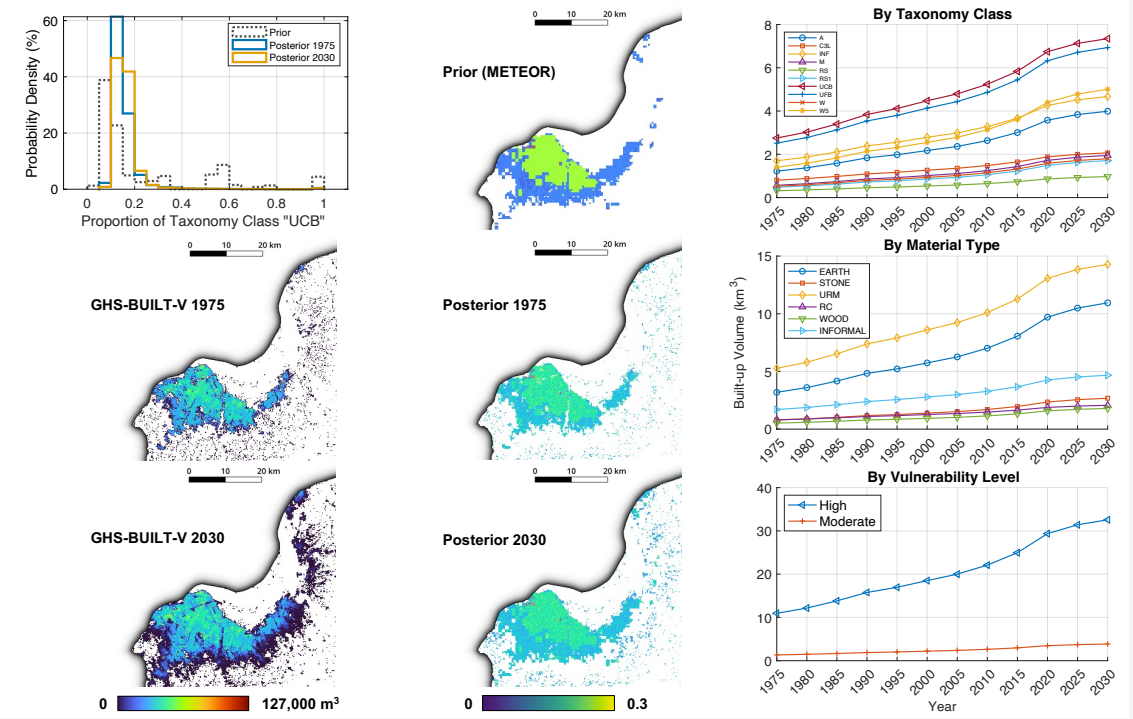

B.10 COM: Grande Comore, Comoros

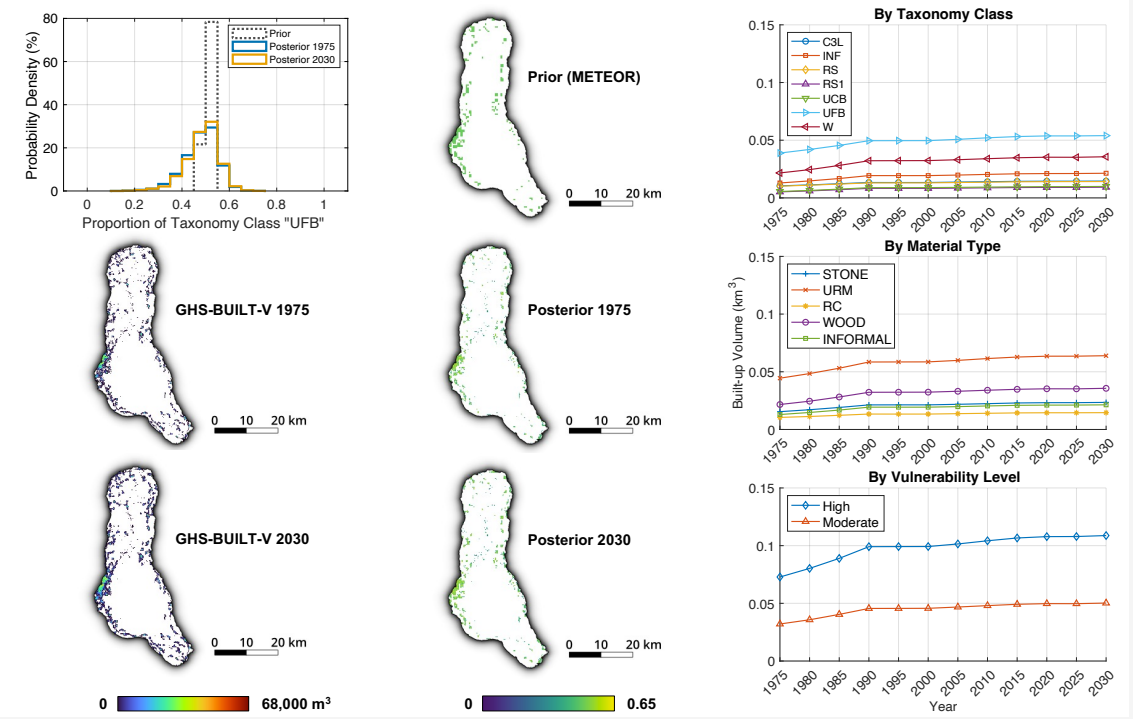

B.11 DJI: Djibouti

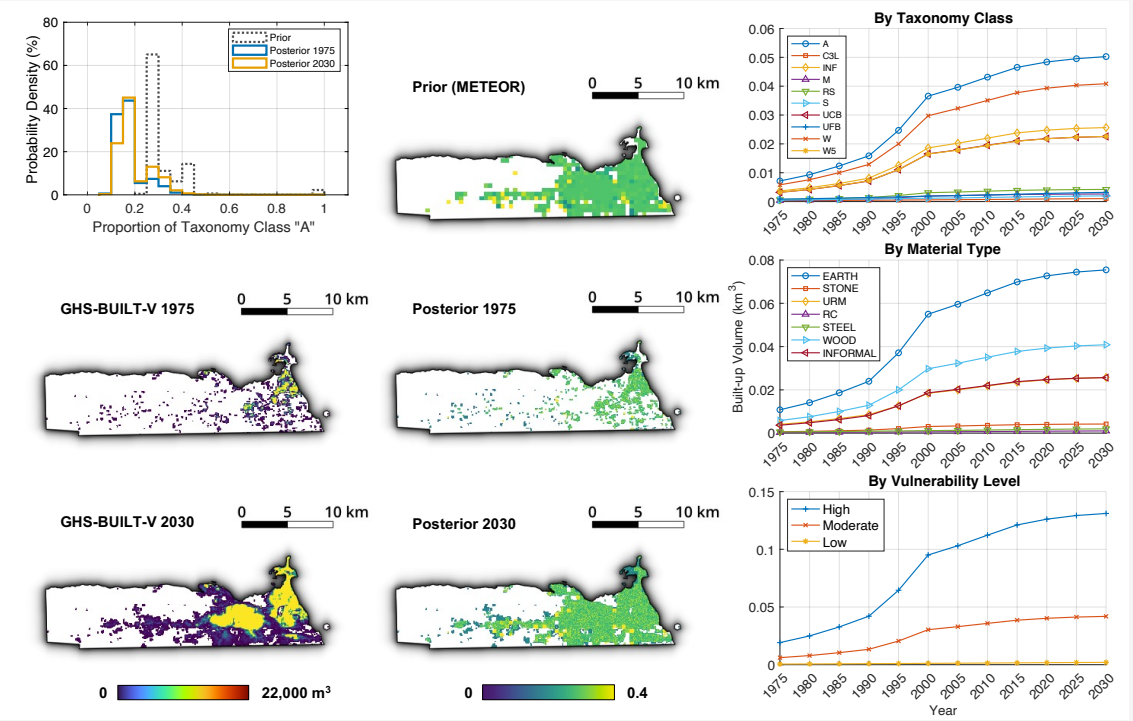

B.12 ERI: Maekel, Eritrea

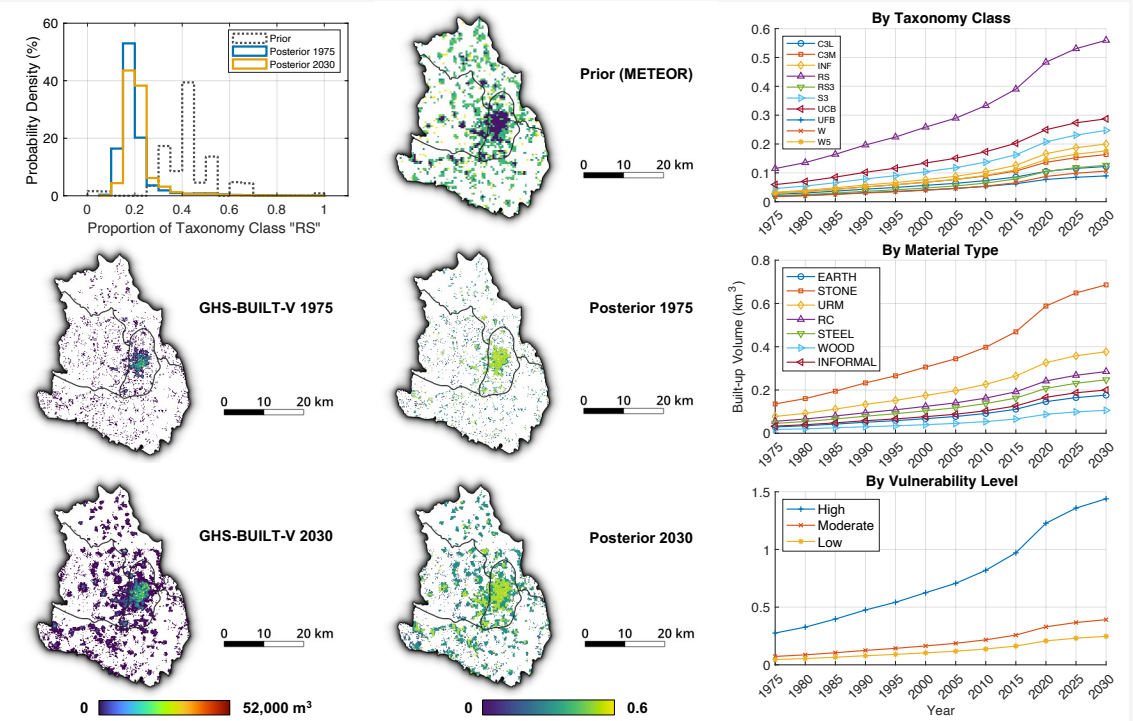

B.13 ETH: Addis Abeba, Ethiopia

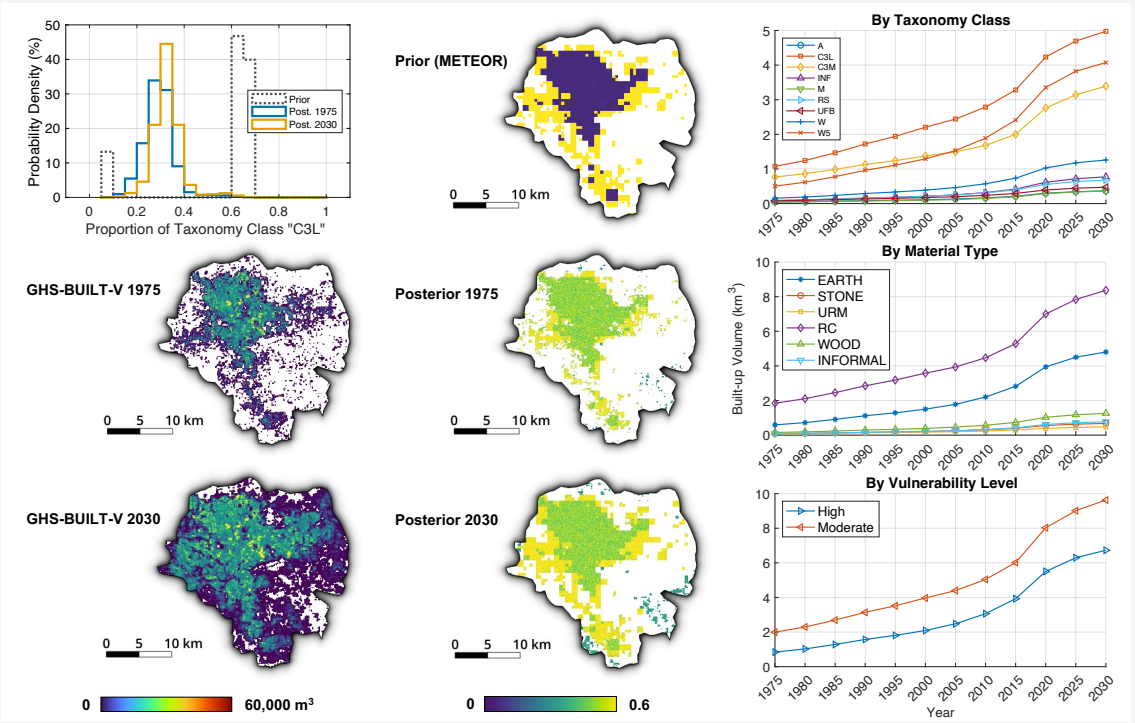

B.14 GIN: Conakry, Guinea

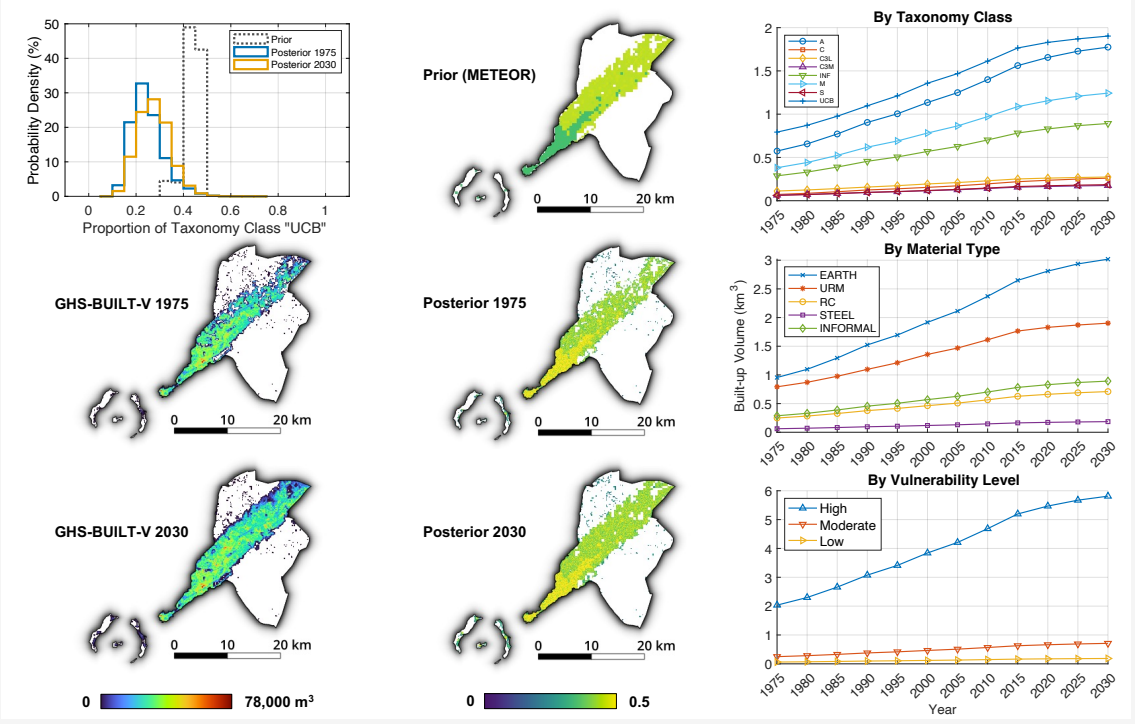

B.15 GMB: Banjul & Kombo, The Gambia

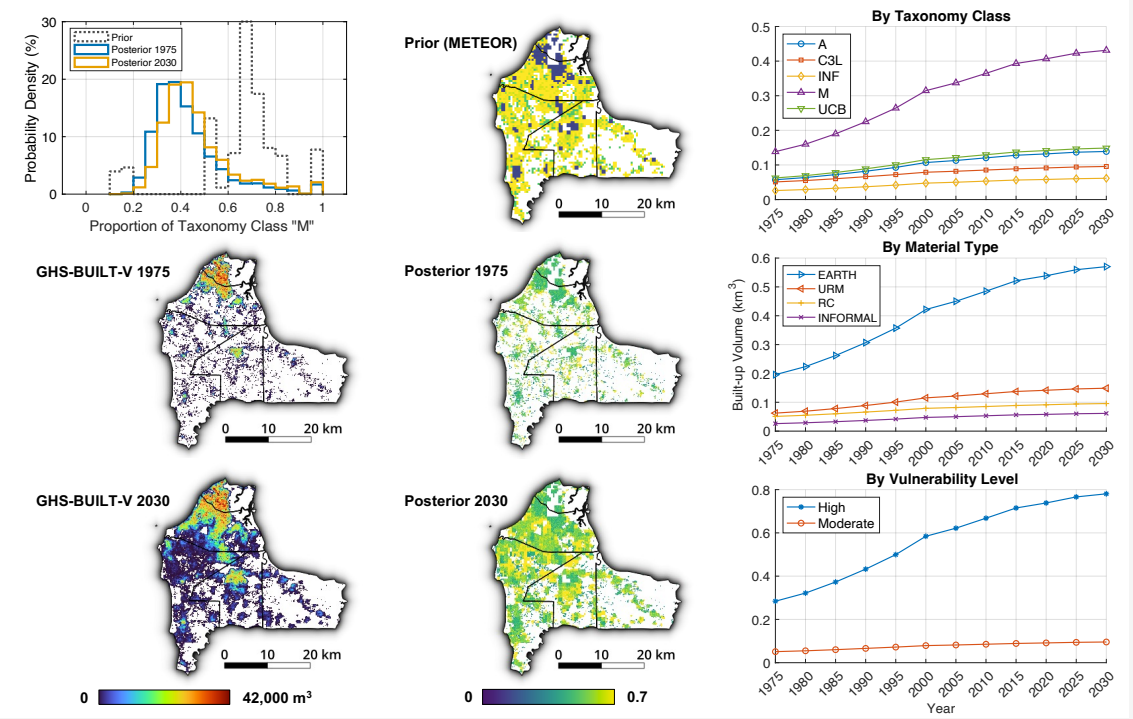

B.16 GNB: Bissau & Biombo, Guinea-Bissau

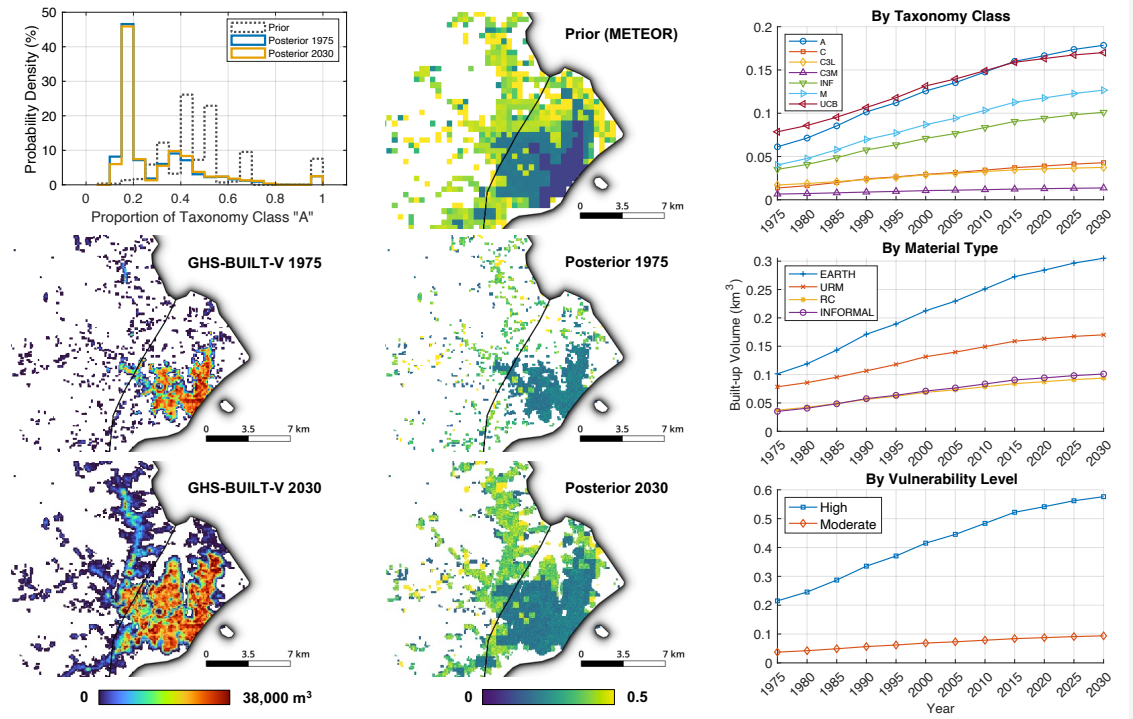

B.17 HTI: Port-au-Prince, Haiti

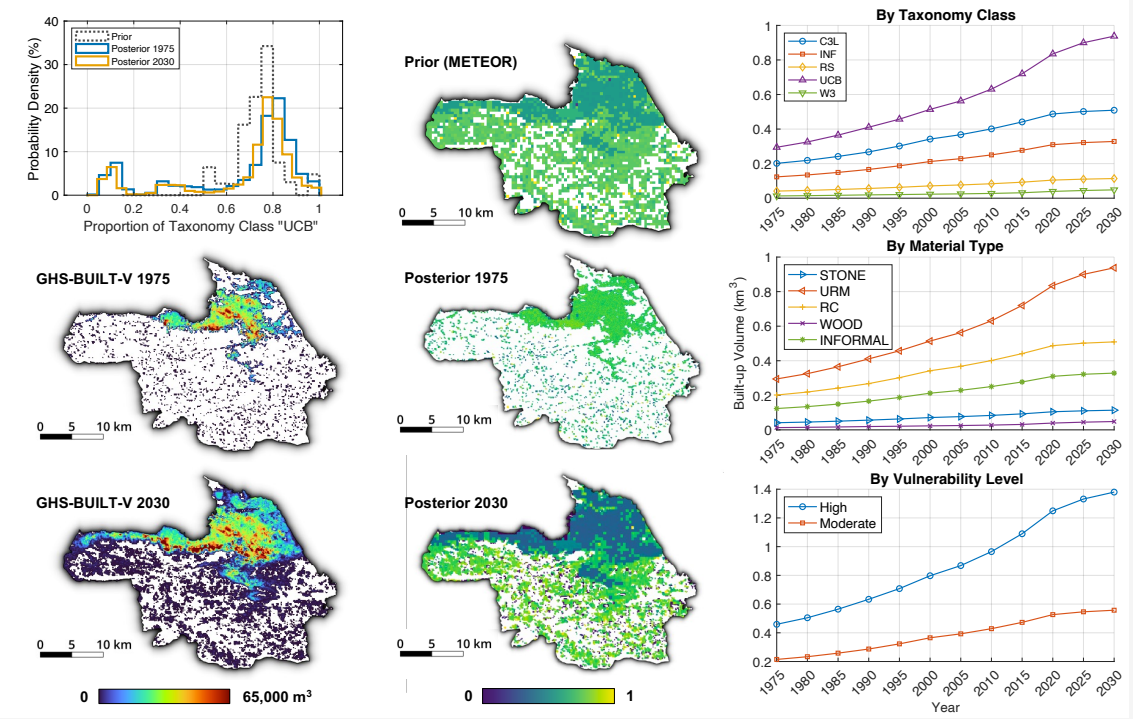

B.18 KHM: Phnom Penh, Cambodia

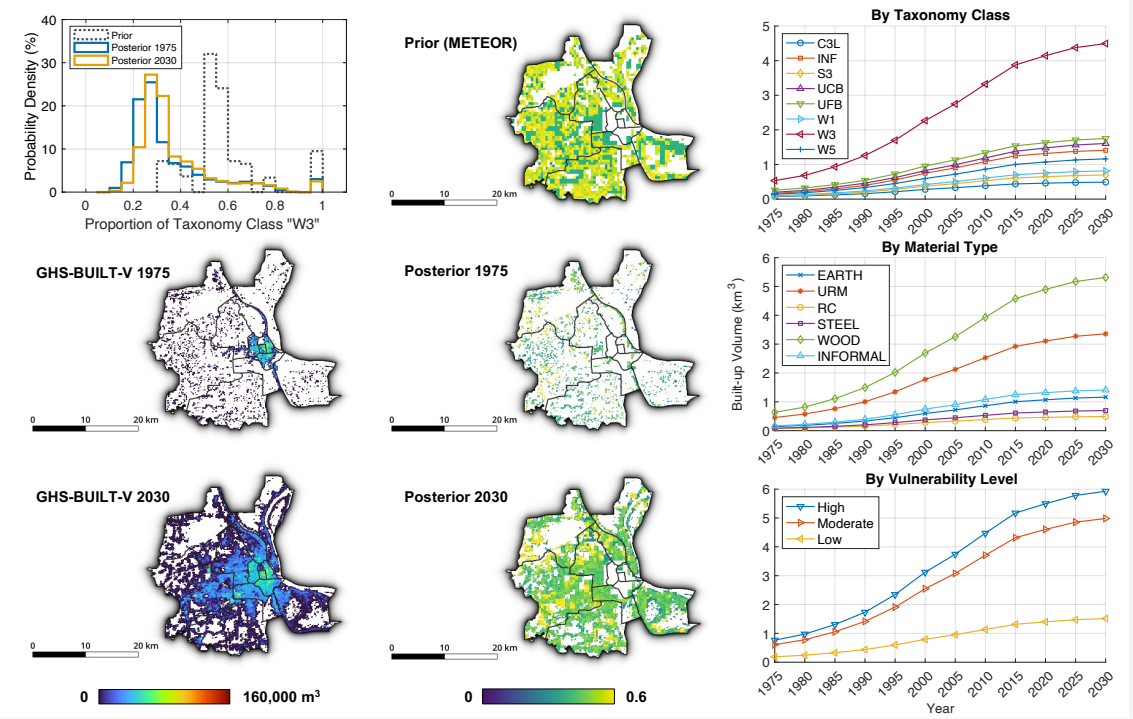

B.19 LAO: Vientiane, Laos

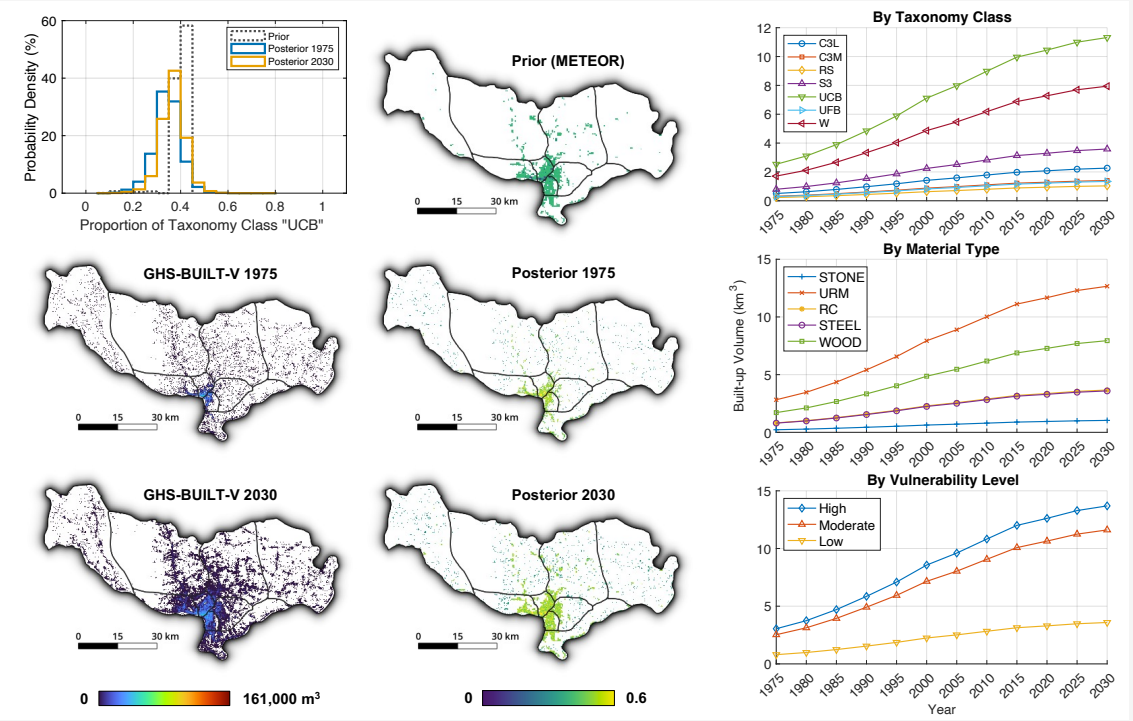

B.20 LBR: Montserrado, Liberia

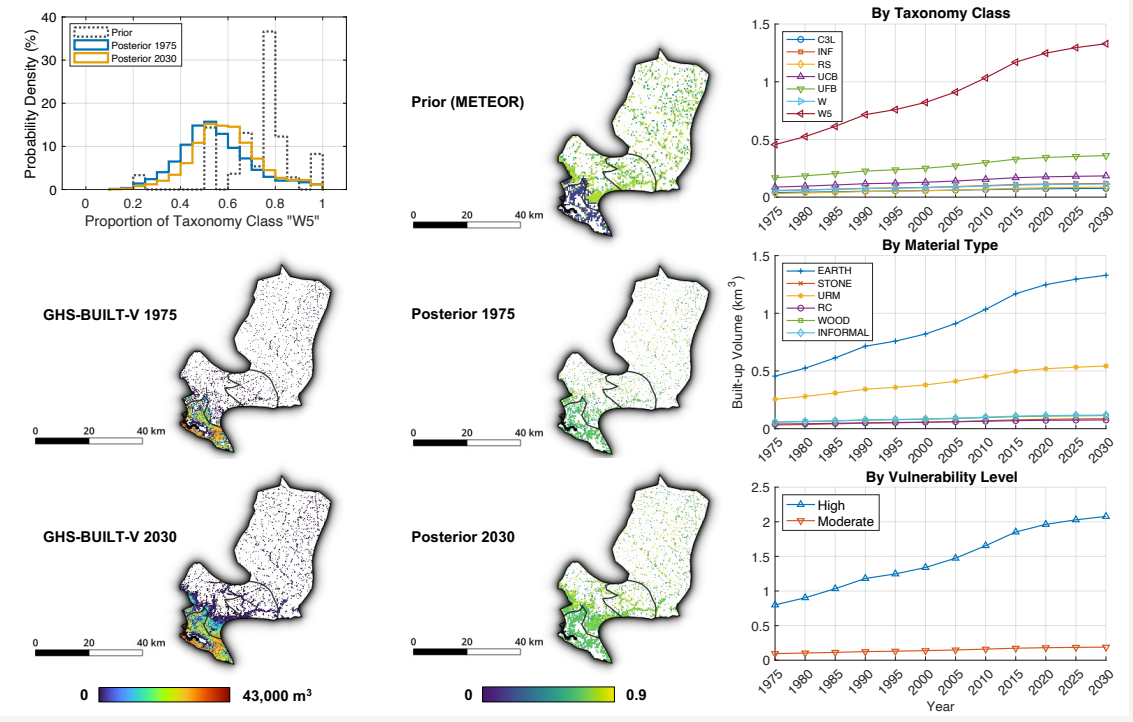

B.21 LSO: Maseru, Lesotho

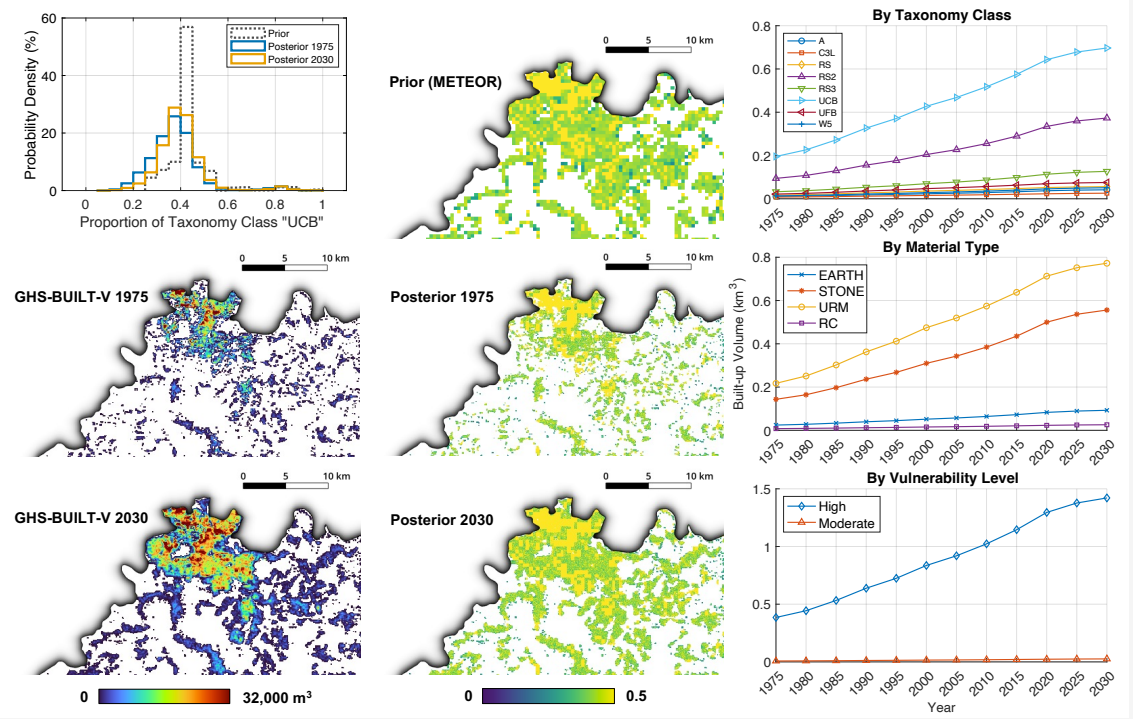

B.22 MDG: Analamanga, Madagascar

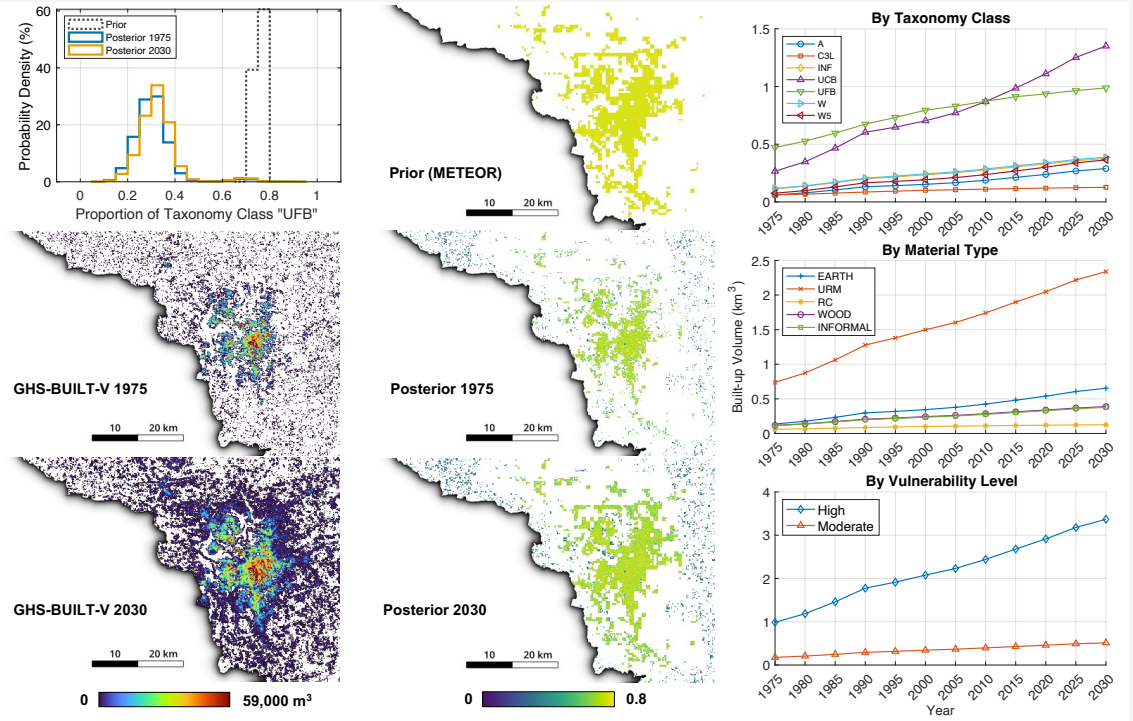

B.23 MLI: Bamako & Kati, Mali

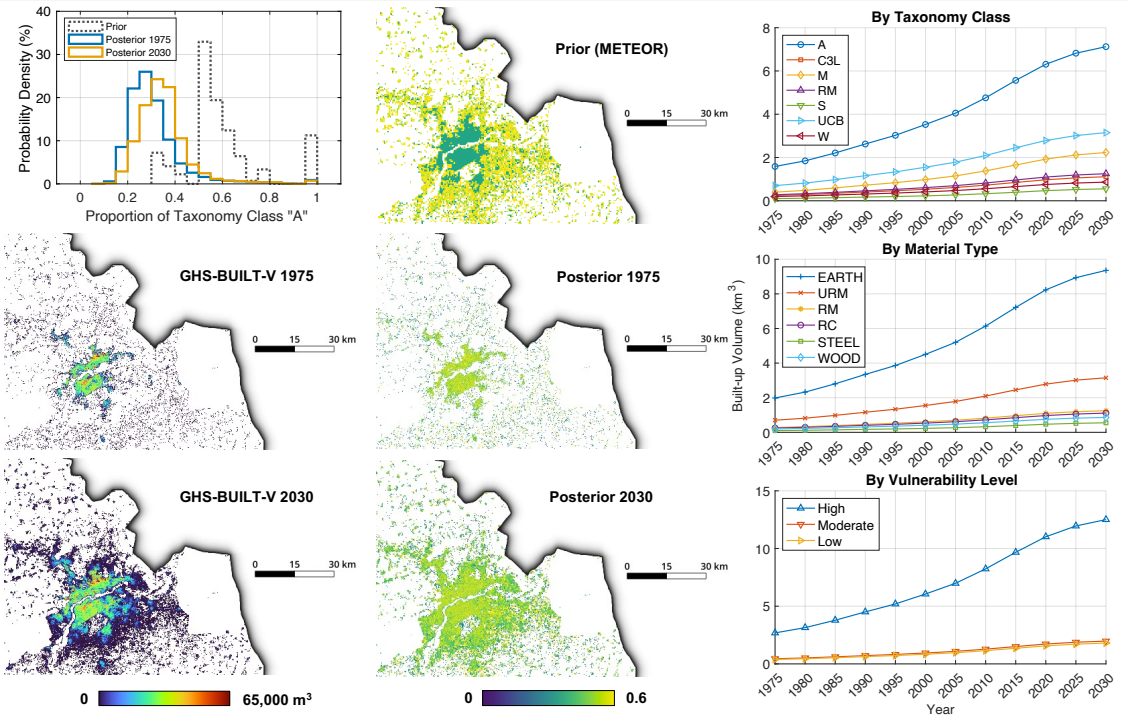

B.24 MMR: Yangon, Myanmar

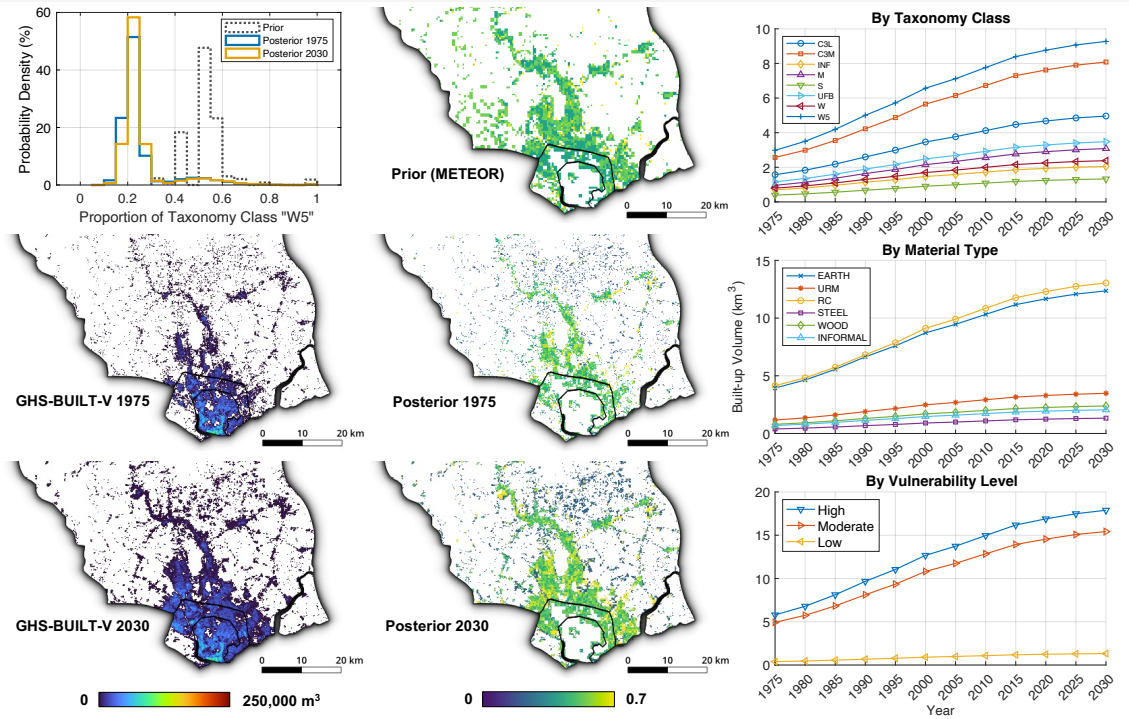

B.25 MOZ: Cidade Da Beira, Mozambique

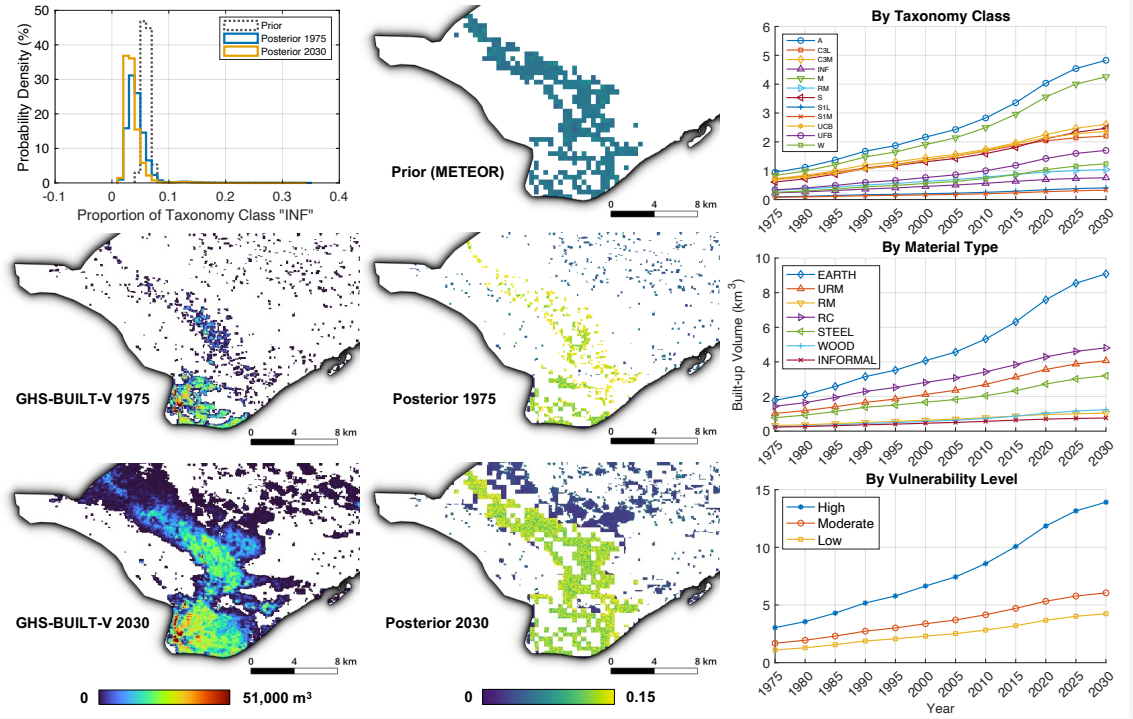

B.26 MRT: Nouakchott, Mauritania

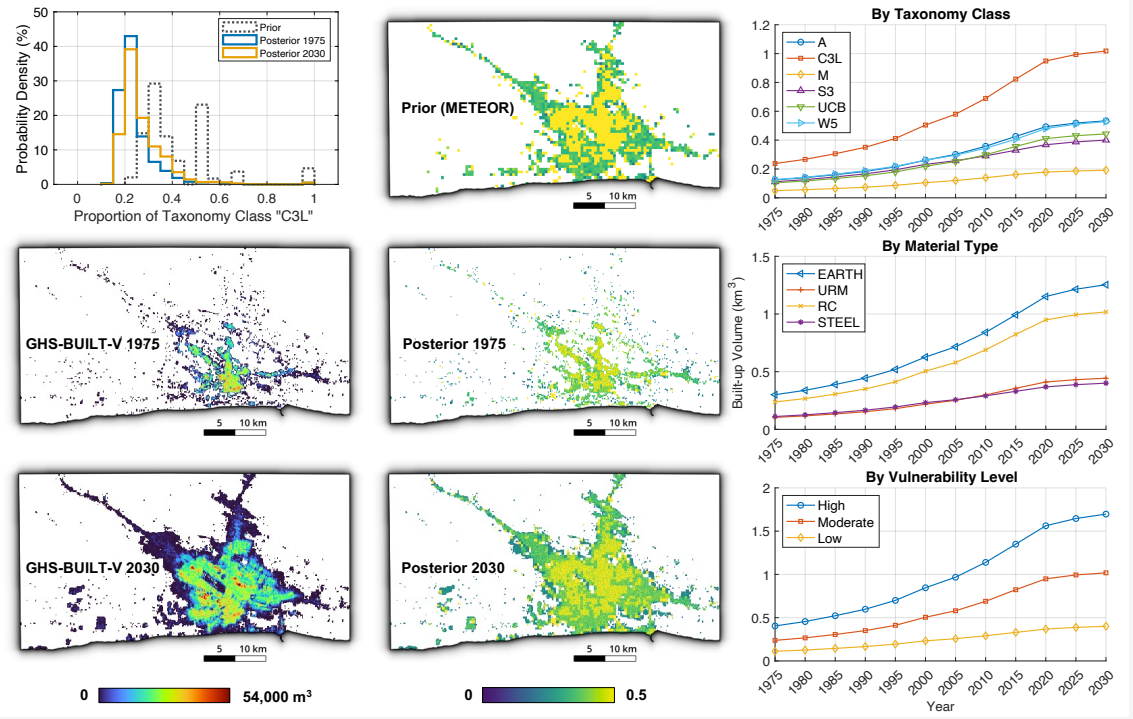

B.27 MWI: Blantyre, Malawi

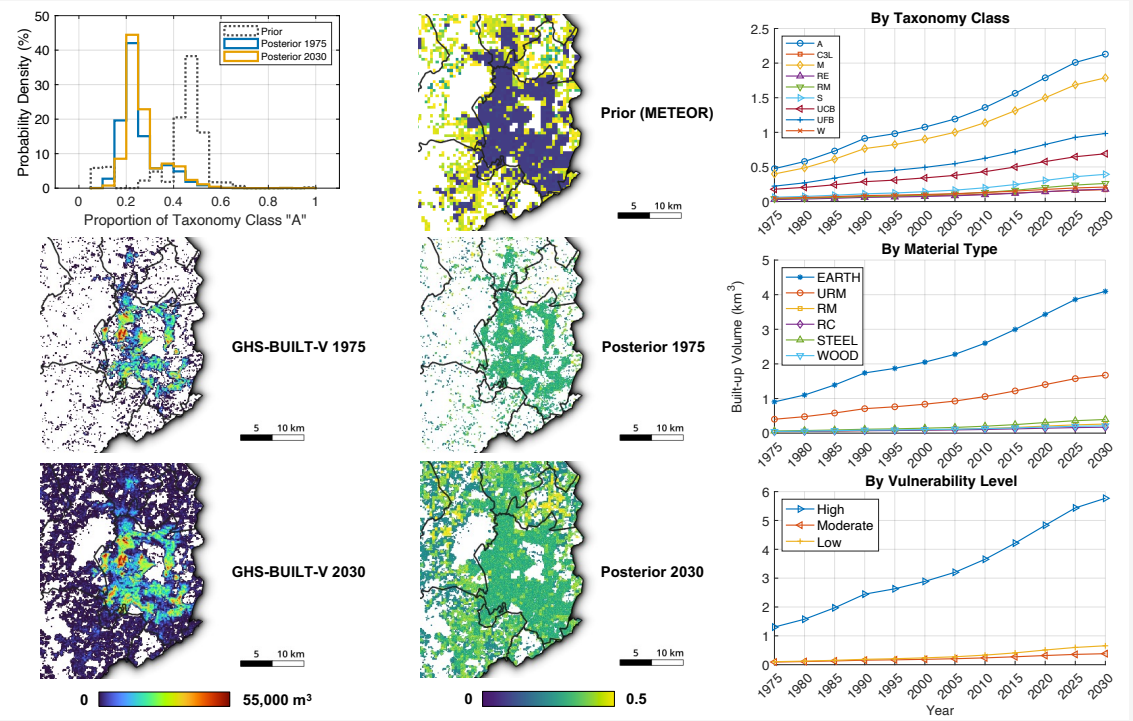

B.28 NER: Niamey, Niger

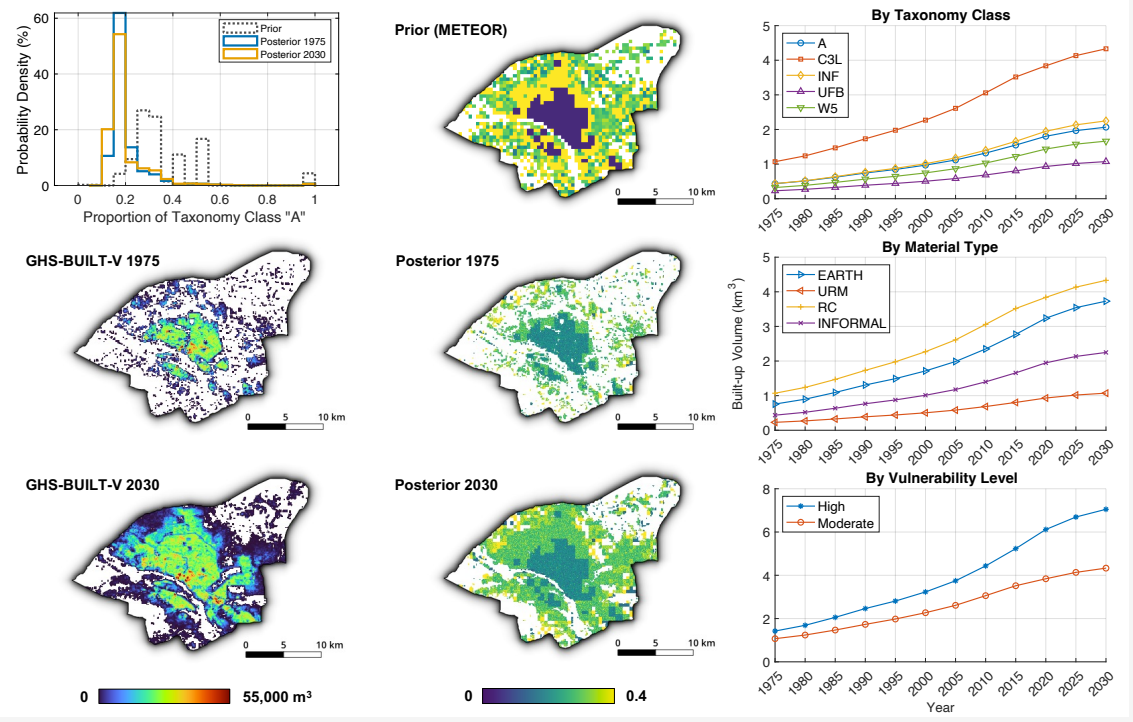

B.29 NPL: Biratnagar, Nepal

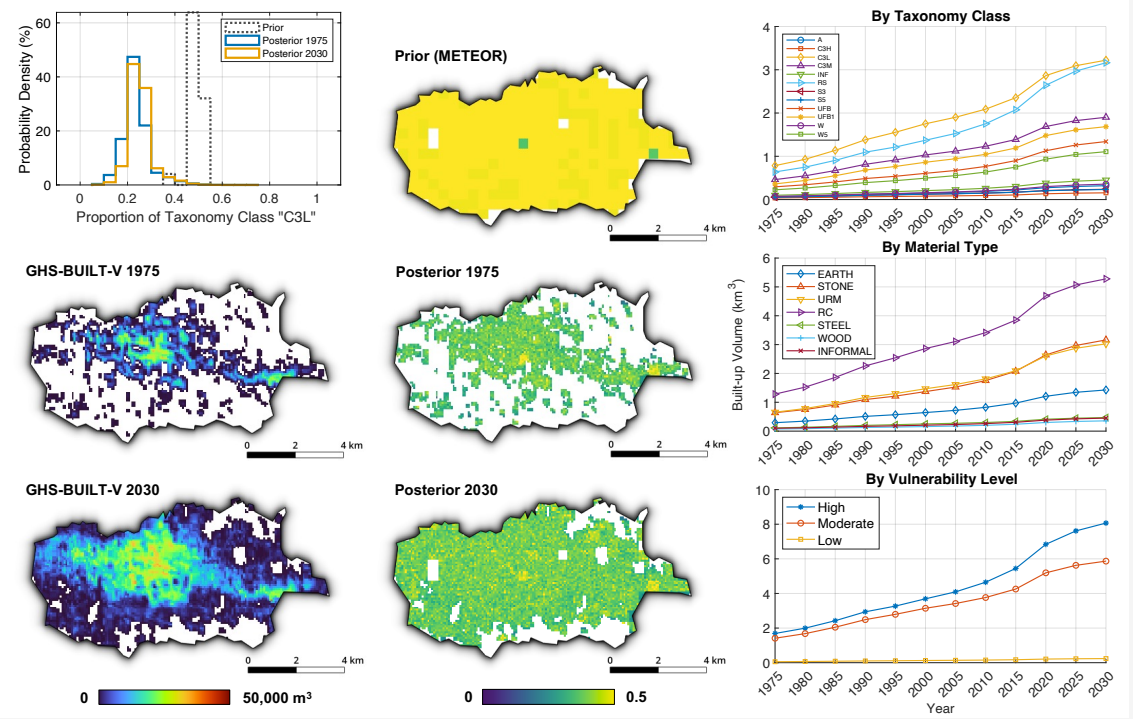

B.30 RWA: Kigali, Rwanda

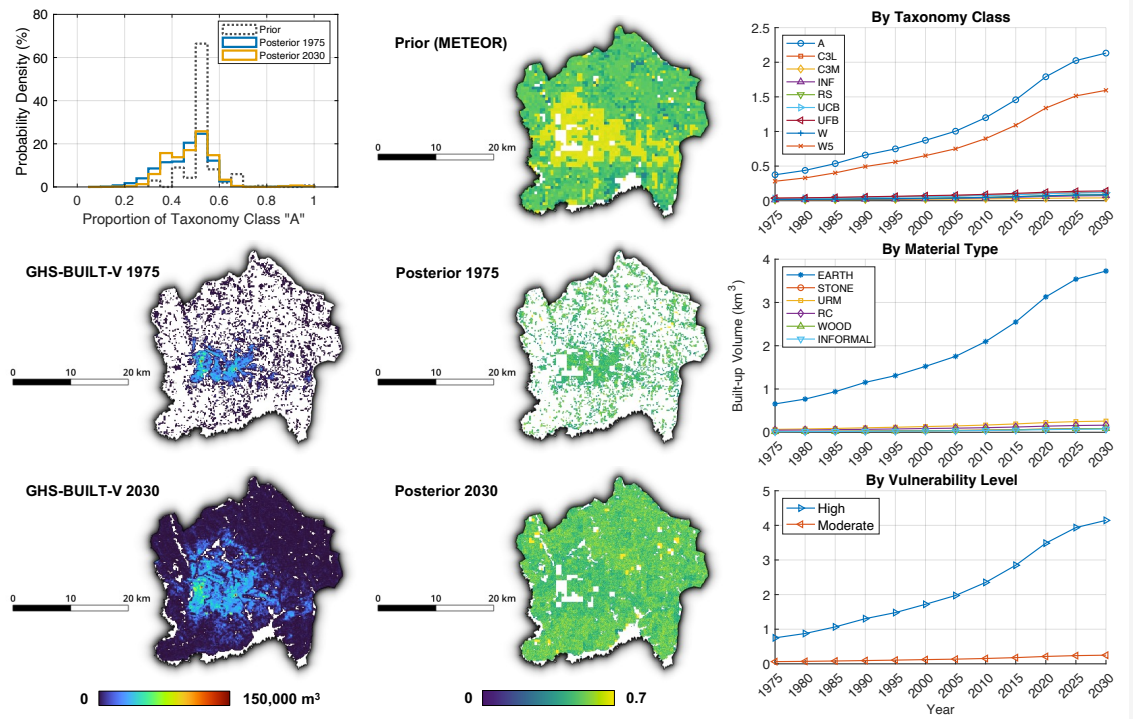

B.31 SDN: Khartoum, Sudan

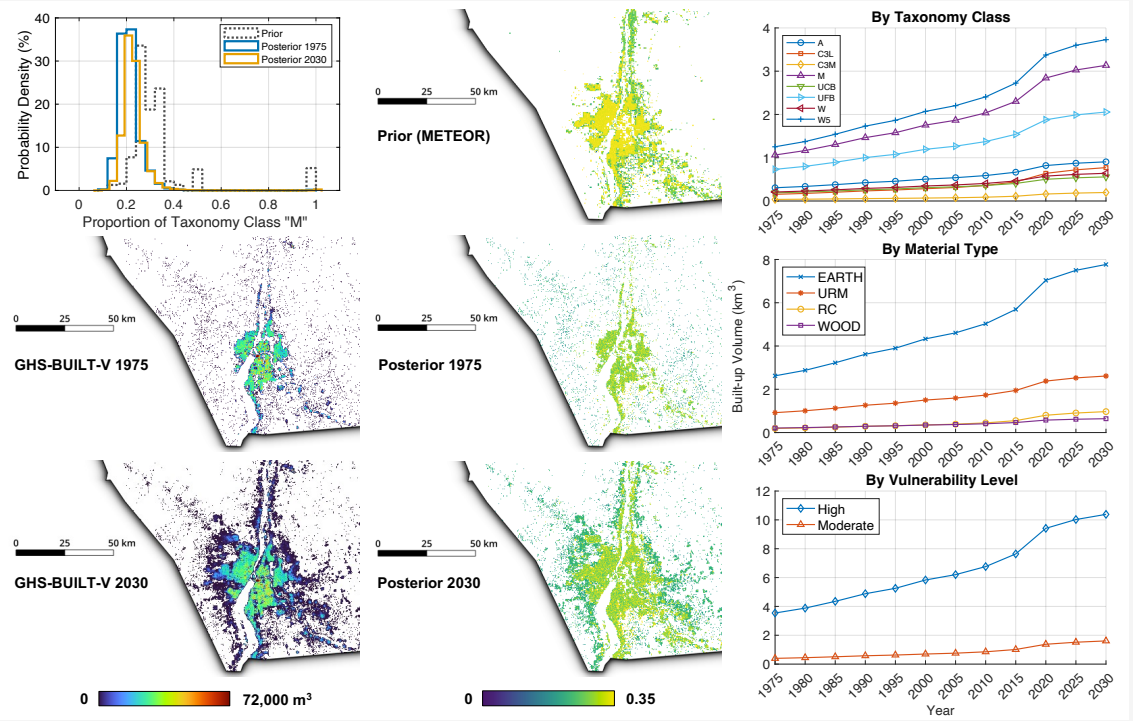

B.32 SEN: Dakar, Senegal

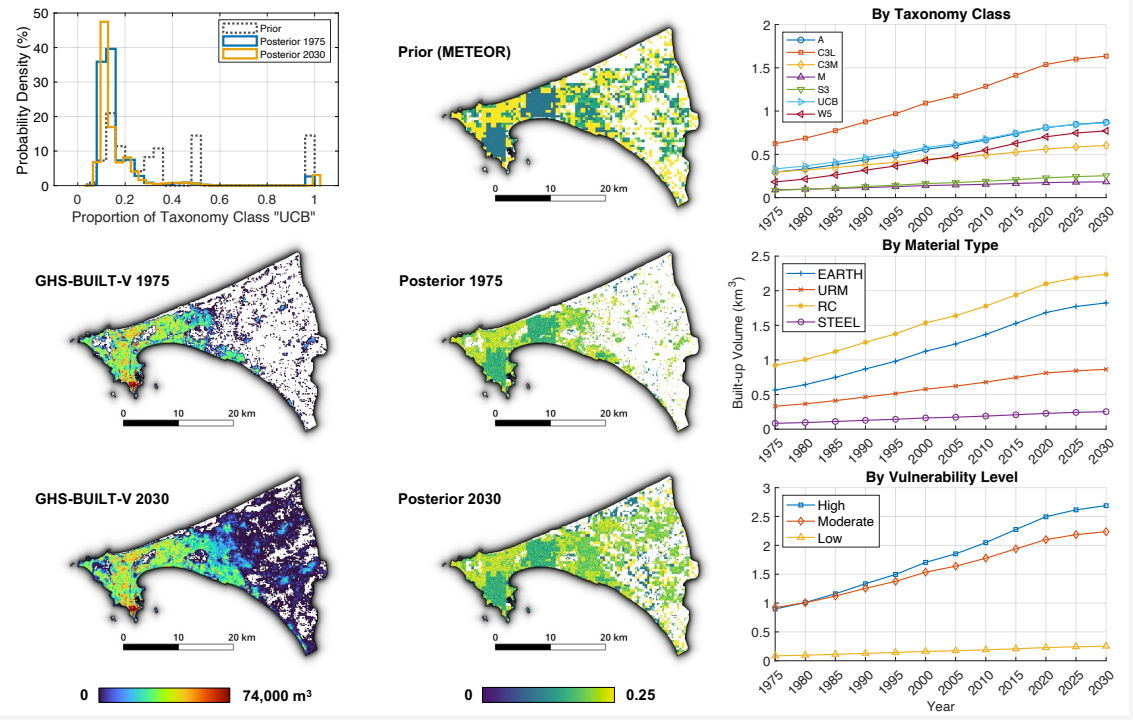

B.33 SLB: Honiara, Solomon Islands

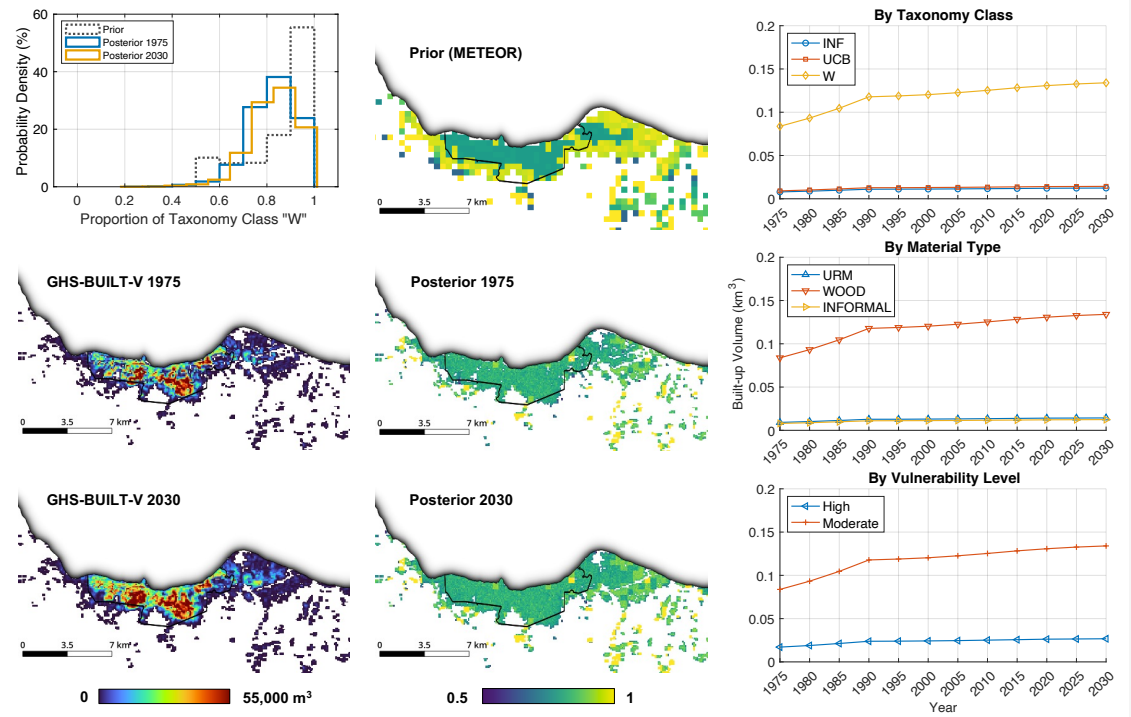

B.34 SLE: Freetown, Sierra Leone

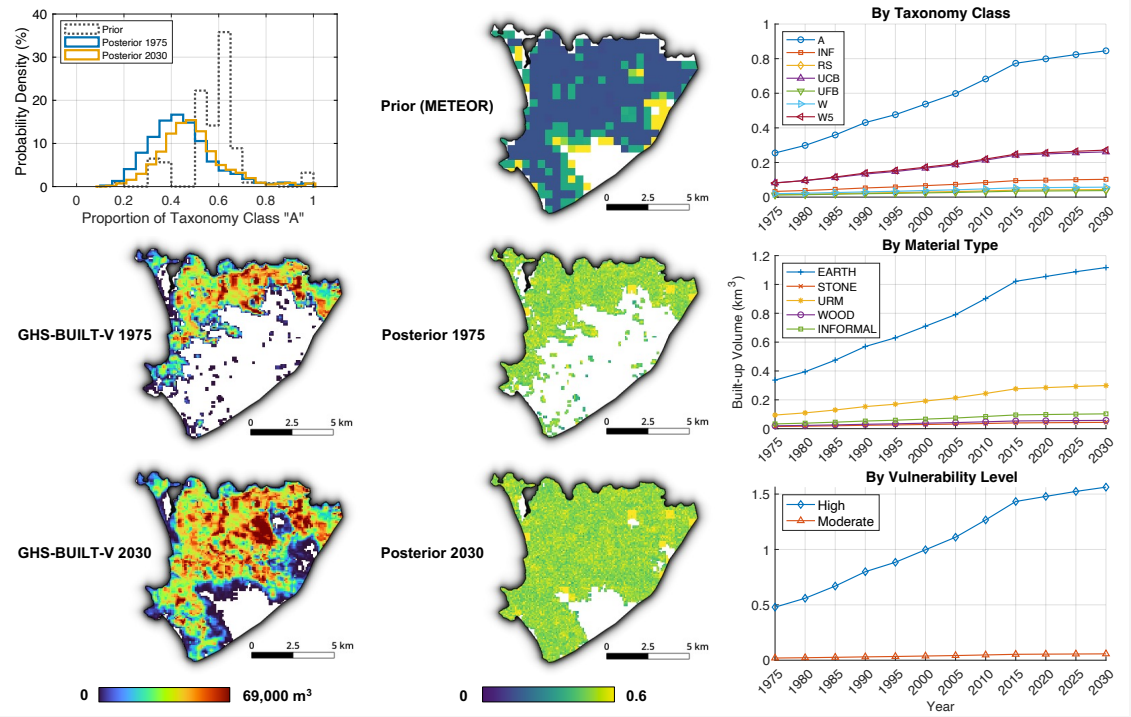

B.35 SOM: Mogadisho, Somalia

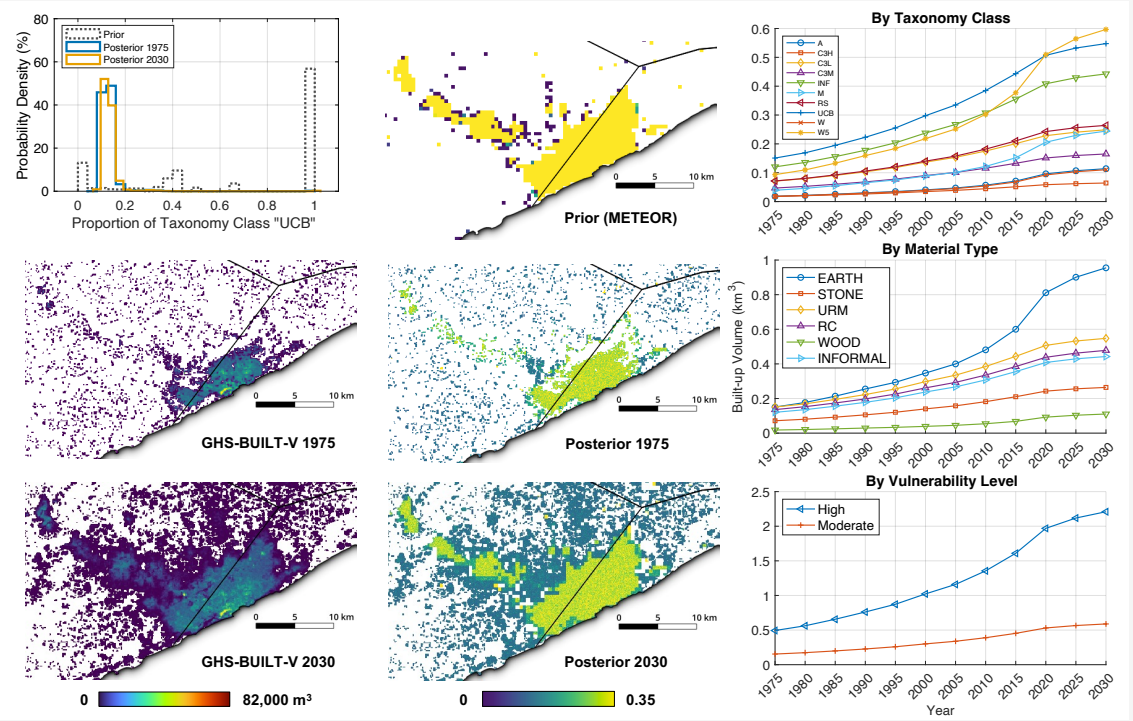

B.36 SSD: Bentiu, South Sudan

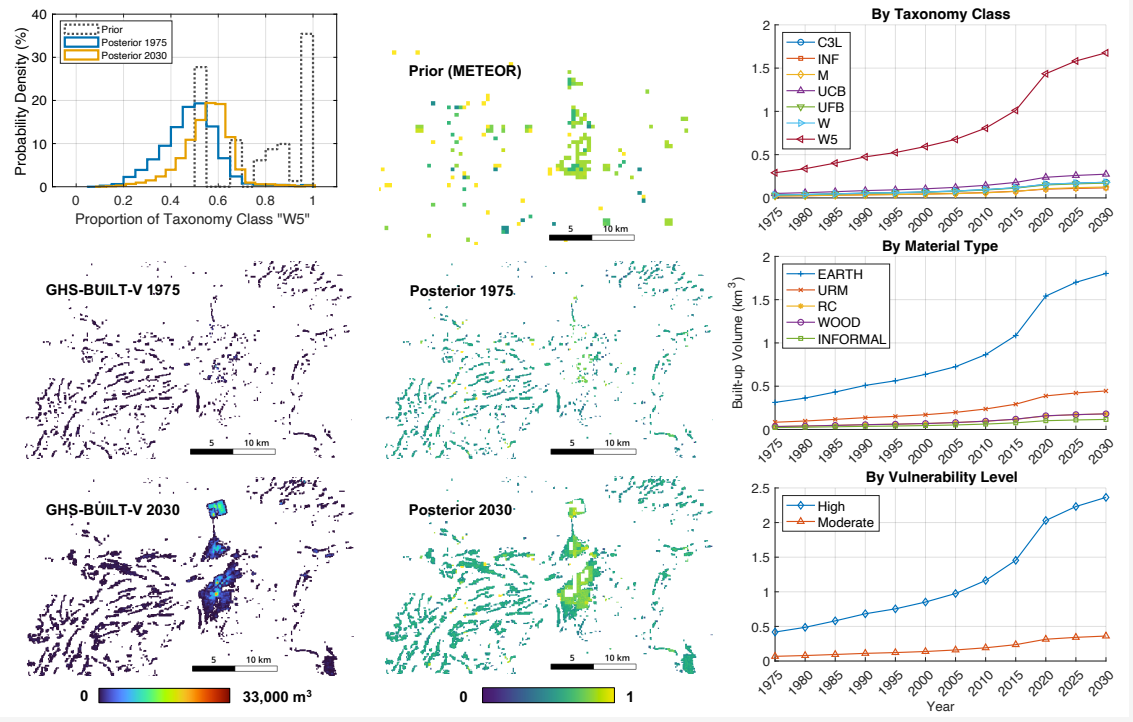

B.37 STP: Agua Grande, São Tomé and Príncipe

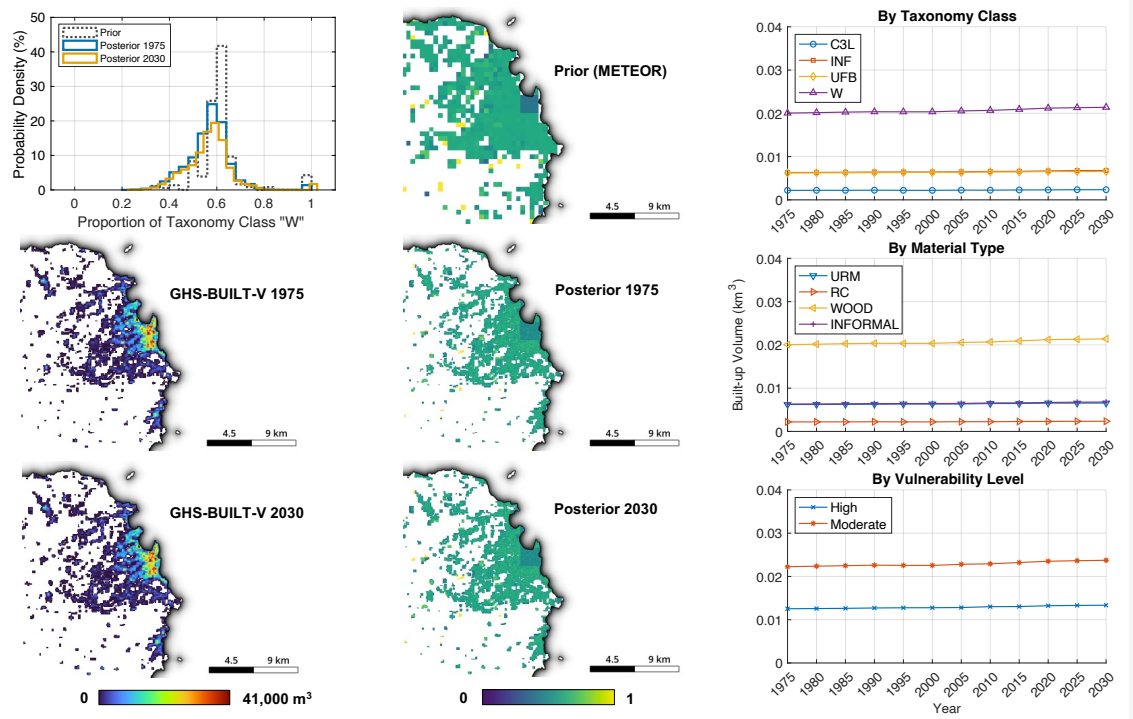

B.38 TCD: N'Djamena, Chad

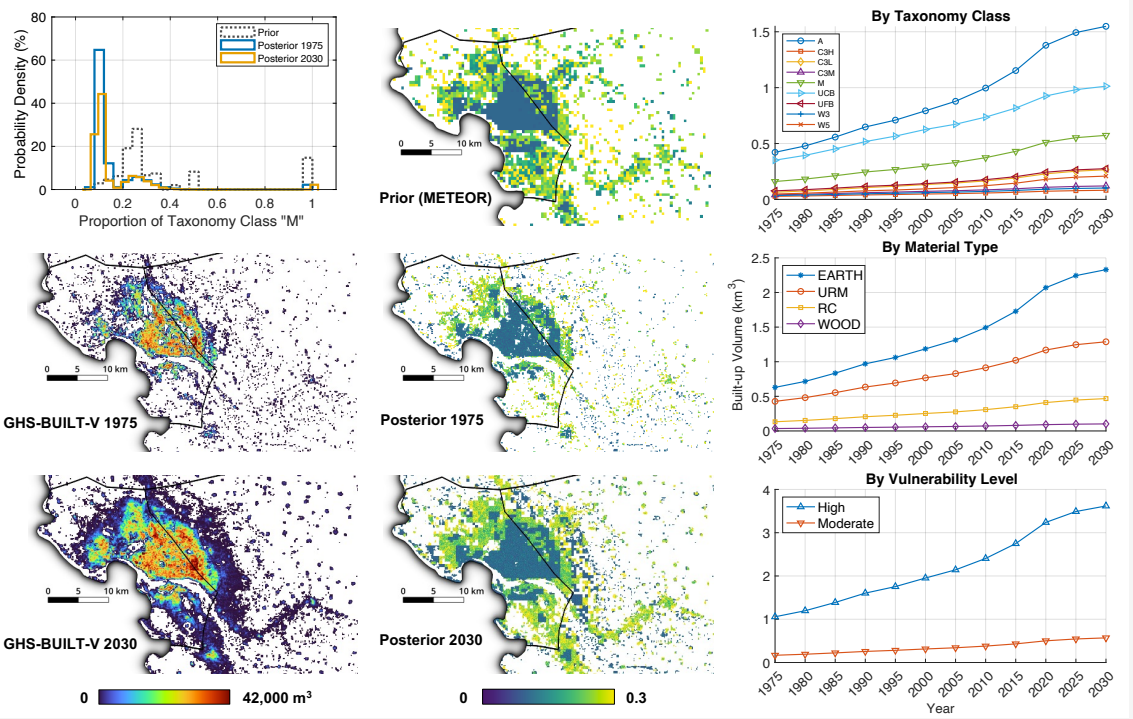

B.39 TGO: Lomé (and Neighboring Areas), Togo

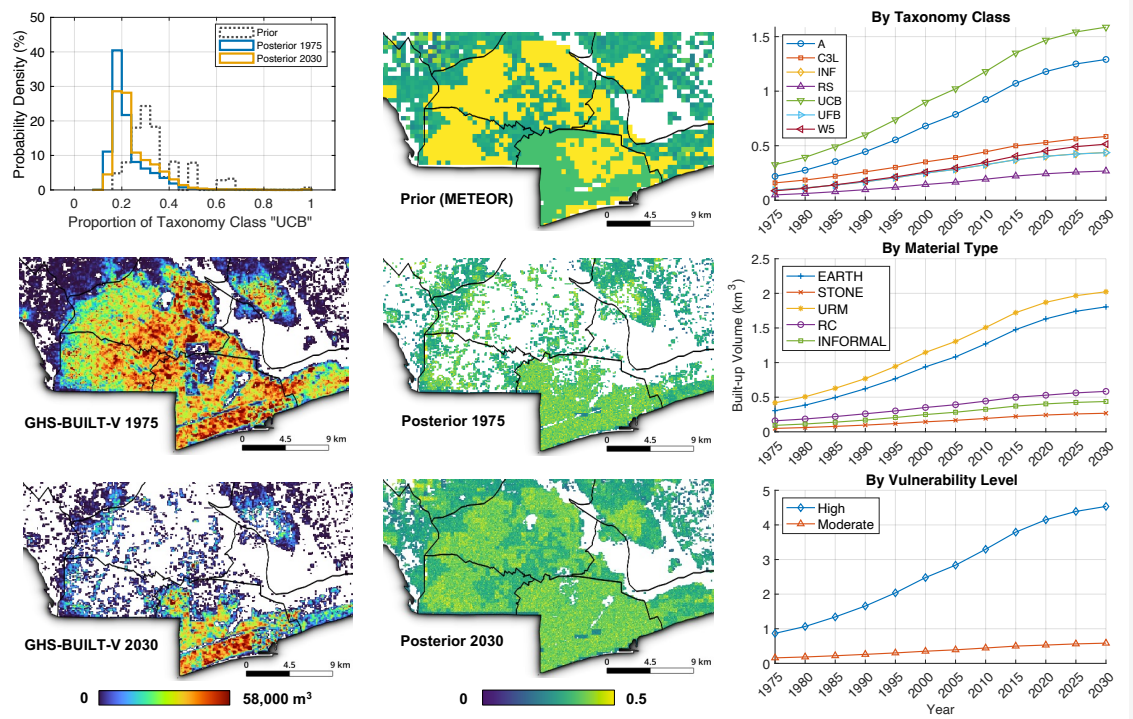

B.40 TLS: Dili, Timor-Leste

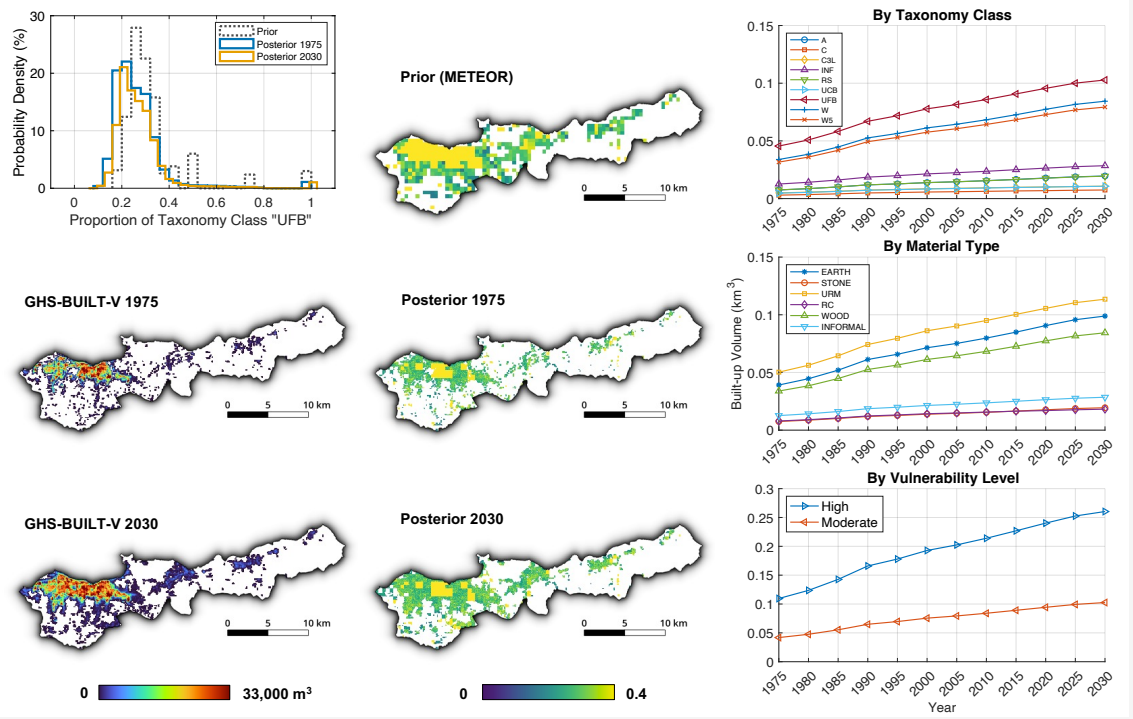

B.41 TUV: Funafuti, Tuvalu

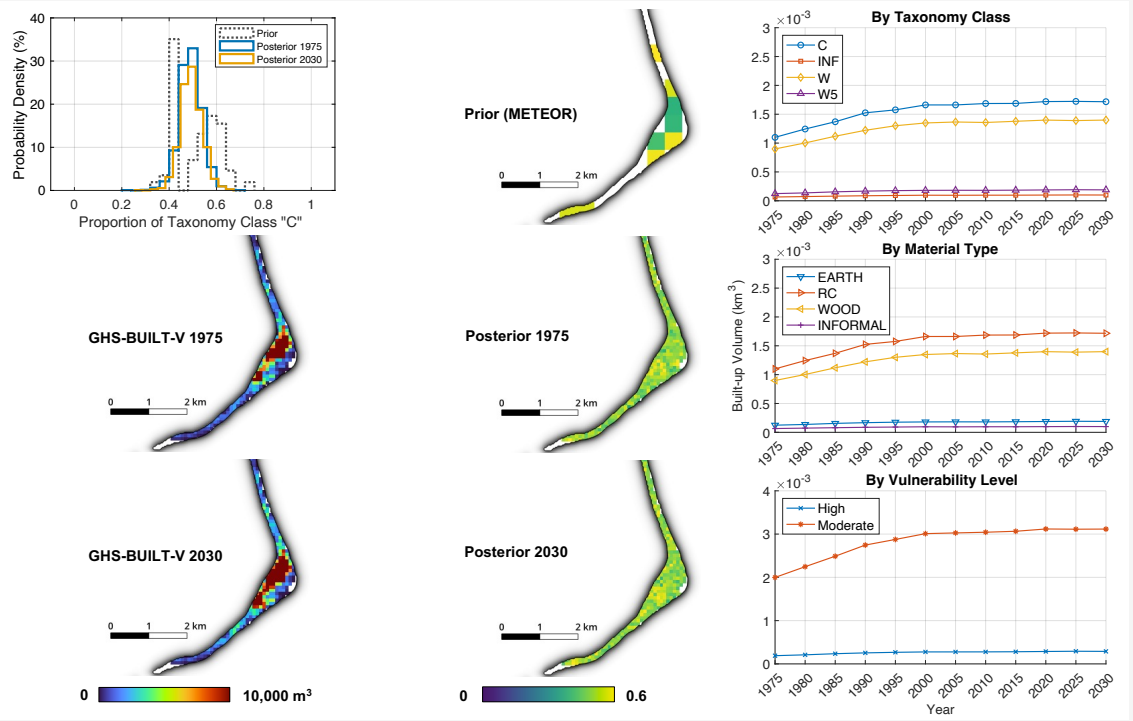

B.42 TZA: Dar es Salaam, Tanzania

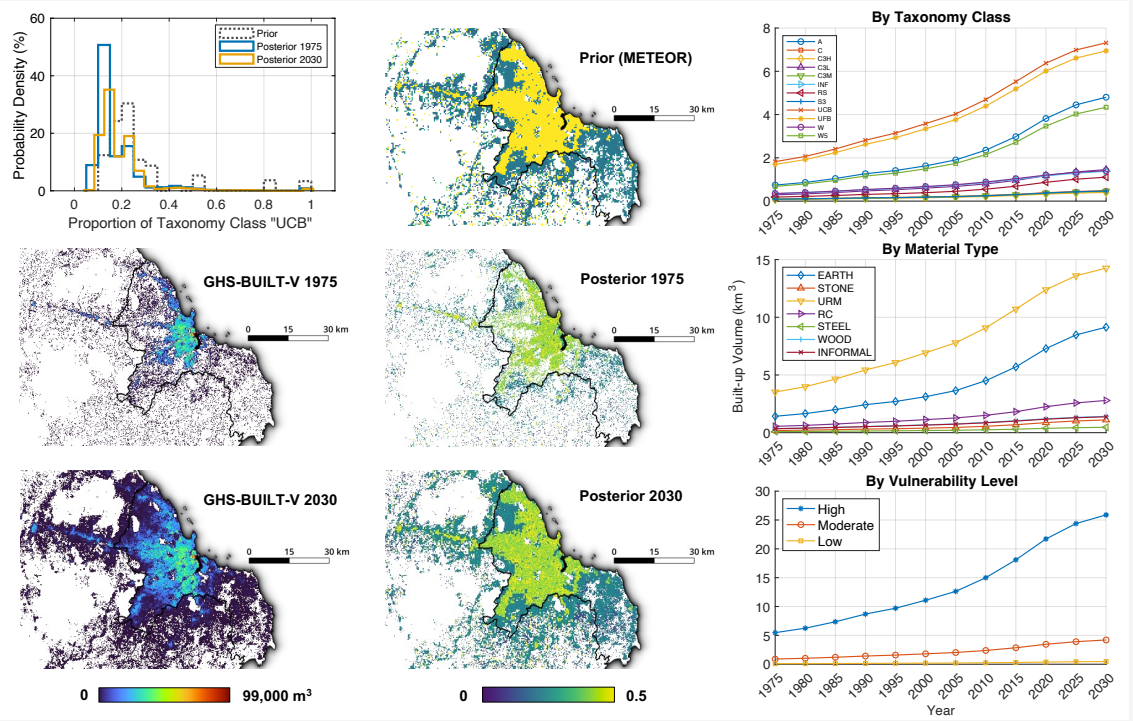

B.43 UGA: Kampala & Wakiso, Uganda

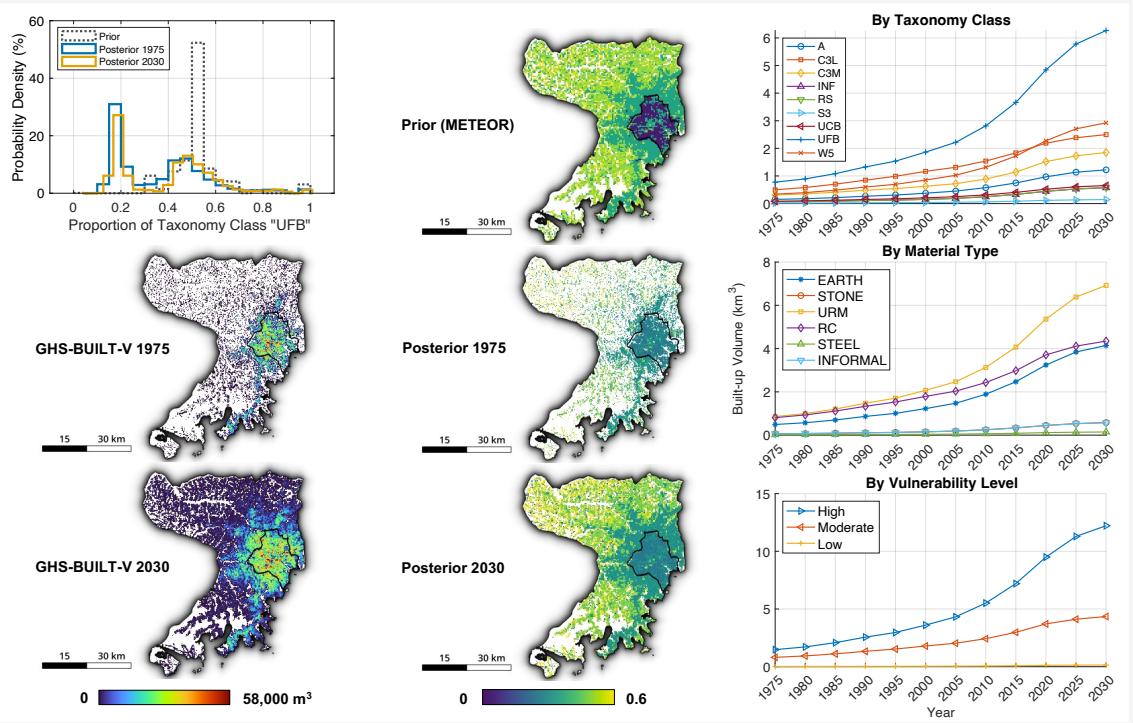

B.44 VUT: Port Vila, Vanuatu

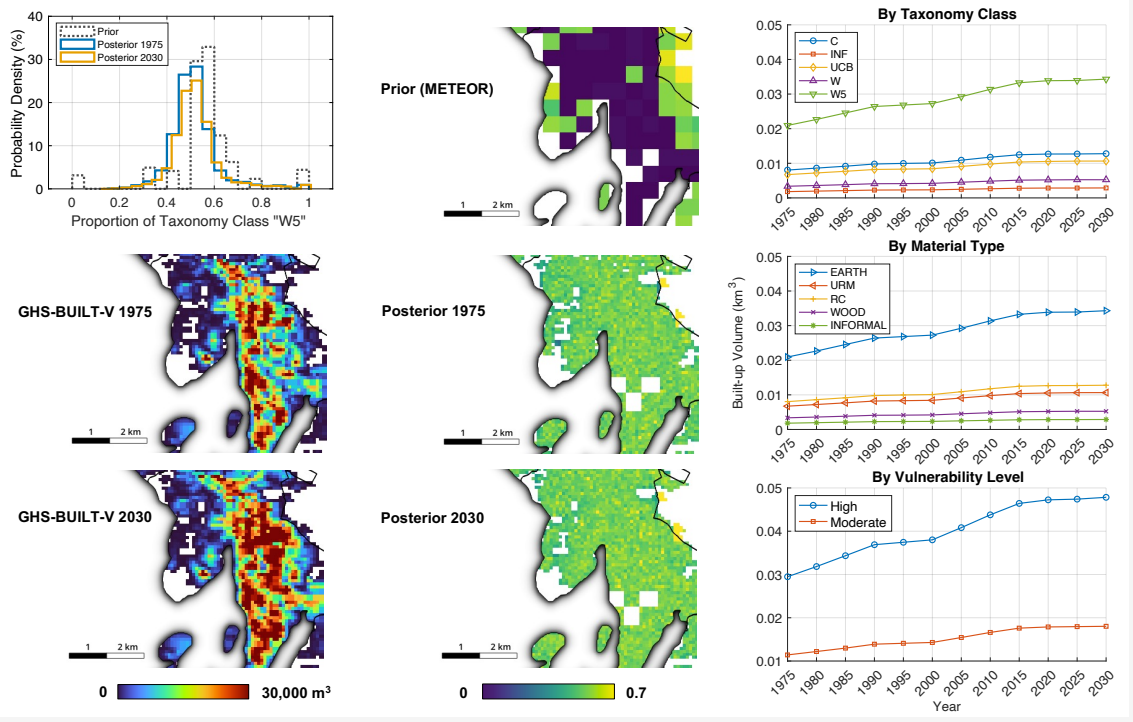

B.45 YEM: Adan, Yemen

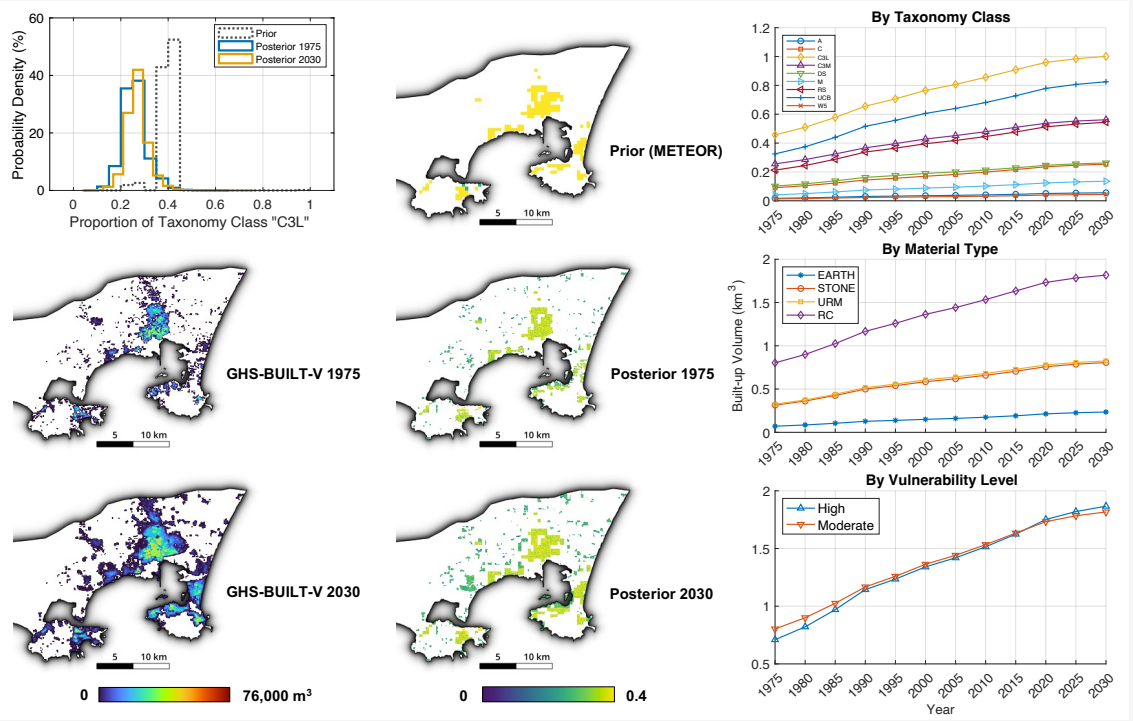

B.46 ZMB: Lusaka, Zambia